DISCLAIMER NOTICE

THIS DOCUMENT IS THE BEST QUALITY AVAILABLE.

COPY FURNISHED CONTAINED A SIGNIFICANT NUMBER OF PAGES WHICH DO NOT REPRODUCE LEGIBLY.

GENERAL APPLIED SCIENCE LABORATORIES, INC.

(4) NA (5) 350 320

Copy No. 6 of 10

Total Pages - iv and 124

#2 = AD-412 677

(6) STUDIES OF THE ELECTROMAGNETIC CHARACTERISTICS OF MOVING IONIZED GASES. (7)-(8) NA

(9) (11) SEMIANNUAL TECHNICAL SUMMARY REPORT, no. 2,

(14) TECHNICAL RPT. no. 290 (11)

(17) (19) NA (20) U

(16) ARPA Order No. 207-61

(15) Contract No. Nonr 3475(00)

Period: October 1 1961 - March 31 1962.

(10) NA

(11) 30 Apr 62,

(12) 124p. (13) NA

(2) Report on Title of Project

"Studies of the Electromagnetic Characteristics of Moving Ionized Gases"

Prepared for

Director
Advanced Research Projects Agency
Department of Defense
The Pentagon
Washington 25, D. C.

ARPA Cont. No. 4557

Prepared by

General Applied Science Laboratories, Inc.
Merrick and Stewart Avenues
Westbury, L. I., New York

April 30, 1962

Approved by: _____
Antonio Ferri
President

TABLE OF CONTENTS

TABLE OF CONTENTS (CONT.)

STUDIES OF THE ELECTROMAGNETIC CHARACTERISTICS OF MOVING IONIZED GASES

The Project Scientist for this task is Dr. Manlio Abele.

The investigations of the microscopic and macroscopic properties in a weakly ionized gas reported in Chapters II and III of this summary report were carried out under the direction of Professors Piero Caldirola and Luigi Napolitano, respectively, and under the general direction of Prof. Piero Caldirola.

The experimental investigation described in Chapter IV has been carried out by Messrs. R. Tomboulian, M. Wecker and H. Medecki under the direct supervision of Dr. Abele.

In Chapter V, preliminary calculations have been conducted by Dr. Bruce Gavril in the evaluation of the electromagnetic properties on the basis of the experimental information obtained with the shock tube facility.

CHAPTER I

STATUS SUMMARY OF THE RESEARCH

The present semi-annual progress report covers the theoretical and experimental research performed during the period from October 1, 1961 to April 1, 1962, in connection with the study of electromagnetic properties of nonuniform plasmas.

Detailed calculations of the distribution function of the electrons are presented, with the basic assumption of a weakly ionized gas where only electron-neutral particle collisions are taken into account. ~~Following the procedure described in Chapter II,~~ the calculations will be extended to the case of interactions between electrons and ions. The results obtained ~~in Chapter II~~ will be applied first to a one-dimensional problem where a temperature gradient is assumed in the plasma, and the electron diffusion and electric properties of the ionized gas will be computed. ~~Chapter III presents the theoretical macroscopic analysis of the properties of a plasma in the absence of an applied magnetic field.~~ The electric field, induced by nonhomogeneous thermodynamic properties, and the electric conductivity of the plasma are evaluated. The analysis is performed for the case of weakly ionized gas in the imperfect Lorentz gas approximation.

This analysis ~~has been~~ WAS extended to the case of a nonisotropic plasma, which corresponds to an applied magnetic field. The results obtained will be presented in an additional report.

The experimental program has been conducted, with the technique described in the previous progress report, in a nonuniform argon plasma obtained in the shock tube facility. Chapter IV presents the experimental

results of the electron density profile of the ionized argon behind the shock for several initial conditions of the driven section. In the limited range of frequencies which have been used in these experiments, the results show the high resolving power of the technique. In the preliminary part discussed herein, only the case of small absorption of the microwaves has been analyzed.

In connection with the program of computing the electromagnetic properties of the plasma from experimental results, the analysis of the propagation of electromagnetic waves in the nonuniform medium inside the cylindrical wave guide is still in progress. The analysis is carried out assuming that the complex dielectric constant of the medium is unknown, and the propagation equations are solved in terms of measured quantities at the surface of the wave guide. The measured quantities correspond to the signals obtained with the electric and magnetic probes which are located at the surface of the wave guide. Chapter V presents the results obtained assuming that the electromagnetic properties of the plasma are constant in a cross-section of the tube and depend only upon the axial distance from the shock. These results will be applied to the calculation of electromagnetic properties on the basis of the results described in Chapter IV. The analysis will be extended to the case of nonuniform transverse distribution, assuming a suitable model for the radial dependence based on theoretical calculations of the flow field behind the shock.

CHAPTER II

ELECTROMAGNETIC PROPERTIES OF NONUNIFORM PLASMAS FROM MICROSCOPIC CONSIDERATIONS

INTRODUCTION

The main object of our research was to examine, in a microscopic way, some effects in a plasma, due to inhomogeneities, so as to estimate the importance of such effects on the principal electromagnetic properties of the plasma, as, for instance, conductivity. In order to reach such results from our view point, it is necessary to calculate certain distribution functions, directly deducible from Boltzmann's equations. If inhomogeneities are present (due to gradients of concentration, of temperature, etc.), as far as we know, no actually developed method of calculation exists.

For this reason we decided to examine various models beginning with the simplest ones:

1. Plasma assimilated to a weakly ionized Lorentzian gas, considering electrons and neutral molecules and neglecting Coulomb interactions.

2. Three component plasma (electrons, ions, neutral molecules) taking Coulomb interactions into account.

Since the analysis of model 2. has appeared particularly difficult from a general point of view (for the reason that it implies the solution of a system of Boltzmann's equations), first of all we decided to carry out in a detailed way, a method of actual calculation, in order to face the simplest model 1. even if it is not very realistic. In addition, for the scheme 1. we have decided to examine separately the various inhomogeneity effects and also, to keep near

to the model studied from the macroscopic view point, we have selected the detailed examination of the influence of temperature gradient in a slab containing the plasma, whose walls are absorbing and emitting with a Maxwellian distribution.

First, in Section 1., the complete mathematical-physical characteristics (in our opinion not so wholly developed in the literature) of model 1. are described up to the deduction of final equations.

Next, in Section 2., a known analytical method used for solving the equations of Section 1. (series expansion of eigen functions of the collision operator) is described.

1. MATHEMATICAL-PHYSICAL CHARACTERISTICS OF MODEL 1

We consider, as in the Lorentz gas model, a binary mixture of a single kind of neutral molecules and electrons. That is to say, we consider a weakly ionized gas ($n \ll N$) which allows us to neglect (within the limits of an initial research whose aim is to test a methematical method for studying Boltzmann equation for a nonhomogeneous system) the ion effects, provided that their density is of the order of n.

We shall indicate with $f(\underline{x}, \underline{v}, t)$ and $F(\underline{x}, \underline{V}, t)$ respectively the electronic and molecular distribution functions.

In the corresponding system of the two Boltzmann equations :

$$Df = J_{ee}(f) + J_{em}(f)$$

$$DF = J_{mm}(F) + J_{me}(F)$$

we can neglect $J_{ee}(f)$ and $J_{me}(F)$.

Assuming, then, the following system for the temporal behavior of f and F,

$$Df = J_{em}(f) \tag{1.1}$$

$$DF = J_{mm}(F) \tag{1.2}$$

we may note that:

a) From the Equation (1.2) the temporal behavior of the molecules is entirely independent of the presence of electrons, while the electron gas depends upon the presence of molecules, through the collision term J_{em}.

b) The temporal behavior of the electron gas, given by Equation (1.1) is affected by the molecular gas, as we shall see later, only through the

following phenomenological parameters:

molecular density, mean velocity and mean square velocity.

As a result it is not necessary in solving Equation (1.1) to integrate the Boltzmann Equation (1.2):

$$DF = J_{mm}(F)$$

for we only need the knowledge of the above mentioned phenomenological parameters.

We shall begin by expanding the electronic distribution function $f(\underline{x}, \underline{v}, t)$ in spherical harmonics, writing:

$$f(\underline{x}, \underline{v}, t) = \sum_{\substack{e=0 \\ o \le m \le e}}^{\infty} \left[a_{em}(\underline{x}, \underline{v}, t)\, C_{em} + \beta_{em}(\underline{x}, \underline{v}, t)\, S_{em} \right] \tag{1.3}$$

where

$$C_{em} = v^e\, \Theta_{em}(\theta) \cos m\omega$$

$$S_{em} = v^e\, \Theta_{em}(\theta) \sin m\omega$$

$\Theta_{em}(\theta)$ being the associated Legendre functions:

$$\Theta_{em}(\theta) = \sin^m\theta\ P_e^{(m)}(\cos\theta)$$

We may write the expansion (1.3) in the form

$$f(\underline{v}) = f_o(v) + \frac{\underline{v}}{v} \cdot \underline{f}_1(v) + \chi(\underline{v}) \tag{1.4}$$

where f_o represents the isotropic part of the distribution function f, $\underline{f}_1$ is the coefficient of the first anisotropy and χ is simply the remaining part of the expansion.

Introducing (1.3) into the Boltzmann Equation (1.1) we obtain a hierarchy of equations, which is easily obtained provided that we know the resul' of the application of the linear collision operator J over each term of the expansion (1.3).

To this end, we may note that the operator J, in an approximation for which one has simply $\frac{m}{M} = 0$ (perfect Lorentz gas), possesses the following properties, for each isotropic function $a(v)$:

$$\begin{aligned} J_{em}(a) &= 0 \\ J_{em}(aC_{em}) &= -\nu_e aC_{em} \\ J_{em}(aS_{em}) &= -\nu_e aS_{em} \end{aligned} \tag{1.5}$$

In the imperfect Lorentz gas scheme, we shall have:

$$\begin{aligned} J_{em}(a) &= O_1\left(\frac{m}{M}\right) \\ J_{em}(aC_{em}) &= -\nu_e aC_{em}\left[1 + O_2\left(\frac{m}{M}\right)\right] \\ J_{em}(aS_{em}) &= -\nu_e aS_{em}\left[1 + O_3\left(\frac{m}{M}\right)\right] \end{aligned} \tag{1.6}$$

where we have used the Landau symbol $O_1(x)$, meaning a quantity which is simply of the order of x.

The quantity $O_1\left(\frac{m}{M}\right)$ has been calculated by others (2) under the hypothesis of a Maxwellian molecular distribution F, obtaining:

$$J_{em}(a) = \frac{m}{M}\,\frac{1}{v^2}\,\frac{\partial}{\partial v}\left[\nu_1 v^3\left(a + \frac{kT}{mv}\,\frac{\partial a}{\partial v}\right)\right] \tag{1.7}$$

On the other hand, we have proceeded to the evaluation of the quantity $O_1(m/M)$ keeping an entirely arbitrary (and hence generally anisotropic) molecular distribution.

The results of our calculation is given by:

$$J_{em}(a) = \frac{1}{v^2}\frac{\partial}{\partial v}\left\{A(v) + B(v)\frac{\underline{v}}{v}\cdot\overline{\underline{V}} + C(v)\frac{\underline{\underline{v^{\circ}v}}}{v^2} : \overline{\underline{V}\underline{V}}\right\} \tag{1.8}$$

where:

$$A(v) = \frac{m}{M}\,4\nu_1 v^3 a + \nu_1 v^3 \frac{\overline{V^2}}{3}\frac{\partial a}{\partial v}$$

$$B(v) = \nu_1 v^2 a$$

$$C(v) = (\nu_1 - \frac{1}{2}\nu_2)v^2\frac{\partial a}{\partial v} + 3\left[(\nu_1 - \frac{1}{2}\nu_2)v - \frac{1}{6}\frac{\partial \nu_2}{\partial v}v^2\right]a \tag{1.9}$$

We have followed Chapman and Cowling's notation, in writing

$$\underline{\underline{v^{\circ}v}} : \overline{\underline{V}\underline{V}} = \sum_{ij=1}^{3}(v_i v_j - \frac{1}{3}v^2\delta_{ij})\overline{V_j V_i}$$

while ν_1 and ν_2 are the first two relaxation frequencies [1]:

$$\begin{aligned}\nu_1(v) &= 2\pi N v\int_0^{\pi}\sin\theta\left[1 - P_1(\cos\theta)\right]\sigma(\theta, v)\,d\theta\\ \nu_2(v) &= 2\pi N v\int_0^{\pi}\sin\theta\left[1 - P_2(\cos\theta)\right]\sigma(\theta, v)\,d\theta\end{aligned} \tag{1.10}$$

$\sigma(\theta_1\left|\underline{v} - \underline{V}\right|)$ being the differential cross section for electron-molecule collision, in a frame of reference fixed with one of the two particles. The determination of $J_{em}(aC_{em})$, $J_{em}(aS_{em})$ has been done disregarding the O_2, O_3 terms.

A general account of the method followed in the derivation of formula (1.8) is given in Appendix 1.

Taking into accout that f_o is an isotropic function and $\underline{f}_1 \cdot \frac{\underline{v}}{v}$ is simply a linear combination with isotropic coefficients of C_{1o}, C_{11}, S_{11}, we are now able to calculate $J_{em}(f_o)$, $J_{em}(\frac{\underline{v}}{v} \cdot \underline{f}_1)$

If we perform a further approximation(*) forgetting the term $\chi(\underline{v})$ in (1.4), we at last arrive at the following:

$$Df = J_{em}(f) = \frac{1}{v^2} \frac{\partial}{\partial v} \left\{ A(v) + B(v) \frac{\underline{v}}{v} \cdot \underline{V} + C(v) \frac{\underline{v}\,\underline{v}}{v^2} : \overline{\underline{V}\,\underline{V}} \right\} - \nu_1 \frac{\underline{v}}{v} \cdot \underline{f}_1 \tag{1.11}$$

where A(v), B(v) and C(v) are given by (1.9).

The calculation of Df is immediate. Finally, by means of the orthogonality properties of the spherical harmonics functions on the unit sphere, we obtain the following system:

$$\left.\begin{aligned} &\frac{\partial f_o}{\partial t} + \frac{v}{3} \underline{\nabla} \cdot \underline{f}_1 + \frac{e}{3mv^2} \frac{\partial}{\partial v} (v^2 \underline{E} \cdot \underline{f}_1) = \frac{m}{M} \frac{1}{v^2} \frac{\partial}{\partial v} \left[\nu_1 v^3 (f_o + \frac{M \overline{V^2}}{3mv} \frac{\partial f_o}{\partial v}) \right] \\ &\frac{\partial \underline{f}_1}{\partial t} + v \underline{\nabla} f_o + \frac{e}{m} \frac{\partial f_o}{\partial v} \underline{E} + \frac{e}{mc} (\underline{H} \times \underline{f}_1) = \frac{1}{v^2} \frac{\partial}{\partial v} (\nu_1 v^2 f_o) \underline{V} - \nu_1 \underline{f}_1 \end{aligned}\right\} \tag{1.12}$$

in the unknown functions f_o, $\underline{f}_1$.

(*) As usual in this kind of reasoning, we may evaluate "a posteriori" the usefulness of this approximation, by calculating explicitly the difference between the results obtained and those based on the successive approximation, or "a priori" we may introduce some plausible arguments, like those used by Davydov (3) and Gurevitch (4).

APPENDIX 1 - DERIVATION OF EQUATIONS 1.8 AND 1.9

Let us state here some formulas which we shall use later on, directly deducible from the dynamics of elastic (classical) collision between two particles (in our case, electron and molecule).

Let us consider an elastic electron-molecule encounter, with velocity $\underline{v}$, $\underline{V}$ respectively, well before the collision.

Let us put:

$$\underline{g} = \underline{V} - \underline{v}$$

where $\underline{g}$ is the relative velocity of approach of the molecule in a frame of reference fixed with the electron (see Figures 1 and 2 at the end of this Appendix).

ϑ is the scattering angle; from Figure 2 we have at once:

$$\underline{g} - \underline{g}' = 2g \sin \frac{\vartheta}{2} \; \underline{k} = 2 (\underline{g} \cdot \underline{k}) \underline{k}$$

where $\underline{k}$ (apse line unit vector) represents the direction of the external bisectrix of the angle between the asymptotes of the relative molecular trajectory.

We have thus:

$$\underline{V} - \underline{v} = \underline{V}' - \underline{v}' + 2g \sin \frac{\vartheta}{2} \; \underline{k}$$

from which, by momentum-conservation:

$$\underline{V}' - \underline{V} = - \frac{m}{M} \; (\underline{v}' - \underline{v})$$

$$\left.\begin{aligned} \underline{v}' - \underline{v} &= \frac{2}{1 + A} \; (\underline{g} \cdot \underline{k}) \underline{k} \\ \underline{V}' - \underline{V} &= - \frac{2A}{1 + A} \; (\underline{g} \cdot \underline{k}) \underline{k} \end{aligned}\right\} \qquad \text{(A1-1)}$$

having stated $A = \frac{m}{M}$

In the frame of reference sketched in Figure 3, we see that the components of $\underline{k}$ are

$$k_{x'} = -\cos\frac{\theta}{2}\cos\varphi$$

$$k_{y'} = -\cos\frac{\theta}{2}\sin\varphi$$

$$k_{z'} = \sin\frac{\theta}{2}$$

We pass from this frame to the one sketched in Figure 4 through:

$$x = -x'\sin\beta + y'\sin\epsilon\cos\beta + z'\cos\epsilon\cos\beta$$

$$y = x'\cos\beta + y'\sin\epsilon\sin\beta + z'\cos\epsilon\sin\beta$$

$$z = y'\cos\epsilon - z'\sin\epsilon$$

where (see Figure 4):

$$\sin\epsilon = \frac{v}{g} - \frac{V}{g}\cos\alpha$$

$$\cos\epsilon = \frac{V}{g}\sin\alpha$$

So we can calculate the components of $\underline{k}$ in the frame of reference of Figure 4. Using the first of (A1-1) we have the following:

$$\begin{aligned}
v'_x(1+A) &= -\left[(v - V\cos\alpha)\sin\theta\sin\varphi - V(1-\cos\theta)\sin\alpha\right]\cos\beta \\
&\quad + g\sin\theta\sin\beta\cos\varphi \\
v'_y(1+A) &= -\left[(v - V\cos\alpha)\sin\theta\sin\varphi - V(1-\cos\theta)\sin\alpha\right]\sin\beta \\
&\quad - g\sin\theta\cos\beta\cos\varphi \\
v'_z(1+A) &= v(A+\cos\theta) + V\left[(1-\cos\theta)\cos\alpha - \sin\theta\sin\alpha\sin\varphi\right]
\end{aligned} \tag{A1-2}$$

So, squaring and summing:

$$v' = \frac{v}{1+A}\left\{1 + 2A\cos\theta + A^2 + 2B^2(1-\cos\theta) + 2B\left[(A-1)\cos\alpha(1-\cos\theta) - (A+1)\sin\alpha\sin\theta\sin\varphi\right]\right\}^{1/2} \tag{A1-3}$$

where we have put:

$$B = \frac{V}{v}$$

We now treat A and B as infinitesimal quantities and eliminate quantities which contain A^2, A^3 ..., B^3, B^4 ....., AB, ...

(A1-3) becomes :

$$v' = v\left\{1 + A\cos\theta - A + B^2(1-\cos\theta) - B\left[\cos\alpha(1-\cos\theta) + \sin\theta\sin\alpha\sin\varphi\right] - \frac{B^2}{2}\left[\cos\alpha(1-\cos\theta) + \sin\alpha\sin\theta\sin\varphi\right]^2\right\} \tag{A1-4}$$

To the same order:

$$v' - v = v\left\{(B^2 - A)(1-\cos\theta) - B\left[\cos\alpha(1-\cos\theta) + \sin\alpha\sin\theta\sin\varphi\right] - \frac{B^2}{2}\left[\cos\alpha(1-\cos\theta) + \sin\alpha\sin\theta\sin\varphi\right]^2\right\} \tag{A1-5}$$

$$(v'-v)^2 = v^2B^2\left[\cos\alpha(1-\cos\theta) + \sin\alpha\sin\theta\sin\varphi\right]^2 \tag{A1-6}$$

$$g = v\left[1 + B^2 - 2B\cos\alpha\right]^{1/2} = v\left[1 + \frac{B^2}{2}\sin^2\alpha - B\cos\alpha\right] \tag{A1-7}$$

$$\sigma(\theta, g) = \sigma(\theta, v) + v\left[\frac{B^2}{2}\sin^2\alpha - B\cos\alpha\right]\frac{\partial\sigma}{\partial v} + \frac{B^2}{2}v^2\cos^2\alpha\,\frac{\partial^2\sigma}{\partial v^2} \tag{A1-8}$$

$$\sigma(\theta, g)\, g = \sigma(\theta, v)\, v - B\cos\alpha\left(v\frac{\partial\sigma}{\partial v} + \sigma\right) + O(B^2) \tag{A1-9}$$

We must now simply evaluate the behavior of the operator J_{em} over an arbitrary isotropic function $a(v)$, that is the quantity:

$$J_{em}(a) = \int (a'F' - aF)\, g\sigma(\theta, g)\, d\Omega dV \tag{A1-10}$$

The preceeding collision term has been evaluated by noting that in each electron-molecule collision, the variation of the modulus v of the electron velocity is given by:

$$v' - v = O\left[\left(\frac{m}{M}\right)^{1/2}\right] \qquad \text{(A1-11)}$$

(see (A1-5))

As a consequence, the integral operator J_{em} can be put in a differential form, following the same technique used in the transformation of the Boltzmann elastic collision operator into the Fokker-Planck form (references (5) (6))

Let us introduce a suitable, but largely arbitrary isotropic function ϕ (v); according to a general well known rule:(*)

$$\int J_{em}(a)\,\phi(v)\,d\underline{v} = \int \left[\phi(v') - \phi(v)\right] g\, a(v)\, F\sigma(\Omega, g)\, d\Omega d\underline{V}\, d\underline{v} \qquad \text{(A1-12)}$$

Furthermore, retaining only terms of the order of m/M, we have according to (A1-11):

$$\phi(v') - \phi(v) = (v'-v)\frac{\partial \phi}{\partial v} + \frac{1}{2}(v'-v)^2 \frac{\partial^2 \phi}{\partial v^2} \qquad \text{(A1-13)}$$

Inserting (A1-13) into (A1-12) and integrating by parts, we find:

$$J_{em}(a) = \frac{1}{v^2}\frac{\partial}{\partial v}\left[-v^2 \mu(v)\, a(v) + \frac{1}{2}\frac{\partial}{\partial v}\left(v^2 \lambda(v)\, a(v)\right)\right] \qquad \text{(A1-14)}$$

where

$$\mu(v) = \int \sigma(\Omega, g)\, g\, F\, (v'-v)\, d\Omega\, d\underline{V}$$
$$\lambda(v) = \int \sigma(\Omega, g)\, g\, F\, (v'-v)^2\, d\Omega\, d\underline{V} \qquad \text{(A1-15)}$$

(*) See, for instance references (2), (7).

So far as we choose $\phi(v)$ to satisfy the following relations:

$$\left[a\mu\phi v^2\right]_{v=o}^{\infty} = \left[a\lambda \frac{\partial \phi}{\partial v} v^2\right]_{v=o}^{\infty} = \left[\frac{\partial}{\partial v}(v^2 a \lambda)\phi\right]_{v=o}^{\infty} = 0$$

In a way consistent with the approximations used, the two preceding functions $\mu(v)$ and $\lambda(v)$ have to be evaluated to the first order in the quantity m/M.

To the first order, $\sigma(\theta, g)g(v'-v)$ is given by formulae (A1-5) and (A1-9) as follows:

$$\sigma g(v'-v) \cong \sigma(\theta, v)\, v^2 B^2 (1-\cos\theta) - \sigma(\theta, v)\, v^2 A (1-\cos\theta)$$

$$- \sigma v^2 B \cos\alpha (1-\cos\theta) - \sigma v^2 \frac{B^2}{2} \cos^2\alpha (1-\cos\theta)^2$$

$$- \sigma v^2 \frac{B^2}{2} \sin^2\theta \sin^2\alpha \sin^2\omega + B^2 \cos^2\alpha\, v^2 \left(v \frac{\partial \sigma}{\partial v} + \sigma\right)(1-\cos\theta)$$

where quantities containing $\sin\omega$ have been overlooked, because a successive integration is performed over ω, from o to 2π. From the definition (A1-15) of $\mu(v)$ we can obtain it from the preceding relation, by integration over θ and ω and over all the velocity space $\underline{V}$.

Leaving aside the (direct) integration, we have:

$$\mu(v) = \frac{\nu_1}{v} \overline{V}^2 - A\nu_1 v - \nu_1 \overline{V_{//}} - \frac{1}{2}\frac{1}{v}\left[a \overline{V_{//}^2} + \frac{b}{2} \underline{V_{\perp}^2}\right] + \frac{\partial \nu_1}{\partial v} \overline{V_{//}^2} \qquad \text{(A1-16)}$$

where

$$\nu_1 = 2\pi N v \int_o^{\pi} \sin\theta\, (1-\cos\theta)\, \sigma(\theta, v)\, d\theta$$

$$a = 2\pi N v \int_o^{\pi} \sin\theta\, (1-\cos\theta)^2 \sigma(\theta, v)\, d\theta$$

$$b = 2\pi N v \int_o^{\pi} \sin^3\theta\, \sigma(\theta, v)\, d\theta$$

and having stated:

$$\overline{V_{//}} = \frac{1}{N} \int d\underline{V}\ V \cos a\ F$$

$$\overline{V^2_{//}} = \frac{1}{N} \int d\underline{V}\ V^2 \cos^2 a\ F$$

$$\overline{V^2_{\perp}} = \frac{1}{N} \int d\underline{V}\ V^2 \sin^2 a \sin^2 \varphi\ F$$

In the same way, to the first order in m/M, $\sigma(\theta, g)\ g\ (v' - v)^2$ following formulae (A1-6) (A1-9) is given by:

$$\sigma(\theta\text{-}g)\ g(v'\text{-}v)^2 \cong \sigma v\ V^2 \cos^2 a\ (1\text{-}\cos\theta)^2 + \sigma v\ V^2\ \sin^2\theta \sin^2 a \sin^2 \varphi$$

overlooking quantities containing $\sin \varepsilon$.

Following the definition (A1-15) we have therefore:

$$\lambda(v) = a\ \overline{V^2_{//}} + \frac{b}{2}\ \overline{V^2_{\perp}} \qquad \text{(A1-18)}$$

Let us now introduce the quantity:

$$\nu_2 = 2\pi N v \int_0^{\pi} \sin\theta \left[1 - \left(\frac{3}{2} \cos^2\theta - \frac{1}{2}\right)\right] \sigma(\theta, v)\, d\theta \qquad \text{(A1-19)}$$

(A1-18) can be written:

$$\lambda(v) = (2\nu_1 - \nu_2)\ \overline{V^2_{//}} + \frac{1}{3}\ \nu_2\ \overline{V^2}\ , \qquad \text{(A1-20)}$$

with

$$\overline{V^2_{//}} + \overline{V^2_{\perp}} = \overline{V^2}$$

Introducing now (A1-16) and (A1-20) into (A1-14), and leaving aside the direct calculations, we have:

$$J_{em}(a) = \frac{1}{V^2} \frac{\partial}{\partial v} \left\{ A'(v) + B'(v)\ \overline{V_{//}} + C'(v)\ \overline{V^2_{//}} \right\}$$

where:

$$\begin{cases} A(v) = \dfrac{m}{M}\,\nu_1\, v^3 a + v\left(\dfrac{1}{2}\nu_2 - \nu_1\right)\overline{V^2}\, a + \dfrac{1}{6} v^2 \dfrac{\partial \nu^2}{\partial v}\, V^2 a + \dfrac{1}{6}\, v^2 \nu_2 \dfrac{\partial a}{\partial v}\, \overline{V^2} \\ B'(v) = \nu_1\, v^2\, a \\ C'(v) = -3v\left(\dfrac{1}{2}\nu_2 - \nu_1\right) a - \dfrac{1}{2}\, v^2 \dfrac{\partial \nu_2}{\partial v}\, a - v^2\left(\dfrac{1}{2}\nu_2 - \nu_1\right)\dfrac{\partial a}{\partial v} \end{cases}$$

Furthermore, by noting that:

$$\overline{V_{\parallel}} = \frac{\underline{v}}{v} \cdot \overline{\underline{V}}$$

$$\overline{V_{\parallel}^2} = \frac{1}{2}\, \underline{v}\,\underline{v} : \overline{\underline{V}\,\underline{V}}$$

and puting:

$$\underline{v}^{\circ}\,\underline{v} = \underline{v}\,\underline{v} - \frac{1}{3}\, v^2\, \underline{\underline{\delta}}$$

we have at last:

$$J_{em}(a) = \frac{1}{v^2}\,\frac{\partial}{\partial v}\left\{ A(v) + B(v)\,\frac{\underline{v}}{v} \cdot \overline{\underline{V}} + C(v)\,\frac{\underline{\underline{v}^{\circ}\underline{v}}}{v^2} : \overline{\underline{V}\,\underline{V}} \right\} \qquad \text{(A1-21)}$$

where

$$\begin{cases} A(v) = \dfrac{m}{M}\,\nu_1\, v^3 a + \nu_1\, v^3\, \dfrac{\overline{V^2}}{3}\, \dfrac{\partial a}{\partial v} \\ B(v) = \nu_1\, v^2\, a \\ C(v) = \left(\nu_1 - \dfrac{1}{2}\,\nu_2\right) v^2\, \dfrac{\partial a}{\partial v} + 3\left[\left(\nu_1 - \dfrac{1}{2}\,\nu_2\right) v - \dfrac{1}{6}\,\dfrac{\partial \nu_2}{\partial v}\, v^2\right] a \end{cases} \qquad \text{(A1-22)}$$

that is formulae (1.8), (1.9) of Section 1.

(A1-22) can be put in the form:

$$J_{em}(a) = \frac{1}{v^2}\,\frac{\partial A}{\partial v} + \frac{1}{v^2}\,\frac{\partial B}{\partial v}\,\frac{\underline{\underline{v}^{\circ}\underline{v}}}{v^2} : \overline{\underline{V}\,\underline{V}}\,. \qquad \text{(A1-23)}$$

At this point, we are able to calculate the quantity:

$$J_{em}(f)$$

where f is the electronic distribution function:

$$f = f_o(v) + \frac{\underline{v}}{v} \cdot \underline{f_1}(v)$$

Taking account that J_{em} is a linear operator, we have:

$$J_{em}(f) = J_{em}(f_o) - \nu_1 \frac{\underline{v}}{v} \cdot \underline{f_1}$$

by using the Bayet-Delcroix-Denisse approximation (see Reference (1)) . One can evaluate $J_{em}(f_o)$ from (A1-23) by simply substituting a with f_o and arrive at the formula (1.11) of Section 1.

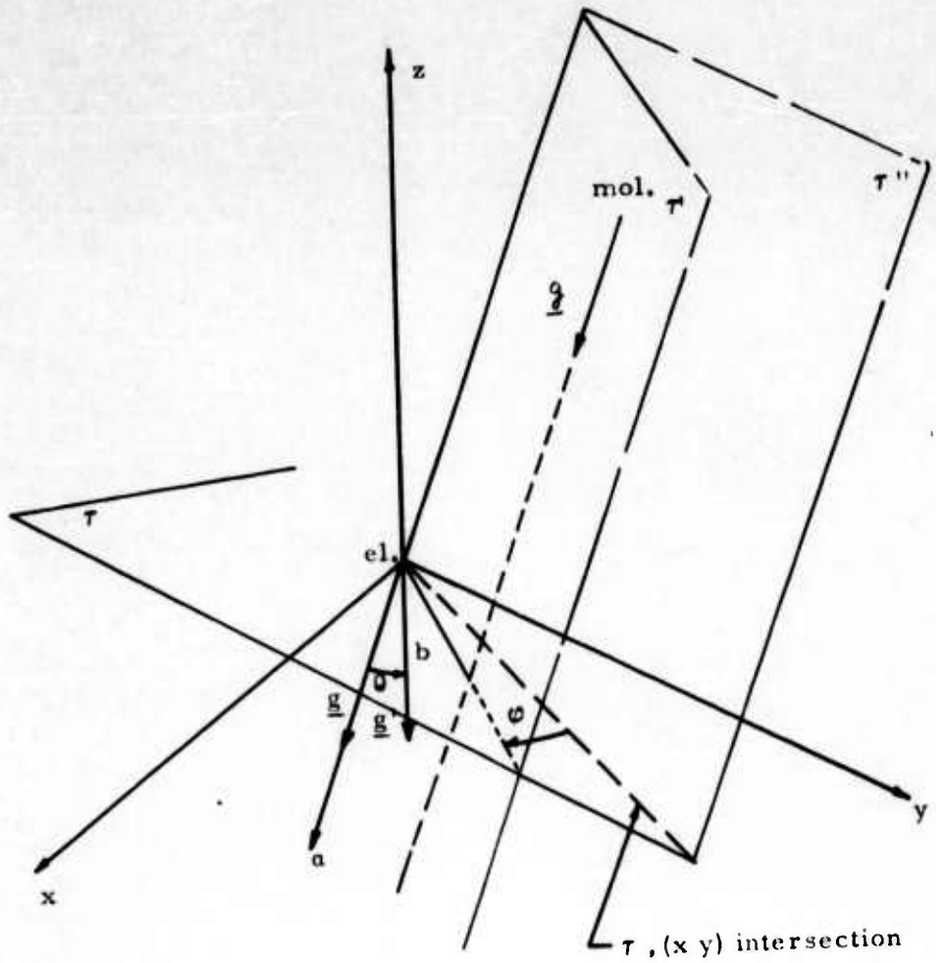

FIGURE 1

τ = plane through the origin, perpendicular to the incoming molecule
τ' = half-plane terminated by the straight line a, over which moves the incoming molecule.
τ'' = reference half-plane
b = inpact parameters
φ = azimuthal angle
θ = scattering angle
$\underline{g}'$ = relative molecular velocity after encounter

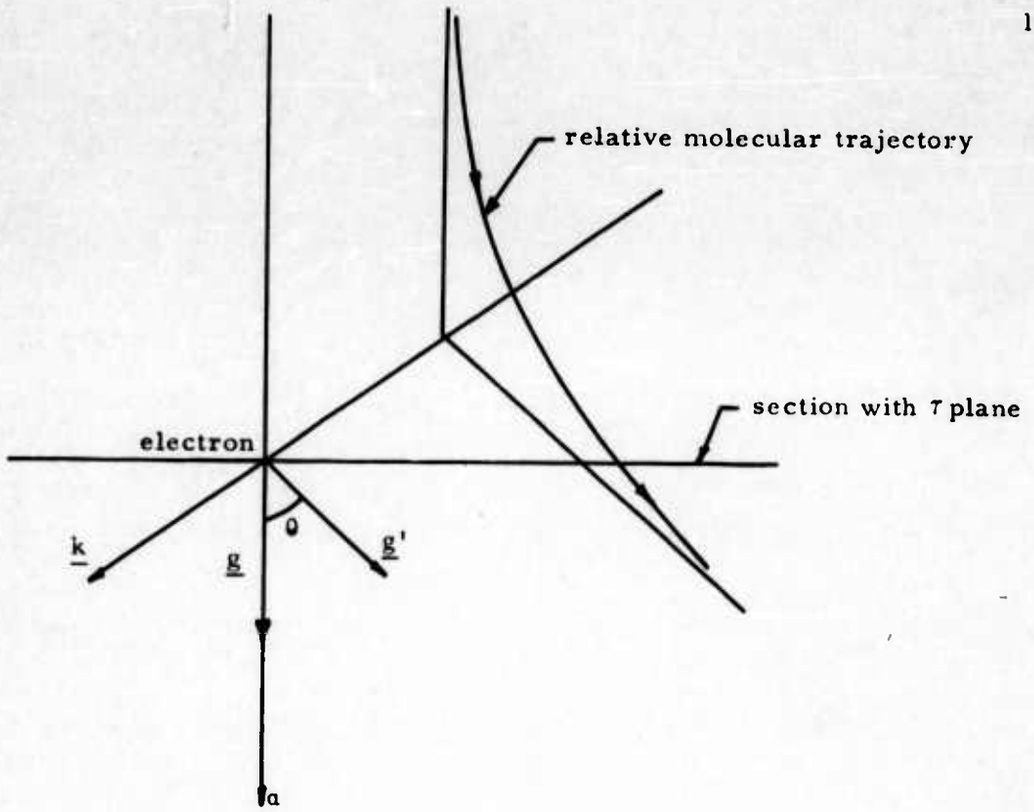

FIGURE 2 (This Figure is intended to be traced on the τ' half-plane of the preceding Figure 1; $\underline{k}$ is the unit vector of the so called "apse" line.)

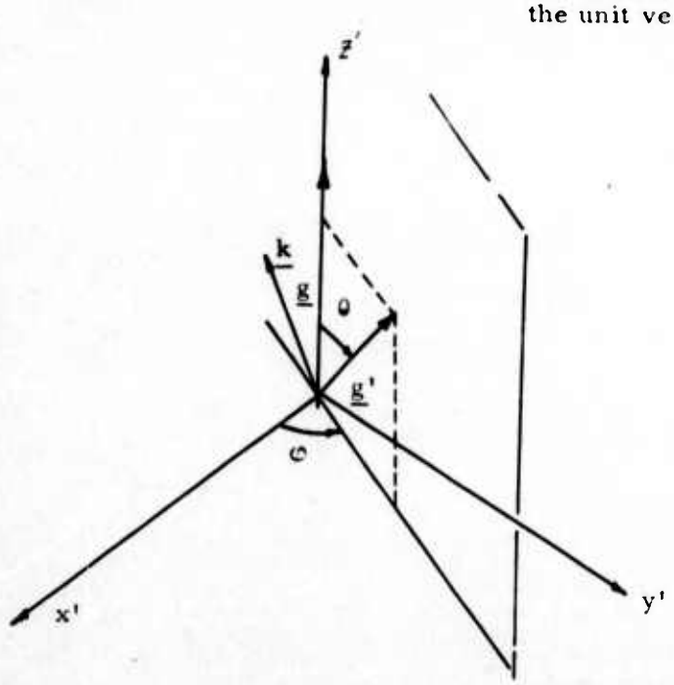

FIGURE 3

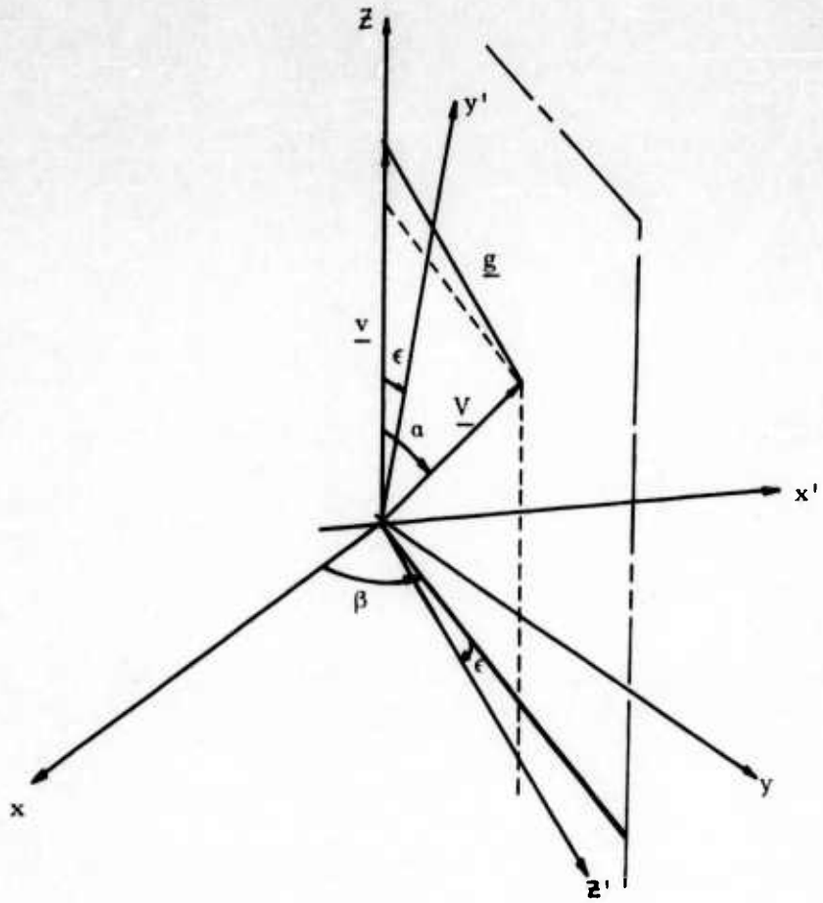

FIGURE 4

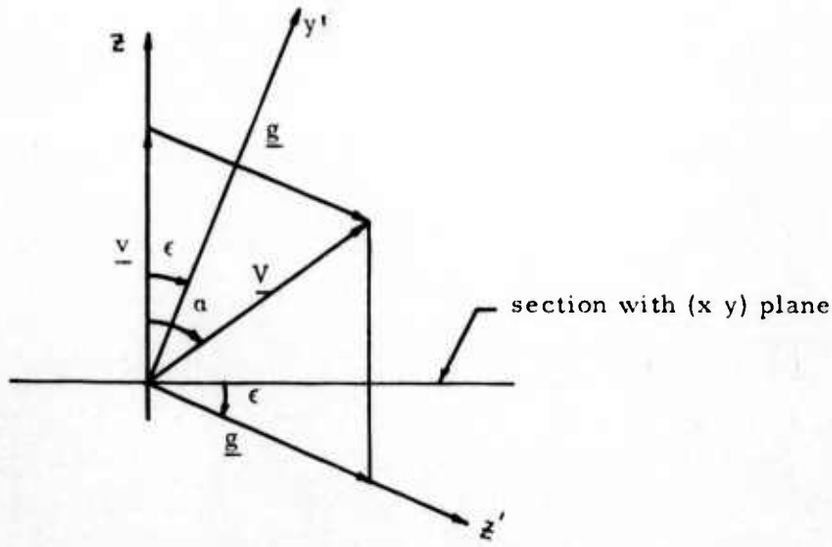

(This part of Figure 4 is traced in (x'y') plane)

2. ANALYTICAL METHOD FOR SOLVING EQUATIONS

We now approach the study of the system (1.12) limiting ouselves to the stationary state when there is no magnetic field.

It is thus possible to express $\underline{f}_1(\underline{x}, v)$ as a function of $f_o(\underline{x}, v)$ and to reduce the system to only one differential equation in $f_o(\underline{x}, v)$

$$\frac{v}{3}\underline{\nabla}\cdot\left\{-\frac{v}{\nu}\underline{\nabla} f_o - \frac{e}{m\nu}\frac{\partial f_o}{\partial v}\underline{E} + \frac{1}{v^2\nu}\frac{\partial}{\partial v}(\nu_1 v^2 f_o)\overline{\underline{V}}\right\} + \frac{e}{3mv^2}\frac{\partial}{\partial v}(v^2\underline{E}\cdot\underline{f}_1) = \frac{m}{M}\frac{1}{v^2}\frac{\partial}{\partial v}\left[\nu_1 v^3\left(f_o + \frac{M\overline{V^2}}{3mv}\frac{\partial f_o}{\partial v}\right)\right] \tag{2.1}$$

Then we studied this elliptic partial differential equation in the variables $\underline{x}$ and v.

As we said before, the presence of the molecular gas appears only through the mean molecular velocity $\overline{\underline{V}}$, $\overline{V^2}$ and the molecular concentration N.

We developed $f_o(\underline{x}, v)$ in a series expansion of eigenfunctions of the operator $J = \frac{m}{M}\frac{1}{v^2}\frac{\partial}{\partial v}\left[\nu_1 v^3\left(f_o + \frac{M\overline{V}^2}{3mv}\frac{\partial f_o}{\partial v}\right)\right]$. In doing so it was necessary to specify the type of electron-molecule interaction we were considering.

We have considered two cases corresponding to central interaction of the Maxwellian type and the rigid spheres type (see Appendix 2).

In the first case the eigenfunctions of J are:

$$\left\{e^{-\frac{mv^2}{2kT}} L_n^{(1/2)}\left(\frac{mv^2}{2kT}\right)\right\} \equiv \left\{e^{-\epsilon} L_n^{(1/2)}(\epsilon)\right\} \tag{2.2}$$

(where $\epsilon = \frac{mv^2}{2kT}$ is the non-dimensional electron kinetic energy); in the second case they are:

$$\left\{ e^{-\frac{mv^2}{2kT}} L_n^{(1)}\left(\frac{mv^2}{2kT}\right) \right\} \equiv \left\{ e^{-\epsilon} L_n^{(1)}(\epsilon) \right\} \tag{2.3}$$

Thus we have:

a) For Maxwellian interaction:

$$f_o = \sum_{n=0}^{\infty} a_n(\underline{x})\, e^{-\epsilon} L_n^{(1/2)}(\epsilon) \tag{2.4}$$

b) For rigid spheres interaction:

$$f_o = \sum_{n=0}^{\infty} a_n(\underline{x})\, e^{-\epsilon} L_n^{(1)}(\epsilon) \tag{2.5}$$

Using the orthogonality properties of the $L_n^{(k)}$ polynomials, we arrive at two systems of infinite differential equations in $a_n(\underline{x})$ and $a_n(\underline{x})$ which, if the electric field is neglected and $\underline{V} = 0$, takes the form:

case of elastic - spheres interactions: (2.6)

$$\mathcal{L}(a_n(\underline{x})) + (n+2)\mathcal{B}(a_n(\underline{x})) + (n+2)(n+3)\mathcal{C}(a_n(\underline{x})) -$$

$$- n\mathcal{B}(a_{n-1}(\underline{x})) - 2n(n+2)\mathcal{C}(a_{n-1}(\underline{x})) + n(n-1)\mathcal{C}(a_{n-2}(\underline{x})) =$$

$$= 3\nu_o^2 N^2 \frac{2m}{M} n a_n(\underline{x})$$

$(n = 0, 1, 2, \ldots)$

Case of Maxwellian interaction: (2.7)

$$\left\{ - n(n-1)(n-2)\mathcal{C}(a_{n-3}(\underline{x})) + \left[n(n-1)\mathcal{B}(a_{n-2}(\underline{x}) + n(n-1)(4n+\frac{5}{2})\mathcal{C}(a_{n-2}(\underline{x})) \right] - \right.$$

$$- \left[n\mathcal{L}(a_{n-1}) + n(3n+2)\mathcal{B}(a_{n-1}) + n(n+\frac{3}{2})(6n+\frac{9}{2})\mathcal{C}(a_{n-1}) \right] +$$

$$+ \left[(2n+\frac{3}{2})\mathcal{L}(a_n) + (n+\frac{3}{2})(3n+\frac{5}{2})\mathcal{B}(a_n) + (n+\frac{3}{2})(n+\frac{5}{2})(4n+\frac{7}{2})\mathcal{C}(a_n) \right] -$$

$$\left. - \left[(n+\frac{3}{2})\mathcal{L}(a_{n+1}) + (n+\frac{3}{2})(n+\frac{5}{2})\mathcal{B}(a_{n+1}) + (n+\frac{3}{2})(n+\frac{5}{2})(n+\frac{7}{2})\mathcal{C}(a_{n+1}) \right] \right\} =$$

$$= \frac{3m^2\nu_o^2 N^2}{MkT} \, n\, a_n(\underline{x}) \qquad (n = 0, 1, 2, \ldots)$$

where :

$$\begin{cases} \mathcal{L} \equiv \nabla^2 - \nabla \log N \cdot \underline{\nabla} \\ \mathcal{B} \equiv 2\underline{\nabla} \log T \cdot \underline{\nabla} + \nabla^2 \log T - (\underline{\nabla} \log T)^2 - \underline{\nabla} \log N \cdot \underline{\nabla} \log T \\ \mathcal{C} \equiv (\underline{\nabla} \log T)^2 \end{cases}$$

In the Maxwellian interaction case we have **also evaluated** the contribution due, separately, to the presence of both an electric field and of a mean molecular velocity.

APPENDIX 2 - EIGENFUNCTIONS AND EIGENVALUES OF THE COLLISION OPERATOR J

a) Maxwellian interaction (*)

$$J_M(\varphi) = \frac{6m\nu_o^2}{M} \epsilon^{1/2} \frac{d}{d\epsilon} \left[\epsilon^{3/2} \left(\varphi + \frac{d\varphi}{d\epsilon} \right) \right] \qquad (A2\text{-}1)$$

We consider the following eigenvalue problem:

$$J_M(\varphi) = -\lambda \varphi \qquad (A2\text{-}2)$$

or

$$2\epsilon \frac{d^2\varphi}{d\epsilon^2} + (2\epsilon + 3) \frac{d\varphi}{d\epsilon} + \left(3 + \frac{M\lambda}{3m\nu_o^2}\right) \varphi = 0 \qquad (A2\text{-}3)$$

Introducing the new function

$$\psi(\epsilon) = e^{+\epsilon} \varphi(\epsilon)$$

(A2-3) becomes:

$$\epsilon \frac{d^2\psi}{d\epsilon^2} + \left(\frac{3}{2} - \epsilon\right) \frac{d\psi}{d\epsilon} + \frac{M\lambda}{6m\nu_o^2} \psi = 0 \qquad (A2\text{-}4)$$

Imposing on $\psi(\epsilon)$, as boundary conditions in ϵ-space, analyticity in $\epsilon = 0$ and polynomial behavior for $\epsilon \to \infty$, the solutions of (A2-4) are the Laguerre's generalized polynomials of order 1/2:

$$L_n^{(1/2)}(\epsilon) = \sum_{\nu=0}^{n} (-1)^{\nu} \binom{n+1/2}{n-\nu} \frac{\epsilon^{\nu}}{\nu!}$$

(*) The maxwellian electron-molecule interaction model corresponds to a repulsive force varying as the inverse fifth power of their distance apart. In this case the collision frequency does not depend on the electron velocity: $\nu = \nu_o N$.

corresponding to the eigenvalues

$$\lambda_n = \frac{6m\nu_o^2}{M} n \qquad (n=0, 1, 2\ldots) \tag{A2-5}$$

b) Rigid sphere interaction (*)

$$J_R(\varphi) \frac{6m\nu_o^2}{M} \epsilon^{-1} \frac{d}{d\epsilon} \left[\epsilon^2 \left(\varphi + \frac{d\varphi}{d\epsilon} \right) \right] \tag{A2-6}$$

We consider the following eigenvalue problem

$$J_R(\varphi) = -\lambda\varphi$$

or

$$\epsilon^2 \frac{d^2\varphi}{d\epsilon^2} + (2+\epsilon) \frac{d\varphi}{d\epsilon} + \left(2 + \frac{M\lambda}{6m\nu_o^2}\right)\varphi = 0 \tag{A2-8}$$

Introducing the new function

$$\psi(\epsilon) = e^{\epsilon}\varphi(\epsilon)$$

(A2-8) becomes:

$$\epsilon \frac{d^2\psi}{d\epsilon^2} + (2-\epsilon) \frac{d\psi}{d\epsilon} + \frac{M\lambda}{6m\nu_o^2} \psi = 0 \tag{A2-9}$$

Imposing on $\psi(\epsilon)$ the same boundary conditions in ϵ-space as in the Maxwellian case, the solutions of (A2-9) are the Laguerre's generalized polynomials of order 1, $\left[L_n^{(1)}(\epsilon) \right]$ corresponding to the eigenvalues

$$\lambda_n = \frac{6m\nu_o^2}{M} n \qquad (n = 0, 1, 2, \ldots) \tag{A2-10}$$

(*) In this model we suppose electrons and molecules are rigid spheres. In this case the collision frequency depends linearly on the electron velocity $\nu = \nu_o N v$.

SYMBOLS

c	light velocity in vacuum
k	Boltzmann constant
m	electron mass
e	electron charge
r	electron (classical) radius
n	electron density
$\underline{v}$	electron velocity (modulus v)
M	molecular mass
R	molecular radius
$\underline{V}$	molecular velocity (modulus $\underline{V}$)
N	molecular concentration
T	molecular Temperature
$\overline{\underline{V}}$	mean molecular velocity
$\overline{V}^2$	mean square molecular velocity
$\underline{E}$	electric field
$\underline{H}$	magnetic field
D	differential Boltzmann operator

$$D \equiv \frac{\partial}{\partial t} + \underline{v} \cdot \underline{\nabla} + \underline{x} \cdot \underline{\nabla}_{\underline{v}}$$

J	integral Boltzmann operator

$\nu = \nu_o N v = \pi (R+r)^2 N v$ collision frequency for rigid spheres interactions

$\nu = \nu'_o N$ = collision frequency for Maxwellian interaction

$A = \frac{dT}{dx}$ constant temperature gradient.

τ^{-1} = knudsen number

REFERENCES

1. Bayet - Delcroix - Denisse - J. Phys. Rad. 15 795 (1954)
2. Chapman - Cowling - "The Mathematical Theory of Non-Uniform Gases", Cambridge (1953).
3. Davydov - Phys. Zeisch. Der Sow. 12 269 (1937)
4. Gurevitch, A.V., Jetp - 3 895 (1957)
5. Uhlenbech - Wang , Rev. Mod. Phys. 17 323 (1945)
6. Allis - Hand.der Phys. (Springer) 21
7. H. Grad , Hand.der Phys. (Springer) 12 also: "Kinetic Theory and Statistical Mechanics"- Lectures at the N.Y. Univ. (1950)

CHAPTER III

STUDY OF ELECTROMAGNETIC PROPERTIES OF NONUNIFORM PLASMAS IN THERMAL EQUILIBRIUM, ISOTROPIC CASE

INTRODUCTION

In this chapter results of the study of the electromagnetic properties of a nonuniform, macroscopically neutral plasma are reported.

The line of approach is a macroscopic one, based on the thermodynamics of irreversible processes.

A three fluid model is assumed; the plasma is considered to be at rest in a suitable reference frame, the components are in mutual thermal equilibrium and imposed magnetic fields are absent. The nonuniformities are those connected with the presence of gradients of state parameters such as temperature, density and concentrations.

The presence of these gradients induces an electric field (i.e.f.) in the medium, even in the absence of external electric fields. It will be shown that, in the stationary state and in conditions of macroscopic neutrality, the induced e.f. depends only on one independent gradient which, for convenience, is taken to be that of temperature. An expression for the i.e.f. is derived, which is valid for a most general medium and which is later simplified to the case of an imperfect Lorentz gas (i.e., weakly ionized plasma for which the mass ratio between the negative charge and neutral molecules is much smaller than one).

The electrical conductivity σ defined as the ratio between the electric current I and the electric potential gradient in a first-order stationary state

in which a given nonuniform distribution of $\nabla\phi$ is maintained on the boundaries of a system is also determined.

The phenomenological coefficients are first expressed in terms of thermodynamic properties of the plasma. It is shown how these coefficients can be expressed in terms of only simple binary molecular diffusion coefficients and thermal diffusion coefficients pertinent to the plasma constituents.

This last step makes it possible, by utilizing the available experimental and/or theoretical data on electron-ion, electron-molecule, and ion-molecule collisions, to express the phenomenological coefficients in terms of the local thermodynamic state of the medium.

These results provide the necessary preliminary information needed to proceed to the actual solutions of fluid dynamic and/or electromagnetic phenomena in a nonuniform plasma. In addition, they already lend themselves to interesting order of magnitude analysis on the effects induced by the nonuniformities. They can be used, for instance, to define ranges within which these inhomogeneties can be neglected and the medium treated as homogeneous, and to lend theoretical substantiation to experimental findings. During the last two years, for instance, some experiments were made by S. Klein at Saclay (France) on the direct conversion of thermal energy into electrical energy (Reference 13).

The experiments were performed with a glass ball in which two metallic electrodes were immersed in an ionized mercury gas at rest. The electrodes were kept at two different temperatures and the ionization was obtained through an H.F. source. As a consequence of the temperature gradient an induced electric field was detected and measured as a potential drop between the two

electrodes. It was possible to observe that the i.e.f. increased with the temperature difference and the degree of ionization. These results qualitatively agree with the theoretical conclusions which are arrived at in the present report.

The steps of the analysis herein reported are as follows: In Section 1., Part 1., the irreversible thermodynamic description of the system is performed. The extensive and intensive state parameters and the pertinent mass and energy fluxes for a mixture of three fluids, one with negative and one with positive charges, are defined. The dynamic relations between fluxes and generalized forces are established and, through suitable use of the basic theorems of the thermodynamics of irreversible processes, the general expression for the mass fluxes in terms of electron concentration, temperature, and electric potential gradients is arrived at.

In Section 1., Parts 2. and 4., the general expressions for the i.e.f. and the electrical conductivity are obtained.

In Section 1., Part 3., the problem of relating these phenomenological coefficients to binary transport coefficients is considered. By suitable transformation of fluxes and affinities it is shown how they can be expressed in terms of three binary diffusion coefficients D_{12}, D_{23}, D_{13} and two thermal diffusion coefficients D_1^T, D_2^T, which refer to the plasma constituents.

In Section 2, Part 1., the evaluation of the molecular and thermal diffusion coefficients for a plasma is carried out and in Part 2. an analysis of the order of magnitude for the transport coefficients is performed for the case of a weakly ionized imperfect Lorentz's gas.

Section 3. deals with an actual determination of the order of magnitude of the phenomenological coefficients, with discussions of their properties and with their actual evaluation for indicative cases.

SECTION 1

1.1. IRREVERSIBLE THERMODYNAMIC DESCRIPTION OF THE MEDIUM

We consider a plasma formed by electrons (subscript 1) ions (2) and neutral molecules (3) in mutual thermal equilibrium (i.e., $T_1 = T_2 = T_3 = T$). It is further assumed that the plasma is at rest in a suitable reference frame and that no imposed magnetic field is present.

It is of basic importance, for a clear understanding of the physics of the phenomena being studied, to proceed to a rigorous irreversible thermodynamic description of the system. This procedure will also help, on one hand, to point out the number and types of simplifying assumptions which will be made and, on the other hand, to have a clear overall picture of the kind of results that can be obtained with this approach.

The fundamental extensive thermodynamics variables X_k for the subject system are: the internal energy U, the volume V, the masses M_1, M_2, and M_3 of the three species and the total electric positive and negative charges E_1 and E_2 present in the volume V. The fundamental relation $S = S(X_k)$ (see Reference 23) can then be written as:

$$TS = U + pV - \sum_{i=1}^{3} g_i M_i - \sum_{i=1}^{2} f_i E_i \qquad (1)$$

where S is the total entropy; T the temperature, p the pressure of the mixture. The quantities g_i and f_i are, respectively, energies per unit mass and energies per unit electric charge and are thermodynamically defined in terms of the partial derivatives of S with respect to the corresponding extensive variable.

We make the following fundamental hypotheses:

$$E_i = e_i M_i$$

$$g_i(X_k) = \mu_i(U, V, M_i)$$

$$f_i(X_k) = \phi$$

That is:

The total electric charges are proportional to the total masses M_1 and M_2. This implies, among other things, that there is only one type of negative and positive charge carrier.

The quantities g_i coincide with the chemical potential μ_i pertinent to the mixture considered in the absence of electric charges ($e_i = 0$).

The quantities f_i are independent of the extensive variables X_k and thus coincide with the electric potential ϕ.

It can be shown that these two latter hypotheses are equivalent to the hypothesis of separability of the energy* U, in the sense that the total energy of the system is simply the sum of the "mechanical energy" of the noncharged system for given S, V, M_i ($e_i = 0$) plus the "electrical energy" $(e_1 M_1 + e_2 M_2)\phi$. This hypothesis is certainly valid in the subject case (cfr. Reference 19).

Equation (1) can then be written as:

$$S = \frac{U}{T} + \frac{p}{T} V - \sum_{i=1}^{3} \frac{\bar{\mu}_i}{T} M_i \qquad (2)$$

where $\bar{\mu}_i$ is the electromechanical potential defined as:

$$\bar{\mu}_i = \mu_i + e_i \phi \qquad (3)$$

and, obviously, $\bar{\mu}_3 = \mu_3$.

---

* A rigorous statement would involve the concept of free energies (cfr. Ref. 19). It can be shown, however, that if the "free energy" is separable, so is the internal energy.

If J_u and J_i ($i = 1, 2, 3$) are the energy and mass fluxes, respectively, using the basic assumption of the thermodynamics of irreversible processes one writes:

$$
\begin{aligned}
J_u &= L_{00}\nabla\left(\frac{1}{T}\right) + L_{01}\nabla\left(-\frac{\bar{\mu}_1}{T}\right) + L_{02}\nabla\left(-\frac{\bar{\mu}_2}{T}\right) + L_{03}\nabla\left(-\frac{\mu_3}{T}\right) \\
J_1 &= L_{10}\nabla\left(\frac{1}{T}\right) + L_{11}\nabla\left(-\frac{\bar{\mu}_1}{T}\right) + L_{12}\nabla\left(-\frac{\bar{\mu}_2}{T}\right) + L_{13}\nabla\left(-\frac{\mu_3}{T}\right) \qquad (4) \\
J_2 &= L_{20}\nabla\left(\frac{1}{T}\right) + L_{21}\nabla\left(-\frac{\bar{\mu}_1}{T}\right) + L_{22}\nabla\left(-\frac{\bar{\mu}_2}{T}\right) + L_{23}\nabla\left(-\frac{\mu_3}{T}\right)
\end{aligned}
$$

The last relation follows from the mass conservation. The quantities L_{ij} are the phenomenological (or kinetic) coefficients which, in the subject case of absence of imposed magnetic field, are scalar quantities. The Onsager's reciprocity relation $L_{ij} = L_{ji}$ holds. The gradients of the intensive variables appearing in equations (4) are the generalized forces, or affinities.

Different alternative forms, each suitable for a number of specific uses, can be given to the system (4) by performing suitable linear transformations of the affinities and/or the fluxes, according to a well defined set of rules. If A_i indicates the direct affinity for the flux J_i and if a prime indicates the transformed quantities, then the following relations hold: (Ref. 23)

$$
\begin{aligned}
A_i' &= \sum_{k=1}^{3} \beta_{ik} A_k \\
J_i' &= \sum_{k=1}^{3} \beta_{ik}^{-1} J_k \qquad (5) \\
L_{im}' &= L_{mi}' = \sum_{j,k} \beta_{ik}^{-1} L_{ik} \beta_{mj}^{-1}
\end{aligned}
$$

where β_{ik}^{-1} is the reciprocal of the element β_{ik} in the square matrix $|\beta_{ik}|$ which defines the linear transformation of the affinities.

We shall make use of few such transformations during the development of the analysis. A particular transformation is however very instructive for an introductive survey of the nature and types of results which we will get.

We notice first of all, that the local thermodynamic state of the mixture, in the subject case of thermal equilibrium among the constituents, is characterized, as follows from eq. (2) when accounting for the presence of the electric potential ϕ, by five independent variables. Going from one set of variables to another is accomplished through the "state equations" of the mixture. It proves convenient to assume the following set of parameters ϕ, T, p, c_i (i= 1, 2), where the c_i's are the mass concentrations of the charged components, as the basic set of independent thermodynamic variables.

The gradients of these variables are not all independent since there are a number of conservation equations to be satisfied and there is, in addition, the requirement of macroscopic neutrality. The latter amounts to the relation

$$e_1 \nabla c_1 + e_2 \nabla c_2 = 0 \qquad (6)$$

between the two concentration gradients, while the momentum conservation requires, under the subject assumptions of macroscopic neutrality and absence of mass motion, that the gradient of p vanish identically throughout the field.

One is thus left with only three independent gradients: say ∇T, $\nabla \phi$ and ∇c_1 .

It is most profitable and instructive to assume as new generalized forces these three independent gradients and express, accordingly, the dynamic equations (eqs. 4) in terms of these forces. This can be done by expressing, through the pertinent state equations, the gradients appearing in eqs. (4) as linear combinations of $\nabla T, \nabla\phi, \nabla c_1$ and then applying eqs. (5).

As a result, the dynamical equations will read:

$$\begin{aligned} J_0' &= L_{00}' \nabla T + L_{01}' \nabla c_1 + L_{02}' \nabla\phi \\ J_1' &= L_{10}' \nabla T + L_{11}' \nabla c_1 + L_{12}' \nabla\phi \\ J_2' &= L_{20}' \nabla T + L_{21}' \nabla c_1 + L_{22}' \nabla\phi \end{aligned} \tag{7}$$

$$\begin{aligned} A_0' &= \nabla T \\ A_1' &= \nabla c_1 \\ A_2' &= \nabla\phi \end{aligned} \tag{8}$$

and the new fluxes J_i' will be given by:

$$\begin{aligned} J_0' &= \frac{1}{T}\left[J_S - (s_1 J_1 + s_2 J_2 + s_3 J_3)\right] = \frac{J_S^c}{T} \\ J_1' &= \frac{1}{T}\left\{\left[\frac{\partial(\mu_1 - \mu_3)}{\partial c_1} - \frac{e_1}{e_2}\frac{\partial(\mu_1 - \mu_3)}{\partial c_2}\right] J_1 + \right. \\ &\quad \left. + \left[\frac{\partial(\mu_2 - \mu_3)}{\partial c_1} - \frac{e_1}{e_2}\frac{\partial(\mu_2 - \mu_3)}{\partial c_2}\right] J_2\right\} \\ J_2' &= \frac{1}{T}\left[e_1 J_1 + e_2 J_2\right] = \frac{I}{T} \end{aligned} \tag{9}$$

where s_i's are the specific entropies of the constituents, and J_s is the total entropy flux:

$$J_s = \frac{Ju}{T} - \frac{\bar{\mu}_1 J_1}{T} - \frac{\bar{\mu}_2 J_2}{T} - \frac{\mu_3 J_3}{T} \tag{10}$$

The quantity J_o' can be thought of as the "conduction" flux of entropy. The flux TJ_2' has the clear physical meaning of the electric current. No direct physical interpretation can be given to the flux J_1' which is a particular linear combination of the mass fluxes J_1 and J_2. The thermodynamic derivate appearing in eq. (9) are computed holding T and p constant.

The L_{ij}''s are the new phenomenological coefficients in the present context; there is no need for expressing L_{ij}' in terms of the original ones L_{ij}.

The system of eqs. (9), containing the three truly independent gradients $\nabla\phi$, ∇T, ∇c_1, is in the appropriate form for the proper application of the theorems of the thermodynamics of irreversible processes.

Suppose we maintain, from outside, a constant temperature gradient on the boundaries of the system.

Eventually a steady state will be reached, referred to as a stationary states of first order, in which the direct flux J_o' is the only flux different from zero. System (9) will then contain only four "unknowns" (the aforementioned gradients plus J_o') so that three of them can be expressed as function of the gradient of temperature. One thus obtains relations of the type:

$$\begin{aligned} \nabla\phi &= a(s)\ \nabla T \\ \nabla c_1 &= \omega_1(s)\ \nabla T \\ J_o' = \frac{J_s^c}{T} &= \omega_2(s)\ \nabla T \end{aligned} \tag{11}$$

where the symbol (s) stands for "function of the local thermodynamic state of the fluid".

The first relation gives the electric field induced by the non-uniformity (under the restraint of constant gradient on the boundary). The phenomenological coefficient $a(s)$ is thus one of the required "electromagnetic properties" of the medium. The second relation gives the gradient of concentration induced by the temperature gradient in the presence of the induced electric field. The last equation relates the temperature gradient to the energy flux into the system (notice that $J_2' = J_1' = 0$ implies absence of any mass flux throughout the system). When computed at the boundaries, it can be interpreted, in the light of an overall energy balance, as the energy to be supplied from the "ambient" to mantain the induced electric field (or, what amounts to the same, the induced concentration gradients).

Equations (9), as they stand, can be used for order of magntitude analyses of the effects of the non-uniformity herein considered, their degree of accuracy depending, apart from the approximations involved in expliciting the phenomenological coefficients, on the overall dimensions of the system. Obviously, the thermodynamic state of the medium will be a function of the point so that, for instance, the first of eqs. (11) should be written as:

$$\nabla \phi (r) = a \left[s(r) \right] \nabla T(r) \tag{12}$$

where r is a space coordinate. Thus the "complete" solution of the problem calls for the determination of the state parameters throughout the medium (in order to answer, for instance , the question of what is the value of ∇T

throughout the system when a given non-uniform temperature distribution is maintained on its boundaries). This is, obviously, a much more complex matter which must be handled by solving the energy and mass equations $\nabla \cdot J_o = \nabla \cdot J_i = 0$ subject to suitable conditions on the boundaries of the medium.

However, order of magnitude analyses can always be carried out by taking suitable "average" values of the state parameters.

Since, in this case $J_2' = J_1' = 0$ implies also $J_1 = J_2 = 0$, this type of information can also be obtained directly from the system (4) by setting in it $J_1 = J_2 = 0$. This simpler procedure will indeed be followed in the next part.

Consider now the other case in which a given non-uniform distribution of electric potential ϕ is maintained on the boundaries. As before, the principle of stationary states implies that the only flux different from zero is the direct flux J_2' that is the electrical current I. Notice that neither the energy flux nor the mass flux is singularly equal to zero: what vanishes is rather two linear combinations of them, as expressed in terms of J_o' and J_2'. This clearly shows why the principle of stationary states could have not been applied to the dynamical equations in the form given by equations (4). System (9) contains once again only four unknowns so that it can be solved to obtain the following relations:

$$\begin{aligned} I &= \sigma(s)\, \nabla\phi \\ \nabla T &= \omega_3(s)\, \nabla\phi \\ \nabla c_1 &= \omega_4(s)\, \nabla\phi \end{aligned} \qquad (13)$$

The first equation is of foremost interest for the present analysis. It yields the steady state "electrical conductivity" of the non-uniform medium subject to the conditions of a given distribution of electrical potential on its boundaries. In the preceeding case an energy exchange between the medium and its surroundings was necessary to maintain, in the stationary case, the induced electric field. Now an exchange of electric charges between the medium and its surroundings is necessary, its amount being determined by eq. (13) evaluated along the boundaries of the region. Once again, complete quantitative solution of the problem calls for the solution of the mass and energy conservation equations to determine the actual distribution of the state parameters throughout the system considered.

This is the type of information which can be obtained from the present analysis. The remainder of the body of the chapter is devoted to obtaining explicit expressions for the coefficients $\alpha(s)$ and $\sigma(s)$.

2 - Determination of the coefficient α.

From the last section it follows that to determine α one must consider the stationary state for which a given nonuniform temperature distribution is kept constant on the boundaries of a system and the mass fluxes J_1 and J_2 vanish throughout.

It here proves convenient to adopt the following form of the dynamical equations:

$$J_u = \sum_{i=1}^{2} Q_i \; J_i + (L_{\infty} - \sum_{j=1}^{2} L_{jo} Q_j) A_u$$

$$J_i = \sum_{k=1}^{2} L_{ik} \; (A_k - A_3 + Q_k A_u) \qquad (14)$$

where the affinities A_i are now defined as:

$$A_u = - \frac{1}{T} \nabla T$$

$$A_1 = - e_1 \nabla \phi - T \nabla \left(\frac{\mu_1}{T}\right)$$

$$A_2 = - e_2 \nabla \phi - T \nabla \left(\frac{\mu_2}{T}\right) \qquad (15)$$

$$A_3 = - T \nabla \left(\frac{\mu_3}{T}\right)$$

and where the quantities $Q_i (i = 1, 2)$ are the heats of transfer (Ref. 19) defined in terms of the coefficients L_{ij} appearing in eq. (4), as:

$$Q_1 = \frac{L_{10} L_{20} - L_{12} L_{20}}{L_{11} L_{22} - L_{12}^2}$$

$$Q_2 = \frac{L_{11} L_{20} - L_{10} L_{21}}{L_{11} L_{22} - L_{12}^2} \qquad (16)$$

Expressing the gradients of μ_i in terms of the independent gradients ∇T, $\nabla \phi$, ∇e_1, and proceeding as indicated in the last section it can be shown that the coefficient a has the following expression:

$$a = \frac{q_1 \left(b_2/e_2 - a_2/e_1\right) + q_2 \left(a_1/e_1 - b_1/e_1\right)}{e_1 e_2 \left(\frac{a_2 + b_1}{e_1 e_2} - \frac{b_2}{e_2^2} - \frac{a_1}{e_1^2}\right)} \qquad (17)$$

with:

$$a_i = \partial(\mu_i - \mu_3) / \partial c_1$$

$$b_i = \partial(\mu_i - \mu_3) / \partial c_2 \qquad (18)$$

$$\tilde{m}_i = v_i - v_3$$

$$q_i = \frac{1}{T}(Q_i - h_i + h_3)$$

where v_i and h_i are the specific volume and enthalpy of the i-th constituent, respectively.

It appears that the $a_i, b_i, \tilde{m}_i$ are completely determined once the pertinent "state equations" (Ref. 23) of the constituents are given. The quantities q_i depend, in addition, upon the phenomenological coefficients L_{ij} through the heats of transfer Q_i.

Thus, to make any use of eq. (17) one must make some assumptions as to the state equations of the plasma constituents and must determine, either experimentally or by means of statistical mechanics, the phenomenological coefficients L_{ij}.

The expressions for a_i, b_i and $\tilde{m}_i$ are herein derived on the assumption that the plasma constituents are perfect gases. The quantities q_i will be dealt with in the next paragraph.

If one makes the perfect gas assumption, the following relations hold (ref. 23).

$$\mu_i = \frac{1}{m_i} RT \left[\phi_i (T) + \ell n \left(p c_i \frac{m}{m_i} \right) \right]$$

$$v_i = \frac{m_i}{m} \frac{RT}{p c_i} \qquad (19)$$

$$h_i = h_{io} + \int_{T_o}^{T} c_{p_i} \, dT$$

wherein $\phi_i (T)$ is an arbitrary function of the temperature, m_i is the molar mass of the ith component, m is the molar mass of the ith component, m is the molar mass of the mixture, h_o a reference specific enthalpy, and R the molar gas constant.

With these expressions one has:

$$a_1 = RT \left\{ \frac{1}{c_1 m_1} - \frac{1}{m_1} \left(\frac{m}{m_1} - \frac{m}{m_3} \right) + \frac{1}{c_3 m_3} + \frac{1}{m_3} \left(\frac{m}{m_1} - \frac{m}{m_3} \right) \right\}$$

$$b_1 = a_2 = RT \left\{ \frac{1}{m_2} \left(\frac{m}{m_3} - \frac{m}{m_1} \right) + \frac{1}{c_3 m_3} + \frac{1}{m_3} \left(\frac{m}{m_3} - \frac{m}{m_1} \right) \right\}$$

$$b_2 = RT \left\{ \frac{1}{c_2 m_2} - \frac{1}{m_2} \left(\frac{m}{m_2} - \frac{m}{m_3} \right) + \frac{1}{c_3 m_3} + \frac{1}{m_3} \left(\frac{m}{m_2} - \frac{m}{m_3} \right) \right\} \qquad (20)$$

$$\tilde{m}_1 = \frac{RT}{pm} \left(\frac{m_1}{c_1} - \frac{m_3}{c_3} \right)$$

$$\tilde{m}_2 = \frac{RT}{pm} \left(\frac{m_2}{c_2} - \frac{m_3}{c_3} \right)$$

In the case of an imperfect Lorentz's gas (i.e. $m_i/m_3 \ll 1$; $N_1/N_3 \ll 1$; $N_2/N_3 \ll 1$) these formulas are greatly simplified and one obtains:

$$\frac{a_1}{e_1} = \frac{RTN}{\epsilon_1}\,\frac{m}{m_1}$$

$$b_1 = a_2 = 0 \qquad (21)$$

$$\frac{b_2}{e_2} = \frac{RTN}{\epsilon_2}\,\frac{m}{m_2}$$

$$m_i = \frac{RT}{pm}\,\frac{m_i}{c_i}$$

where $\epsilon_i = \frac{e_i}{m_i N_i}$ are the electric charges per unit volume.

The explicit expression for the coefficients a, is found by substitutiing eqs. (20) into eq. (17).

In the case of imperfect Lorentz's gas one obtains:

$$a = - Nm \frac{\frac{q_1}{\epsilon_2 m_2} + \frac{q_2}{\epsilon_1 m_1}}{\frac{\epsilon_1}{\epsilon_2 m_2 c_1} + \frac{\epsilon_2}{\epsilon_1 m_1 c_2}} \qquad (22)$$

The formulae so far developed are all that one can do without specifying the nature of the phenomenological coefficients L_{ij}. Any order of magnitude analysis can be furthered only after having obtained suitable expressions for these coefficients or, what amounts to the same, for the quantities q_i.

This is considered in the next part, where it will be shown how the L_{ij}'s can all be expressed in terms of transport coefficients.

3. Expressions of the pertinent phenomenological coefficients in terms of transport coefficients

To express the coefficients L_{ij} in terms of transport coefficients the following consideration is essential.

In the subject case we have two independent mass fluxes and one energy flux. The number of independent phenomenological coefficients is therefore six, accounting for the three Onsager reciprocity relations. It follows that the behavior of the system is completely characterized by only six independent coefficients. One such a set is that of the three binary diffusion coefficients D_{12}, D_{13}, D_{23} (i.e., coefficients of diffusion of electron-ion, electro-molecule and ion-molecule mixtures) plus the two thermal diffusion coefficients D_1^T, D_2^T (i.e. the coefficients of thermal transport due to diffusion of the electron gas and the ion gas into the neutral-ion and neutral-electron gas, respectively) and the heat conduction coefficient.

It is then natural to think that a suitable linear transformation of fluxes and forces will make it possible to express everything in terms of the above transport coefficients.

This is considered in the next part, where it will be shown how the L_{ij}'s can all be expressed in terms of transport coefficients.

3. Expressions of the pertinent phenomenological coefficients in terms of transport coefficients

To express the coefficients L_{ij} in terms of transport coefficients the following consideration is essential.

In the subject case we have two independent mass fluxes and one energy flux. The number of independent phenomenological coefficients is therefore six, accounting for the three Onsager reciprocity relations. It follows that the behavior of the system is completely characterized by only six independent coefficients. One such a set is that of the three binary diffusion coefficients D_{12}, D_{13}, D_{23} (i.e., coefficients of diffusion of electron-ion, electro-molecule and ion-molecule mixtures) plus the two thermal diffusion coefficients D_1^T, D_2^T (i.e. the coefficients of thermal transport due to diffusion of the electron gas and the ion gas into the neutral-ion and neutral-electron gas, respectively) and the heat conduction coefficient.

It is then natural to think that a suitable linear transformation of fluxes and forces will make it possible to express everything in terms of the above transport coefficients.

This is indeed so. In fact, by defining new generalized forces A_i'' as:

$$A_i'' = A_i + h_i A_u \qquad (i = 1, 2, 3)$$

$$A_o'' = A_u \qquad (23)$$

we find, according to eqs. (23), the following expressions for the new fluxes:

$$J_i'' = J_i \qquad (i = 1, 2, 3)$$

$$J_o'' = J_u - \sum_{i=1}^{3} h_i J_i$$

and the new phenomenological coefficients L_{ij}'':

$$L_{ij}'' = L_{ij} \qquad (i, j = 1, 2, 3)$$

$$L_{oo}'' = L_{oo}$$

$$L_{1o}'' = - L_{11} (h_1 - h_3) - L_{12} (h_2 - h_3) + L_{1o} \qquad (24)$$

$$L_{2o}'' = - L_{21} (h_1 - h_3) - L_{22} (h_2 - h_3) + L_{2o}$$

These new coefficients L''_{ij} are just those used in reference (1) and it is therein shown how they are related to the binary diffusion coefficients D_{ij}, to the thermal diffusion coefficients D_i^T ($i = 1, 2$) and to the thermal conductivity coefficient λ.

The ultimate goal of expressing the q_i's in terms of transport coefficients is thus achieved by performing the necessary substitutions. One gets:

$$q_1 = -\frac{1}{T}\left\{\frac{(L''_{10} + L''_{20})\, L''_{12} + L''_{10}\, L''_{23}}{(L''_{13}\, L''_{12} + L''_{13}\, L''_{23} + L''_{12}\, L''_{23})}\right\}$$

$$q_2 = -\frac{1}{T}\left\{\frac{(L''_{1} + L''_{2})\, L''_{12} + L''_{2}\, L''_{13}}{(L''_{13}\, L''_{12} + L''_{13}\, L''_{23} + L''_{12}\, L''_{23})}\right\} \qquad (25)$$

and by using the expressions for L''_{ij} reported in Ref. (1):

$$q_1 = -\frac{1}{AT}\left\{\left[D_1^T + D_2^T\right] n^2 n_1 n_2 m_1 m_2 \left[n_3 m_3^2 D_{13} D_{23} - m_2 (\rho - n_2 m_2)\right.\right.$$
$$\left. D_{12} D_{23} - m_1 (\rho - n_1 m_1) D_{12} D_{13}\right] + \left[D_1^T\right] n^2 n_2 n_3 m_2 m_3$$
$$\left[n_1 m_1^2 D_{12} D_{13} - m_3 (\rho - n_3 m_3) D_{23} D_{13} - \right. \qquad (26)$$
$$\left.\left. - m_2 (\rho - n_2 m_2) D_{23} D_{12}\right]\right\}$$

and:

$$q_2 = -\frac{1}{AT}\left\{\left[D_1^T + D_2^T\right]\left[n_3 m_3^2 D_{13} D_{23} - m_2 (\rho - n_2 m_2) D_{12} D_{23} - m_1 (\rho - n_1 m_1) D_{12} D_{13}\right] n^2 n_1 n_2 m_1 m_2 + \left[D_2^T\right] n^2 n_1 n_3 m_1 m_3 \left[n_2 m_2^2 D_{12} D_{23} - m_3 (\rho - n_3 m_3) D_{13} D_{23} - m_1 (\rho - n_1 m_1) D_{13} D_{12}\right]\right\} . \quad (27)$$

where:

$$A = \left[\rho^2 p (n_1 D_{23} + n_2 D_{13} + n_3 D_{12})\right]^{-1}\left\{n^2 n_1 n_3 m_1 m_3\left[n_2 m_2^2 D_{12} D_{23} - m_3 (\rho - n_3 m_3) D_{13} D_{23} - m_1 (\rho - n_1 m_1) D_{13} D_{12}\right] n^2 n_1 n_2 m_1 m_2 \left[n_3 m_3^2 D_{13} D_{23} - m_2 (\rho - n_2 m_2) D_{12} D_{23} - m_1 (\rho - n_1 m_1) D_{12} D_{13}\right] + n^2 n_1 n_3 m_1 m_3\left[n_2 m_2^2 D_{12} D_{23} - m_3 (\rho - n_3 m_3) D_{13} D_{23} - m_1 (\rho - n_1 m_1) D_{13} D_{12}\right] n^2 n_2 n_3 m_2 m_3 \left[n_1 m_1^2 D_{12} D_{13} - m_3 (\rho - n_3 m_3) D_{13} D_{23} - m_2 (\rho - n_2 m_2) D_{12} D_{23}\right] + n^2 n_1 n_2 m_1 m_2 \cdot \left[n_3 m_3^2 D_{13} D_{23} - m_2 (\rho - n_2 m_2) D_{12} D_{23} - m_1 (\rho - n_1 m_1) D_{13} D_{12}\right] n^2 n_2 n_3 m_2 m_3 \left[n_1 m_1^2 D_{12} D_{13} - m_3 (\rho - n_3 m_3) D_{13} D_{23} - m_2 (\rho - n_2 m_2) D_{12} D_{23}\right]\right\} . \quad (28)$$

4. - Determination of the electric conductivity of a plasma

As shown in the preceeding parts the determination of the coefficient α in terms of the transport coefficients of the mixture involves essentially two steps. First the dynamical equations are written in the form which is appropriate for the subsequent application of the principle of stationary state which yields the expression of α in terms of some set of kinetic coefficients L'_{ij} and some thermodynamics derivatives. To express the latter ones some assumptions must be made as to the nature of the state equations of the constituent gasses (in particular, the perfect gas hypothesis has been made).

In the second step, suitable linear transformations are introduced which related the kinetic coefficients L_{ij} to a new set of coefficients L''_{ij} which, as shown in Ref. (1), is directly expressible in terms of the transport coefficients.

This same procedure must be followed to determine the electrical conductivity σ, and can be reported now in a condensed form, by skipping all details.

The appropriate form of the dynamic equations is that given in eqs. (7). By definition, the electric conductivity given by the ratio $I/\nabla\Phi$ between the electric current density and the electric field.

This ratio depends on the particular assumptions about the order of the stationary state in which it is evaluated and thus to a certain extent on the number of "constraints" which are imposed at the boundary of the system. It acquires a definite meaning, that is, it can be given a unique expression in terms of the state parameters, only in a particular first order stationary state.

Indeed, in the subject case of a ternary plasma, one could define a third order stationary state in which a given non-uniform electric potential distribution and a uniform temperature and electron concentrations are maintained on the boundaries of the system. In such a state, however, the plasma would certainly not be uniform throughout the region (i.e. ∇T and ∇c_1 would not be identically zero) and the ratio between I and $\nabla \phi$ would also be a function of the other gradients (and/or fluxes) present in the system. Similar considerations hold for a second order stationary state in which a given non-uniform electric potential distribution and a uniform temperature (or electron concentration) are maintained on the boundary of the system. Once again, the gradient of T (or of c_1) would not vanish identically throughout the system, two independent fluxes would be different from zero and no unique definition for the electric conductivity could be given (i.e. the ratio $I/\nabla\phi$ would not depend only on the state of the system but also on some gradients of the state parameters).

Thus the electric conductivity must be defined in a first order stationary state for which a given non uniform distribution of electric potentive is maintained on the boundaries of the system. In this case the electric current will be the only non-vanishing flux and equations (7) can be solved for the ratio $\sigma' = (I/\nabla\phi)_{\nabla\phi = \text{const.}}$ giving:

$$\sigma' = L'_{22} + \frac{2\, L'_{10}\, L'_{21}\, L'_{02} - L'_{00}\, L'^{2}_{21} - L'_{11}\, L'^{2}_{02}}{L'_{00}\, L'_{11} - L'^{2}_{10}} \qquad (29)$$

It is of interest to notice that in a fully ionized neutral plasma (i.e. in a system with one less degree of freedom) in which the electron concentration gradient ∇c_1 is no longer an independent gradient, the expression for σ in the first order stationary state becomes by formally putting $L'_{1j} = 0$ in Eq.(7):

$$\sigma = L'_{22} - \frac{L'^2_{02}}{L'_{00}} \tag{30}$$

This relation, when expressed in terms of the only binary diffusion coefficient existing in this case, reduces, as it is easy to verify, to the well known Einstein-type relation.

To obtain σ in terms of the set of transport coefficients, one only needs a set of relations between the L'_{ij} and the L''_{ij}'s, which, as said before, are related to the transport coefficients as shown in Ref. (1) The subject relationships are:

$$\begin{aligned}
L'_{00} &= L''_{00} \\
L'_{01} &= \bar{b}_1 L''_{01} + \bar{b}_2 L''_{02} \\
L'_{02} &= e_2 L''_{02} + e_1 L''_{01} \\
L'_{11} &= \bar{b}_1^2 L''_{11} + 2\bar{b}_1 \bar{b}_2 L''_{12} + \bar{b}_2^2 L''_{22} \\
L'_{22} &= e_1^2 L''_{11} + 2e_1 e_2 L''_{12} + e_2^2 L''_{22} \\
L'_{21} &= e_1 \bar{b}_1 L''_{11} + (e_2 \bar{b}_1 + e_1 \bar{b}_2) L''_{12} + e_2 \bar{b}_2 L''_{22}
\end{aligned} \tag{31}$$

with:

$$\begin{aligned}
b_1 &= \frac{\partial \mu_1}{\partial c_1} - \frac{\partial \mu_3}{\partial c_1} - \frac{e_1}{e_2}\left(\frac{\partial \mu_1}{\partial c_2} - \frac{\partial \mu_3}{\partial c_2}\right) \\
b_2 &= \frac{\partial \mu_2}{\partial c_1} - \frac{\partial \mu_3}{\partial c_1} - \frac{e_1}{e_2}\left(\frac{\partial \mu_2}{\partial c_2} - \frac{\partial \mu_3}{\partial c_2}\right)
\end{aligned}$$

where all the symbols have the already defined meaning.

SECTION 2

2. 1. - The transport coefficients for a plasma.

In the preceeding section the general expressions for the coefficients α and σ in terms of the transport coefficients D_{12}, D_{13}, D_{23}, D_1^T, D_2^T, λ have been derived.

The next step toward the ultimate goal of expressing α and σ, to within a given degree of approximation, in terms of the thermodynamic parameters of the mixture and of the physical charateristics of the constituent gases requires then the evaluation of the above mentioned transport coefficients in terms of these parameters.

This will be done in this section.

We recall some basic facts on the determination of the transport coefficients.

For conditions not too far from equilibrium the determination of the transport coefficients hinges on the evaluation of the following integrals (see Refs. 1 or 6 details):

1) The deflection angle:

$$\chi(g^*, b^*) = \pi - 2\, b^* \int_{r_m^*}^{\infty} \frac{d\, r^*/r^{*2}}{\left(1 - \frac{b^{*2}}{r^{*2}} - \frac{\phi^*(r^*)}{g^{*2}}\right)^{1/2}} \qquad (32)$$

where:

$$r^* = r/\sigma\,; \quad b^* = b/\sigma\,; \quad \phi^* = \phi/\epsilon\,; \quad T^* = \frac{KT}{\epsilon}\,; \quad g^{*2} = \frac{1}{2}\, m_{ij}\, g^2/\epsilon$$

and where: m_{ij} is the reduced mass, defined as $m_{ij} = m_i m_j / m_i + m_j$ where m_i and m_j are the masses of the particules of species i and j; g is the initial relative velocity of the two particles; b is the impact parameter; r the distance between the mass centers of the two colliding particles; $\phi(r)$ is the interaction potential; r_m the distance of closest approach.

Eq.(32) is valid for elastic collisions between particles assumed to be centers of force fields with spherical symmetry.

The potentials which we shall deal with are all expressible as:

$$\phi(r) = \epsilon f\left(\frac{r}{0}\right)$$

where ϵ and 0 depend on the particular "molecular model" assumed. In particular, 0 corresponds to the molecular diameter in the case of the rigid sphere model.

2) The non-dimensional collision cross section $Q^{(e)*}(g^*)$:

$$Q^{(e)*} = \frac{Q^{(e)}}{Q^{(e)}_{r.s.}} = \frac{2}{\left[1 - \frac{1}{2}\,\frac{1+(-1)^e}{1+e}\right]} \int_0^{\infty} (1 - \cos^e \chi)\, b^*\, db^*$$

where the subscripts r.s. indicate values for the rigid sphere model. It is:

$$Q^{(e)}_{r.s.} = \left[1 - \frac{1}{2}\,\frac{1+(-1)^e}{1+e}\right] \pi 0^2$$

with 0 defined as before.

3) The non dimensional collision integrals:

$$\Omega^{(es)*} = \left[\frac{2}{(s+1)!\ T^{*s+2}} \right] \int_0^\infty e^{-g^{*2}/T}\ g^{*2s+3}\ Q^{(e)*}\, dg^* = \frac{\Omega^{(es)}}{\Omega^{(es)}_{r.s.}}$$

where:

$$\Omega^{(es)}_{r.s.} = \sqrt{\frac{KT}{2\pi m_{ij}}}\ \frac{(s+1)!}{2}\ \left[Q^{(e)}_{r.s.} \right]$$

Notice that, by definiton, all starred quantities are equal to one for the rigid sphere model.

Any transport coefficient is expressible in terms of the above quantities. Indeed, indicating by the subscripts i, j, quantities related to collisions between particles of the ith and jth species one has:

a) D_{ij} - (diffusion coefficient for the ith and jth species in a multicomponent gas mixture) is related to the binaty diffusion coefficients D_{ij} of each pair of species (see eq. 8-2,49, in Ref. (1)). These relations involve in addition, the concentrations of the single species, and the molecular masses.

The coefficient D_{ij}, in turn, is expressible as:

$$D_{ij} = \frac{3}{8}\ \frac{1}{\rho}\ \frac{\sqrt{\pi m_{ij}\ KT}}{\pi \sigma_{ij}^2\ \Omega^{(11)*}} \qquad (33)$$

where:

$$\sigma_{ij} = \frac{1}{2}\ (\sigma_i + \sigma_j)$$

is the collision diameter.

b) The coefficients of thermal diffusion, D_i^T, can be evaluated in terms of the coefficients of binary molecular diffusion and of the coefficients of thermal conductivity for each species (λ_i) and for each pair of species (λ_{ij}). The pertinent explicit expressions are too cumbersome to be reported here; they can be found in Ref. (1) page 543.

It is important, however, to notice that they involve the integrals $\Omega_{ij}^{(22)*}$ and $\Omega_{ij}^{(1,s)*}$, (s = 1, 2, 3).

c) The coefficients of thermal conductivity for the ith species can be evaluated as:

$$\lambda_i = \frac{25}{32} \frac{\sqrt{\pi m_i KT}}{\pi \sigma_i^2 \Omega^{(22)*}} \frac{3}{2} \frac{K}{m_i} \tag{34}$$

This expression is valid for monatomic gases; Eucken's corrections are to be added for polyatomic gases.

The coefficient of thermal conductivity for a binary mixture is given by:

$$\lambda_{ij} = \frac{25}{8} \frac{p D_{ij}}{A_{ij} T} \tag{35}$$

where A_{ij} is a combination of the collision integrals $\Omega_{ij}^{(es)}$. Its value is very close to one.

Table I summarizes the fundamental dependence of the discussed transport coefficients for multicomponent gaseous mixtures (first column) on the related binary transport coefficients (column two) and on the related collision integrals (column three).

The next step is a discussion of the actual evaluation of the transport

coefficients for the particular potentials related to the interactions between the particles present in a plasma.

a) Interaction electron-ions

The force between two charged particles is coulombian.

The interaction potential is given by the equation:

$$\phi(r) = -\frac{Ze_1^2}{r} = -\frac{e_1 e_2}{r} \qquad (36)$$

where Z indicates the number of electric charges carried by the ion and the sign "-" takes into account the attractive nature of the force for distances greater than the threshold of actions of quantic type, for which the force is repulsive.

With the potential given by eq. (36) one faces the well known fact that the collision cross section, as defined by eq. (32) assumes an infinite value.

This problem has been studied extensively, and the difficulty eliminated by a "cut off" of the upper limit of the integral. The cut off distance must be the smaller of the mean distance between the gas particles $D = n^{-1/3}$ and the Debye shielding length:

$$\ell_D = (KT/4\pi n_1 e_1^2)^{1/2} .$$

Consider at first, as pertinent, the collisions for which the impact distance b is less than D.

One evaluates eq. (32) wherein the upper limit becomes b= D.

Substituting for the expression $\frac{1}{2} m_{12} g^2$ its mean value 2kT and neglecting the small variations of the kinetic energy of the particles within the sphere of radius D, one obtains:

$$Q^{(1)}(g) = \frac{1}{4}\left(\frac{Z e_1^2}{2KT}\right)^2 \ln\left[1 + 4\left(\frac{2KTD}{Z e_1^2}\right)^2\right] \tag{37}$$

where, for mixture of electrons-ions it is:

$$D = \left[n_1 + n_2\right]^{-1/3} \tag{38}$$

The corresponding binary diffusion coefficient is obtained by substituting eq. (37) into eq. (33) which results in:

$$D_{12} = \left[\frac{3}{8}\left(\frac{m_{12}\,KT}{\pi}\right)^{1/2}\left(\frac{2\,KT}{e_1 e_2}\right)^2 \frac{1}{\rho}\right] \Bigg/ \left\{\left[\frac{1}{4}\ln\left[1+4\left(\frac{2KTD}{e_1 e_2}\right)^2\right]\right]\right\} \tag{39}$$

In the second case, when the upper limit is put equal to l_D the collision cross section will be:

$$Q^{(1)} = \frac{2\pi e_1^4}{(3/2\ KT)^2}\ln\Lambda \tag{40}$$

where:

$$\Lambda = \frac{3}{2 e_1^3}\left[\frac{K^3 T^3}{\pi\, n_1}\right]^{1/2}$$

The corresponding expression for D_{12} is readily obtained by substituting eq. (40) into eq. (33) and is:

$$D_{12} = \left[\frac{3}{8}\left(\frac{m_{12}\,KT}{\pi}\right)^{1/2}\left(\frac{3}{2}KT\right)^2 \frac{1}{\rho}\right] \Bigg/ \left[2\pi e_1^4 \ln\Lambda\right] \tag{41}$$

More recently a new method to evaluate the coefficient D_{12} has been proposed (Ref. 12) which does not use the cut off for evaluating the collision

cross section. Such a method furnishes, with a more complicated process, an approximation higher than that necessary for our purposes, and it is therefore not used here.

b) Interaction of electrons-neutral molecules and ions-neutral molecules

The interaction between charged particles (electrons or ions) and the neutral molecules can be treated by the following procedure (Ref. 3).

The charged particle produces an electric field that induces an electric dipole into the neutral molecule, which undergoes a separation of electric charges. The induced electric dipole produces an external potential given by:

$$V = + \alpha \frac{e_i}{r^4} \cos \Theta \qquad (i = 1, 2)$$

where α is the polarizability of the molecule, e_i the inducing charge, and Θ the position angle referred to the axis of the dipole.

The interaction potential will then be written as:

$$\phi (r) = - \frac{\alpha}{2} \frac{e_i^2}{r^4} \qquad (42)$$

The negative sign indicates that the forces are attractive up to the distance σ, quantic threshold. It should be noted that the energy of interaction expressed by (42) is only a first approximation to more complicated expressions, because it neglects, for instance, the London's dispersion energy, related to the mutual action between the molecular dipole and the dipole induced by this into the ion. Such a dispersion energy, proportional to the

inverse sixth power of the distance, can amount to 25% of the interaction energy given by (42) for distances between the particles of the order of one collision diameter (Ref. 1, ch. 13).

The polarizability of the atoms and of the molecules has been studied theoretically and experimentally; its values vary, for polyatomic molecules, with the direction of the inducing electric field. It is always possible however to introduce a mean value taken over all directions. This value increases with the molecular complexity; for instance, the mean polarizability varies from $7,9 \times 10^{-25}$ cm^3 to $103,2 \times 10^{25}$ cm^3 for the molecule of hydrogen and the molecule of benzone, respectively. Tables, given in Ref. (1) furnish the more important data.

For a potential expressed by eq. (42) which is nothing but a particular form of the Sutherland's model with $\gamma = 4$, one notices, from the tab. 4 of Ref. (1) that for not too high values of the particle energy, the collision cross sections become very close to the collision cross sections for rigid spheres. For first approximation calculations and for orders of magnitude evaluations and in view of the uncertainty as to the value of a, we can therefore use the results obtained for the simple potential of rigid spheres without too large errors.

We write therefore:

$$D_{13} = \frac{3}{8} \frac{1}{\sigma_{13}^2} \sqrt{\frac{KT}{\pi m_{13}}} \frac{1}{n} \tag{43}$$

$$D_{23} = \frac{3}{8} \frac{1}{\sigma_{23}^2} \sqrt{\frac{KT}{\pi m_{23}}} \frac{1}{n} \tag{44}$$

where:

$$\sigma_{ij} = \frac{1}{2} (\sigma_i + \sigma_j)$$

is the collision diameter.

An alternate procedure for the determination of D_{i3} (i= 1, 2), based on experimental data, can be used.

Recently, experimental evaluations of the total elastic collision cross sections were made for the ions-neutral molecules and the electrons-neutral molecules mixtures.

The total elastic collision cross sections are defined by:

$$Q^{(o)} = 2\pi \int_o^\infty b\, db \tag{45}$$

and one can write:

$$Q^{(1)} = Q^{(o)} \left(\overline{1 - \cos \chi} \right) \tag{46}$$

where $\left(\overline{1 - \cos \chi} \right)$ indicates the mean value of the term (1-cos χ) taken over all angles of collision. Such a mean value, for collision angles equally probable, is equal to one. This occurs for not too elevated values of the energy of the particles.

With this limitation and with not too large errors, one can then assume for $Q^{(1)}$ the values experimentally obtained for $Q^{(o)}$ and hence compute D_{13} and D_{23} by substituting these values in eqs. (43-44).

A more extended discussion of this procedure can be found in Ref. 9.

c) Interaction between neutral molecules

The interaction potential is expressed by:

$$\phi(r) = -\frac{G}{r^6} \tag{47}$$

since the two molecules behave as two mutually inducing dipoles. This potential, corresponding to the Sutherland's model, was studied by Kotani (Ref. 4) and the values of $\Omega^{(es)*}$ are available in tabulated form.

The evaluation of the transport coefficients for this model is thus reduced to the substitution of these tabulated values into the previously described formulae.

The results thus far described are summarized in Table II. For each of the three types of interactions the corresponding expressions for the potential are reported together with the available references for the theoretical and/or experimental evaluation of the collision cross sections.

2. - Analysis of the orders of magnitude of the transport coefficients

The determination of the transport coefficients, as described above, will now be specialized to the case of a weakly ionized, imperfect Lorentz's gas for which, as said, the following inequalities hold by definition:

$$\frac{m_1}{m_2} \simeq \frac{m_1}{m_3} \ll 1; \qquad \frac{n_1}{n_3} \simeq \frac{n_2}{n_3} \ll 1$$

It will be found that in such case a number of terms and/or contributions can be neglected because of smaller order. To lend rigorousness to such an order of magnitude analysis, we shall assume as a reference "order of smallness" the square root of the mass ratio $\delta = (m_1/m_3)^{1/2}$. For the neutral particles we shall be interested in, δ is of the order of 10^{-2}.

Let us begin with the binary diffusion coefficients. It is pointed out that evaluation of their comparative orders of magnitude will be made for given temperature and number density of the plasma.

Eqs. (39-41-43-44) indicate that for given n and T the order of magnitude of the coefficients of binary molecular diffusion depend on both the ratio of the colliding molecular masses and the ratio of the related collision cross sections.

The reduced masses in the present approximation are given by:

$$m_{12} \simeq m_1$$

$$m_{23} \simeq \frac{m_2}{2} \simeq \frac{m_3}{2}$$

The orders of magnitude of the ratios between the collision cross sections are immediately evaluated for any energy level (this being the only parameter on which the Q_{ij} depend). As discussed in Section II, Q_{12} can be obtained theoretically, while either rigid sphere model formulae or experimental results, [reported, for instance, in Refs. (11, 9, 3, 21, 18)] can be used for Q_{13}, Q_{23}.

It is important to observe that the ratios between the collision cross sections, to a first approximation, do not depend on the state parameters. Indeed, consider, for instance, the ratio Q_{12}/Q_{23} in a plasma, when $n_1 = n_2 = 10^6$ part./cm^3.

In the range $1,000 < T < 10,000^\circ$ K, such a ratio varies between 1.68×10^2 and 1.10×10^2. For $n_1 = n_2 = 10^{15}$ part/cm^3, the ratio is roughly doubled. The above reported values for the electron number density are limiting values for the range of variation of n_1, corresponding to the weakly ionized gases of the ionospheric F layer and of the electric strong discharges, respectively.

As a consequence:

$$Q_{23} / Q_{12} \equiv 0 \quad \left[10^{-2}\right] \equiv 0\left[\delta\right]$$
$$Q_{23} / Q_{13} \equiv 0 \quad \left[10^{2}\right] \equiv 0\left[\delta^{-1}\right] \qquad (48)$$
$$Q_{13} / Q_{12} \equiv 0 \quad \left[10^{-4}\right] \equiv \left[\delta^{2}\right]$$

These particular values have been obtained for a plasma whose constituents are N_2, N_2^+, e^-, and at $T = 1,000^{o}K$, $n_1 = n_2 = 10^6$ part/cm^3. The orders of magnitude of these ratios do not essentially vary as functions of the state parameters or, for the usual gases, of the chemical nature of the particles.

Thus, we obtain, for the diffusion coefficients:

$$D_{12} / D_{23} \equiv 0 \left[1\right]$$
$$D_{13} / D_{23} \equiv 0 \left[\delta^{-2}\right] \qquad (49)$$
$$D_{12} / D_{13} \equiv 0 \left[\delta^{2}\right]$$

(b) The evaluation of D_1^T, D_2^T and of their ratio now constitutes the second step.

As mentioned previously, the coefficients of thermal diffusion for each consitiuent species of the mixture is a function of the coefficients of binary molecular diffusion D_{ij} and of the coefficients of thermal conductivity λ_1, λ_2, λ_3.

Since:

$$Q_1 / Q_3 \equiv 0 \left[\delta^{2}\right]$$
$$Q_2 / Q_3 \equiv 0 \left[\delta^{2}\right]' \qquad (50)$$
$$Q_1 / Q_2 \equiv 0 \left[1\right]'$$

one has:

$$\lambda_1 / \lambda_3 \equiv 0 \quad [\delta^{-3}]$$
$$\lambda_2 / \lambda_3 \equiv 0 \quad [\delta^{-2}] \tag{51}$$
$$\lambda_1 / \lambda_2 \equiv 0 \quad [\delta^{-1}]$$

The various terms in the equations for D_1^T and D_2^T can be noticeably simplified from (49) and (51).

Neglecting all the necessary long manipulations, we only state here the pertinent results as follows:

$$D_1^T / D_2^T \equiv 0 \quad [\delta^4] \tag{52}$$

$$D_2^T = \frac{15}{4} \frac{n_2}{n_1} \text{ mn } \mathcal{M} D_{23} \tag{53}$$

where:

$$\mathcal{M} = M_2 (1 + M_3 / M_2) \Big/ (21 M_2 / M_3 + 33/4 \ M_3/M_2 + 12)$$

For convenience, a list of the relative orders of magnitude of all the quantities involved is reported in TABLE III.

SECTION 3

On the basis of the results of the last sections, one can examine more accurately the phenomenological coefficients describing the electrical properties of a non-uniform plasma. Namely, at this point it is possible to evaluate their expressions in terms of the thermodynamic state parameters of the plasma.

1) The Coefficient a .

In section I we have obtained for a , for the imperfect Lorentz's gas, the expression:

$$a = - \frac{q_1 / \epsilon_2 m_2 \quad + \quad q_2 / \epsilon_1 m_1}{\epsilon_1 / \epsilon_2 m_1 m_2 n_1 + \epsilon_2 / \epsilon_1 m_1 m_2 n_2} \tag{54}$$

Since it is possible to evaluate for q_1, and q_2 a relative order of magnitude $q_2/q_1 \equiv 0 \left[\delta\right]$ by analyzing their expression (26-27), one obtains as a consequence:

$$a = - \frac{q_2 \epsilon_2 n_1 n_2 m_2}{\epsilon_1^2 n_2 + \epsilon_2^2 n_1} \tag{55}$$

where q_2 assumes now the following form:

$$q_2 = - \frac{A K D_2^T}{m_2 n_2 D_{23}} \left(1 + \frac{n_1}{n_3} \frac{D_{13}}{D_{12}} \right) \tag{56}$$

Thus:

$$a = - K_e Am F \left(1 + \frac{n_1}{n_3} \frac{D_{13}}{D_{12}} \right) \tag{57}$$

where:

$$F = \left(\frac{15}{4}\,\frac{m^3}{m_3^2 m_2}\,\frac{n^2}{n_3^2}\,\eta\right) : \left(\frac{n_1}{n_2}\,\frac{e_1}{e_2} + \frac{e_2}{e_1}\right)$$

The coefficient α is dimensionally expressed in volt/cm/^{o}K/cm and represents a measure of the electric field induced by a unit gradient of temperature in a plasma.

It has, for an ionized gas, the same significance of the Seebeck's coefficient, usually treated for solid substances. [It is recalled that the Seebeck's coefficient S for solid conductors is defined in the same way as the coefficient α. Indeed S is the ratio between the gradients of electric potential and temperature in a first order stationary state in which no electric current flows. (See Ref. 23, for instance)].

Examining the expression for α one observes that the only fundamental parameter upon which it substantially depends is the degree of ionization.

Indeed, for a weakly ionized gaseous mixture, one can suppose that: $\frac{n_1}{n_2}$; $\left|\frac{e_1}{e_2}\right|$; $\frac{n}{n_3}$; $\frac{m}{m_3}$; are only slightly different from unity; and the coefficient $K_e AmF$ is a constant depending on the mean molecular mass $m = \epsilon_i\ m_i n_i/n$ only.

The ratio between the coefficients of the binary molecular diffusion D_{13}/D_{12}, as we have shown, does not depend on any state parameter. The only parameter that, as a consequence, affects α is the degree of ionization.

An indicative value obtained for α in a particular interesting case follows.

2- Value of α obtained for the ionosphere F layer

Considering a plasma, whose characteristics are those of the air in the ionspheric F layer, we have:

$$T = 1,000^{\circ} F$$

$$\frac{n_1}{n} = 0.5 \times 10^{-4} \qquad \text{(day values).}$$

One can assume that the particles present are essentially of the following three species: electrons, ions N_2^+ and neutral molecules N_2 and thus $m_2/m_1 = 2_1 8 \times 10^4$.

In this case (ref. 2)

$$n_1 = n_2 = 10^6 \text{ part/cm}^3 \qquad \text{(day values, } e_1 \text{ electron charge)}$$

Q_{12} and Q_{13} are respectively: (Ref. 21 to 16):

$$Q_{12} \simeq 8,4 \cdot 10^{-12} \text{ cm}^2$$

$$Q_{13} \simeq 5,2 \cdot 10^{-16} \text{ cm}^2$$

Therefore:

$$\alpha \simeq -10^{-3} \ \frac{\text{volt/cm}}{^{\circ}\text{K/cm}}$$

This value is of the same order of magnitude as the corresponding Seebeck coefficient for semiconductors (Ref. 20) whose indicative values are reported below:

Material	Seebeck coeff.
Ge (n-type)	850
Bi_2 Te_3	250
S_i - Ge - alloy	1

3. - The electric conductivity.

The expression for the electric conductivity (29) can be simplified under the assumptions of the Lorentz's imperfect gas.

It can be shown that the following relationships between the coefficients L''_{ij} and the transport coefficients hold:

$$
\begin{aligned}
L''_{oo} &\cong \lambda_3 \, T \\
L''_{01} &= D_1^T \\
L''_{20} &= D_2^T \\
L''_{11} &= \frac{n_1 n_3 \, m_1^2 \, D_{12} \, D_{13}}{KT(n_2 D_{13} + n_3 D_{12})} \\
L''_{12} &= \frac{n_1 n_2 \, m_1 m_2 \, D_{13} \, D_{23}}{KT(n_2 D_{13} + n_3 D_{12})} \\
L''_{22} &= \frac{n_2 \, m_2^2 \, D_{23}}{KT}
\end{aligned}
\tag{58}
$$

Pertinent orders of magnitude of these parameters are shown in Table III.

When the proper substitutions in the expression for θ are made one finds that:

$$
\begin{aligned}
\theta = L'_{22} + \frac{L'_{10} L'_{02} L'_{21}}{L'_{00} L'_{11} - L'^2_{10}} \left[2 - \frac{L'_{11} L'_{02}}{L'_{01} L'_{21}} - \frac{L'_{00} L'_{21}}{L'_{01} L'_{02}} \right] \simeq \\
\simeq L'_{22} - \frac{L'^2_{21}}{L'_{11}} = 0
\end{aligned}
\tag{59}
$$

since the first two terms in the squared bracket are of order one, while the third term is of order (δ^{-5}). The vanishing of θ is to within terms of order (δ^5).

This important result indicates that in the present case the plasma behaves essentially as a dielectric medium since, in the steady state, a given distribution of a constant electric field on its boundaries does not

originate any appreciable current but produces only a "polarization" of the medium, as indicated by the induction of electron (and ion) concentration gradients. As a matter of fact, it is just the presence of this induced electron concentration gradient which causes the vanishing of the electric current. That this is so can be readily realized by the following considerations. As shown by eqs.(7) the electrical conductivity σ for an isothermal, uniform three-fluid plasma would be simply given by L'_{22} or, for a Lorentzian gas, by:

$$\sigma_1 = \frac{n_1}{n} \frac{e^2}{\sqrt{m_1 KT}} \frac{1}{Q_{13}} \left[\frac{n_2}{n_3} \frac{Q_{12}}{Q_{13}} + 1 \right]^{-1} \left[\frac{3}{2 \pi \sqrt{\pi}} \right] \qquad (60)$$

which is obviously the Lorentz' formula when the ion contribution is neglected. If now we consider, instead, a plasma with uniform composition but non-isothermal, we find, according to eqs. (7), that the conductivity σ_2 would be given by: $L'_{22} - (L'^2_{02}/L'_{00})$. But the second term is of order (δ^5) so that σ_2 is practically equal to σ_1 . Thus the presence of the temperature gradient would not alter σ provided the electron distribution remains uniform. If however we consider the opposite case of an isothermal plasma with non-uniform electron concentration, then, in the steady case, the conductivity σ_3 would be equal to $L'_{22} - L'^2_{21}/L'_{11}$. That is, accounting for the relative orders of magnitude, it would vanish identically. Thus it is just the "reaction" of the electrons, so to speak, which makes the total current vanish identically in a first order stationary state.

CONCLUSIONS

We state the more important conclusions reached in this chapter:

i) For a ternary macroscopically neutral plasma in thermal equilibrium there are five independent state parameters but only three gradients of these parameters are independent.

ii) Chose the gradients of temperature T, of electric potential ϕ and of electron concentration c_1, as such a set of independent gradients. Then, when a given non-uniform temperature distribution is maintained on the boundaries of the system a steady state is eventually reached in which an electric field $\nabla\phi$ is induced throughout the system, and it is given by:

$$\nabla\phi = a\,\nabla T$$

where a is a phenomenological coefficient depending, in general, on the local thermodynamic state of the medium. Similarly, an electron concentration gradient is induced, which is proportional to ∇T according to a state dependent phenomenological coefficient.

iii) The coefficient a, for a weakly ionized imperfect Lorentz-type plasma, is practically a function only of the degree of ionization, increasing with it. Values computed for an indicative case (ionospheric F layer) show that a is of the order 10^{-3} Volt/^{o}K for a degree of ionization of 10^{-4}.

iv) When a given non-uniform distribution of electric potential is maintained on the boundaries of the system (i.e. when the plasma is imbedded into a time independent electric field) a first order stationary state is reached in which the electrical conductivity σ will depend only on the local thermodynamic state of the medium and not on the temperature gradients, say, which are induced by the electric field.

v) For a weakly ionized imperfect Lorentz-type plasma, σ is practically zero, thus indicating that the plasma, in this condition, behaves essentially as a dielectric.

vi) Points ii) and iii) give qualitative theoretical support to some experiments reported in the literature. (Ref. 13).

TABLE I

TRANSPORT COEFFICIENTS INVOLVED

Transp. Coefficient	Dependence On:	
	Binary Transp. Coefficients	Collision integrals
D_{12}, D_{13}, D_{23}	D_{ij}	$\Omega_{ij}^{(11)}$
D_1^T, D_2^T	D_{ij} , λ_i	$\Omega_{ij}^{(22)}$, $\Omega_{ij}^{(1,s)}$ $(s = 1, 2, 3)$
λ	D_{ij} , λ_i	

TABLE II

Interaction	Potential	Collision cross section			
		Theory	Ref.	Exper.	Ref.
Electron-ions	$\phi = -\frac{e_1 e_2}{r}$	cut-off $D = n^{-1/3}$	1	Not available	
		cut-off $D = \ell_D$	15		
		no cut-off	12		
Electron-neutral molecules; Ion-neutral molecules	$\phi = -\alpha \frac{e_i^2}{r^4}$	Not available			3, 9, 11, 18, 21
Neutral-neutral molecules	$\phi = -\frac{G}{r^6}$	Tabulated values	4, 1	Available	See Ref. 1

TABLE III

ORDERS OF MAGNITUDE FOR LORENTZIAN GAS *

$$\delta = (m_1/m_3)^{1/2} = 0\left[10^{-2}\right]$$

$$m_{12} \simeq m_1 \quad ; \quad m_{23} \simeq \frac{m_2}{2} \simeq \frac{m_3}{2} \quad ; \quad \frac{n_2}{n_3} \simeq \frac{n_1}{n_3} \simeq 0\left[\delta^2\right]$$

Quantity	Order	Quantity	Order	Quantity	Order
Q_{23}/Q_{12}	δ	D_{12}/D_{23}	1	q_2/q_1	δ
Q_{23}/Q_{13}	δ^{-1}	D_{13}/D_{23}	δ^{-2}	e_1/e_2	δ^{-2}
Q_{13}/Q_{12}	δ^2	D_{12}/D_{13}	δ^2	b_1/b_2	δ^{-2}
Q_1/Q_3	δ^2	λ_1/λ_3	δ^{-3}	L''_{11}/L''_{12}	1
Q_2/Q_3	δ^2	λ_2/λ_3	δ^{-2}	L''_{12}/L''_{22}	δ^2
Q_1/Q_2	1	λ_1/λ_2	δ^{-1}	L''_{11}/L''_{22}	δ^2
		λ/λ_3	1	$\dfrac{L''_{11}\,L''_{00}}{L''^2_{02}}$	δ^{-1}
		D_1^T/D_2^T	δ^4		
				L''_{10}/L''_{02}	δ^4
				$\dfrac{L'_{22}/L'_{13}}{L'_{12}/L'_{23}}$	1
				$\dfrac{L'_{11}\,L'_{23}}{L'_{12}\,L'_{13}}$	δ^{-5}

* N_2 , N_2^+ , e^-

SYMBOLS

b	impact distance
c	molecular specific heat
c_i	mass concentration of the i-th component
D	molecular mean distance
D^T_i	coefficient of thermal diffusion for the i-th species
D_{ij}	coefficient of molecular diffusion for the species i and j
e_i	electric charge per unit mass of the i-th component
e'_i	electric charge of the particle of the i-th species
e	electric charge of the electron
E	electric field
f	velocity distribution function
F	force
g_i	specific Gibbs potential
g_{ij}	relative speed between two colliding particles
h_i	specific enthalpy for the i-th species
h	Planck's constant
J_i	Mass flow of the i-th species
J_o	Energy flux
K	Boltzmann's constant
m_i	molar mass for the i-th species
m'_i	mass of the particle
m_{ij}	reduced mass
M_i	particle weight with reference to the H_2 atom
m	molar mass of the mixture

n	number density of the mixture
n_i	number density for the i-th species
N_i	molar concentration of the i-th component
p	pressure
r	distance between two particles
R	gas constant
s_i	specific entropy for the i-th species
t	time
T	temperature
U	specific internal energy
v	specific volume
V	volume
V_i	velocity of the particle of i-th species
X_i	molecular concentration for the i-th species
W_i	reduced velocity
Z	number of positive electric charge of an ion
ϵ	electric charge per unit volume
μ	electrochemical potential
ϕ	electric potential
ω	angular wavelength
D_{ij}	coefficient of binary molecular diffusion
δ	Kronecker's del
$1/\zeta$	collision frequency
λ	thermal conductivity coefficient
ρ	density
$\phi(r)$	interaction potential

χ collision angle

$\Omega_{ij}^{(es)}$ collision integral

References

1) HIRSCHFELDER J.O., CURTISS C.F., BIRD R.B.: "Molecular Theory of gases and liquids" Wiley and Sons, 1954

2) ROSSINI F.D. ed.: "Thermodynamics and Physics of Matter" Parts B&D, Princeton Press 1955

3) DELCROIX J.L.: "Introduction to the theory of ionized gases" Interscience Pub. 1960

4) KOTANI M.: "Proc. Phys.-Math. Soc. Jap." 24, 76 (1942)

5) HOLLERAN E.M., HULBURT H.M.: "I. Chem. Phys" 19, 232 (1951)

6) CHAPMAN S., COWLING T.G.: "The Mathematical Theory of non-uniform Gases" Cambridge University Press, 1939

7) CURTISS C.F. HIRSCHFELDER J.O.: "J. Chem. Phys." 17, 550 (1949)

8) LANDOLT BORNSTEIN: "Zahlenwerte and Functionen" Springer 1951

9) FRANCIS G.: "Ionization Phenomena in Gases" Butterworths 1960

10) EUCKEN, A: Physik Z. 14, 324 (1913).

11) GILARDINI A: "Microwave Determination of Collision Frequencies for slow Electrons" III Congresso Internazionale sui fenomeni di ionizzazione nei gas Venezia 1957

12) THOMPSON W.B. HUBBARD J.: "Long range forces and the diffusion coefficients of a plasma" Proc. of a Symp. on magneto-Fluid. Dynamics Williamsburg Jan 1960

13) KLEIN: "The direct conversion of thermal energy into electrical energy" Munich 1961, Acta Symposium on ionized gases.

14) SPITZER: "Physics of fully ionized gases" Interscience Pub.

15) KANTROWITZ, PETSHEK: Magnetohydrodynamics" Stanford Press 1957

16) GLASSTONE, LOVBERG: "Controlled thermonuclear reactions" Van Nostrand

17) CHANDRASECKAR: "Principles of stellar dynamics", Clarendon 1961

18) BAYET M.: "Physique Electronique de Gas et des Solide" Masson 1961

19) DE GROOT S. R .: "Thermodynamics of irreversible processes" 1959

20) EGLI P.G.: "Thermodlectricity" Wiley and Sons 1958

21) BROWN S.C. "Basic data of plasma physics" Wiley 1959

22) DEMETRIADES S.: "Magnetogasdynamic Acceleration of Flowing Gases and Applications" Northrop Co. 1959

23) CALLEN: "Thermodynamics" Wiley 1959

CHAPTER IV

THE EXPERIMENTAL INVESTIGATION

INTRODUCTION

The general aim of the experimental part of this study is to determine the electrodynamic properties of a nonuniform plasma. In particular, the plasma properties of air about a supersonic vehicle at high altitude are of interest.

As was discussed in the first semi-annual report, this investigation would be made in two distinct steps. First, the experimental apparatus and method would be tested and evaluated using an easily generated plasma of the desired characteristics. Only after the first step has been satisfactorily completed, would the more sophisticated measurements in air be attempted. The experimental report will deal primarily with the evaluation of the apparatus and technique. Also presented will be the data obtained by utilizing this technique to examine the plasma production relaxation time in argon. Our purpose in presenting this data on argon is not so much for its intrinsic value (which is dubious because of impurities), but rather to show the type of problem and the accuracy to which the technique can be meaningfully employed.

The experimental technique will be discussed in the following order: First, the shock tube will be considered as the plasma-producing agent; second, the equipment to measure the electrodynamic character of the plasma will be discussed; and third, the experimental technique will be evaluated using the data obtained from experiments run using an argon plasma. This section will conclude with our future objectives.

1. THE PLASMA GENERATOR

Numerous methods of generating plasmas are available to the experimentalist. Unfortunately, at this state of the art, no one has yet devised a plasma generator where all the properties are controllable. At best, it is necessary to make a compromise between the characteristics important to a given experiment and the failings of the plasma production system.

The important requisite for the plasmas in this experiment is that the density can be controlled not only in magnitude but also spacially. Additional requirements are that the gas density and type be controlled and that the plasma can be contained so that the electromagnetic character can be determined. To these ends, a shock tube as a plasma generator is a suitable compromise.

It was shown in the first semi-annual report that the shock tube was capable of producing known plasma densities with or without axial nonuniformities. Further, a discussion was presented as to the controllability of the plasma composition and the use of the shock tube as a wave guide for electrodynamic measurements. As is usually the case, it is not the general behavior of a device that is important, but rather the specific departures that must be analyzed.

In a conventional shock tube, a pressure ratio is established across a diaphragm. When the diaphragm either bursts or is broken, the thermodynamic character of the slug of air behind the shock that is formed can be computed a priori. In principle, by adjusting the initial conditions (in both the driver and driven sections), a plasma can be generated with specific

properties. However, energy dissipation processes which cannot be accurately considered in the predicted shock calculation may substantially attenuate the theoretical shock velocity in the driven section. With a decrease in velocity of about 20%, the predicted electron density in the plasma may be reduced by more than an order of magnitude.

To compound this prediction error, in a shock tube where the diaphragm is self-rupturing, there is an additional uncertainty. The variation of mechanical properties of the diaphragm may introduce an additional order of magnitude of uncertainty in the electron density value.

Since it is desirable in this experiment to obtain plasma densities within a small range for each operation of the shock tube, the following techniques have been employed. First both the initial driver and driven pressures are measured by mechanical ganges. A Wallace and Tiernan 0 - 50 mm gauge is used to measure the initial driven pressure. Unfortunately, this gauge when used below 2 mm Hg requires a long time before an equilibrium value is obtained. In principle, however, the driver-driven pressure ratio can be maintained to within 3% for a driven pressure of 1 mm Hg. After calibration, the absolute value of the initial driven pressure is also accurate to about 3% at 1 mm Hg, improving to .3% at 10 mm Hg.

It might be noted that many shock tubes are operated using metallic diaphragms where the rupture pressures are predictable to within 5%. However, it was deemed imperative that no metallic fragments exist in the shock tube since these might damage the tube and microwave equipment and possibly produce erroneous electrodynamic measurements.

In order to maintain the driver-driven pressure ratio precision, it is necessary to break rather than pressure-rupture the main diaphragm. In the first semi-annual report, a method using hot wires stretched across the diaphragm was described. While this method produced satisfactory breaks with the conditions the tube was then operating, the method was cumbersome since the wires required replacement after each shot. In addition, leaks developed in the complicated nonmetallic diaphragm holder. Further, since in the future it is expected that the temperature of the driven tube would be elevated, tests were run to find a plastic suitable at high temperatures that could be broken using the hot wire technique. No such plastic could be found. The hot wire technique was abandoned in favor of a mechanical cutting system described below.

a Nitrogen chamber
b Second diaphragm
c Piston
d Stops
e Driver tube
f Rod
g Cutter
h Main diaphragm
i Driven tube

Figure 1. Diaphragm Breaker

The main diaphragm consists of four sheets of .010-inch Lexan*. This combination has a rupture strength of about 200 psi for the three-inch tube diameter in this experiment. In normal operation, the pressure differential across the diaphragm is about 150 psi. As shown in Figure 1 above, a four-bladed pointed cutter is attached to a quarter-inch rod that extends the length of the driver tube. On the opposite end of the rod from the cutter, a piston is attached. The piston operates in a chamber which is divided by a second diaphragm consisting of four sheets of Lexan. To break the main diaphragm, the section of the chamber not including the piston is pressurized with nitrogen until the second diaphragm ruptures. Pressure is then exerted on the piston which accelerates the cutter attaining a velocity sufficient to cut the main diaphragm in about one millisecond.

This system has proved highly successful but slightly cumbersome because of the second diaphragm. However, it offers the advantage that any reasonable driven pressure can be used since the thickness of the main diaphragm is not critical. Further, it allows the use of any plastic sheet that can be cut, thus permitting the use of high temperature materials. Modifications of this system are now in progress so as to replace the second diaphragm with a monostable valve assembly.

The present shock tube system operating at an initial driven pressure of about 1 mm Hg and driver pressure of 150 psi has an average deviation from the mean running conditions of about 70 ft/sec at 7000 ft/sec shock velocity or about 1% mean deviation in velocity.

---

* Produced by General Electric Co.

In argon at 7000 ft/sec, this deviation in velocity corresponds to about 30% in the equilibrium electron density. It should be noted that these figures are obtained from the experimental running conditions of this shock tube and represent the mean shot to shot variation that can be expected. If the theoretical equilibrium electron density calculations are made using the actual shock velocity, the initial driven pressure and the gas composition, the equilibrium electron density of any given shot can be determined to about 3%. This is because, for each shot the velocity (which is the important variable) can be determined to about .1% using the reflected microwave signal. It is well known that in the particular case of argon, the approach to equilibrium ionization is slow. Thus the equilibrium calculations must be used only as an indication of the asymptotic value of electron density behind the shock interface.

It has been shown thus far that the shock tube is experimentally capable of generating known average plasma densities in a repeatable manner.

Another source of errors in the interpretation of the experimental results is the nonuniform radial distribution of the plasma properties due to boundary layer effects. For instance, the estimated radial nonuniformity for air is shown in Figures 2 and 3. In the present series of experiments, the microwaves propagate behind the shock interface at a distance where the distortion of the radial distribution of the electromagnetic field is still negligible. Thus these effects were not taken into account in the interpretation of the experimental results. At the present time, calculations are being conducted to include the radial nonuniform distribution in the analysis of the wave guide fundamental mode.

The present experimental investigation is confined to the analysis of the axially nonuniform electron density in argon.

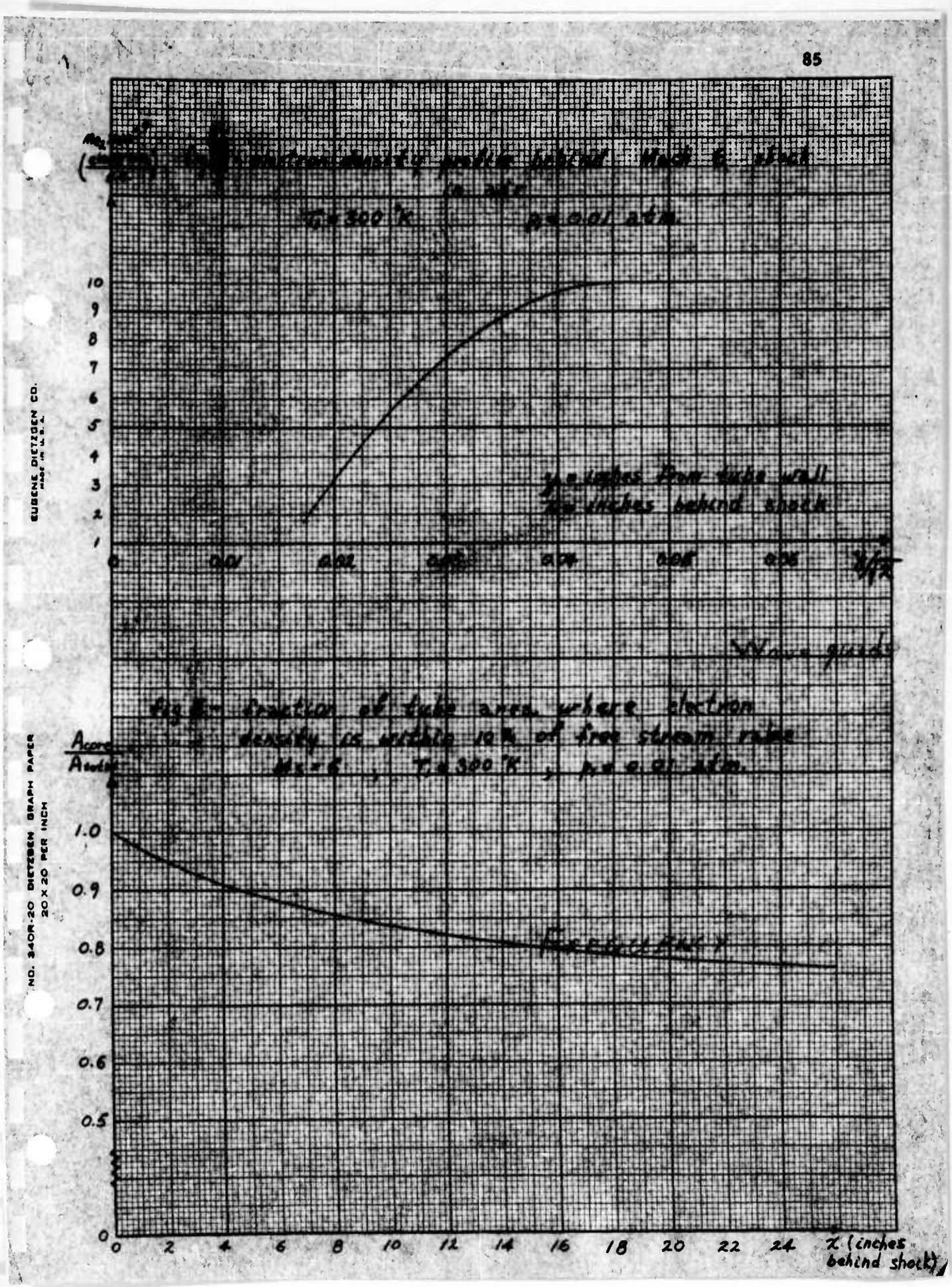
Mx = 6
To = 300 °K
po = 0.01 atm.
Heights from tube wall for inches behind shock
Wave guide
Fig 8 — Fraction of tube area where electron density is within 10% of free stream value
Mx = 6 , To = 300 °K , po = 0.01 atm.
Effective Area
1.0
0.9
0.8
0.7
0.6
0.5
0
0 2 4 6 8 10 12 14 16 18 20 22 24
x (inches behind shock)
EUGENE DIETZGEN CO.
MADE IN U.S.A.
NO. 340R-20 DIETZGEN GRAPH PAPER
20 X 20 PER INCH

The controllability of the density gradient in air, as described in the first report, has not yet been attempted.

2. ELECTROMAGNETIC MEASUREMENTS

In the previous section the shock tube was described as a plasma generator. The salient feature of this experiment is that the shock tube also can be used as a wave guide whose properties depend upon the electromagnetic properties of the generated plasma. The range of frequencies that can be propagated in the fundamental transmission mode TE_{11} is small, which limits the range of electron densities that can be measured. However, it will be shown that within this range, a remarkable degree of precision can be obtained.

It is well known that a cylindrical tube can act as a transmission line for certain frequencies of electromagnetic waves. If the medium in the wave guide is a vacuum, for the TE_{11} mode the cut-off frequency is given by

$$f_c = \frac{1.84\ c}{2\pi R}$$

where R is the tube radius and c is the velocity of light in a vacuum. All frequencies above this "cut-off" frequency can be propagated, but the geometric field configurations become very complicated. Since it is necessary to measure the electric and magnetic fields in this experiment, it is desirable to have a situation where only one mode can propagate in the wave guide. Thus, only frequencies between the cut-off frequency given by the above equation and the cut-off frequency for the next mode are used. This upper frequency limit then is given by

$$f_c = \frac{2.405\ c}{2\pi R}$$

which corresponds to the cut-off frequency of the TM_{01} mode.

For our shock tube with a radius of 3.75 cm, the cutoff values establish the frequency range from 2350 to 3065 mc/sec. Further limitations on this range are imposed by the inability to tune the system as the low frequency limit is approached because the wave guide wavelength becomes very long, extending to infinity at cutoff. Figure 4 shows the relation between the wave guide wavelength and the generated frequency for this shock tube. The propagation limits for the TE_{11} mode are shown. When the wave guide wavelength exceeds about 40 cm, the system becomes difficult to tune. Hence the practical operating range is about 2460 - 3050 mc/sec.

When the wave guide or shock tube contains a uniform plasma the propagation depends upon the plasma frequency and the electron collision frequency in the plasma. In the ideal case where the collision frequency is assumed zero, the propagation constant k_z for the TE_{11} mode is given by:

$$k_z = \sqrt{\frac{\omega^2}{c^2} - \frac{\omega_p^2}{c^2} - \left(\frac{1.84}{R}\right)^2} \qquad (1)$$

where ω is the angular frequency of the electromagnetic wave and

ω_p is the plasma frequency. ω_p is related to the electron density n_e by the equation:

$$\omega_p = 5.64 \times 10^4 \sqrt{n_e} \qquad (2)$$

where n_e measures the number of electrons per cubic centimeter. From equation (1), the cutoff frequency ω_c is given by

$$\omega_c^2 - 2.171 \times 10^{20} = \omega_p^2 \qquad (3)$$

Relating ω_p to the electron density, one obtains:

Wave Guide Wavelength
2.25
2.5
Frequency
2.75
3
Frequency (10⁹ c/sec)
TE11 Cutoff
TM01
EUGENE DIETZGEN CO.
NO. 340R-M DIETZGEN GRAPH PAPER
MILLIMETER

$$\frac{\omega_c^2}{3.18 \times 10^9} - 6.82 \times 10^{10} = n_e \qquad (4)$$

ω_c must be smaller than the cutoff angular frequency of the TM_{01} mode of the wave guide ahead of the plasma interface.

Therefore, with the maximum frequency 3050 mc/sec, the upper limit of electron density at which the electromagnetic field can propagate in the plasma is:

$$n_{e_{max}} \sim 5.2 \times 10^{10} \text{ electrons/cc} \qquad (5)$$

To measure the properties of the plasma, two types of field detectors are used. First, the electric field detector is an antenna which is mounted flush with the wall of the shock tube. This antenna is connected to a microwave diode type IN 23. If the detector is operating in the "square law" region, the output voltage from the diode is proportional to the square of the average electric field at the wall. The maximum output from a typical detector for an input power of 20 milliwatts is about 40 millivolts.

The magnetic detector is like the electric field detector except that between the wall of the tube and antenna, a loop is made. The plane of the loop lies in a plane including the axis of the tube and the microwave antenna. An output comparable to the electric detector is obtained if the diameter of the loop is about .4 cm.

A spurious signal was noted on the electric probe early in the investigation (shown by the arrow in Figure 5). Subsequent investigation without the microwave signal clearly showed that a current was generated in the crystal probe which was directly associated with the shock arrival (see Fig. 6).

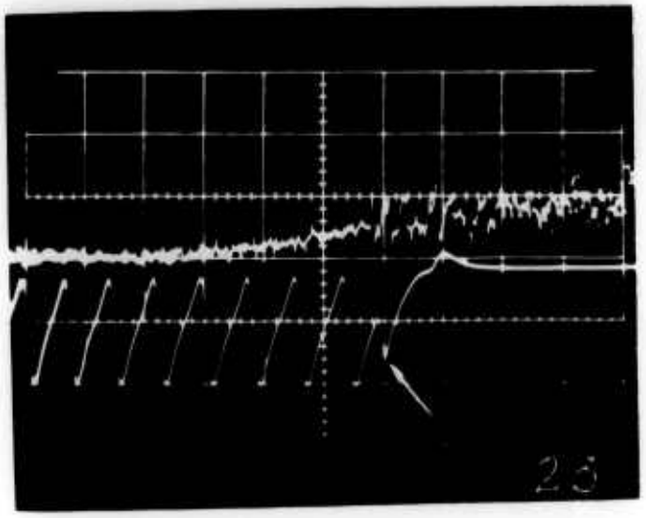

Figure 5.

Shot Number 23
Sweep Speed 50 μsec/cm.
Wavelength 22 cm.
Upper Trace: Pressure Detector
Lower Trace: Signal from microwave detector
Note: White arrow indicates interference signal.

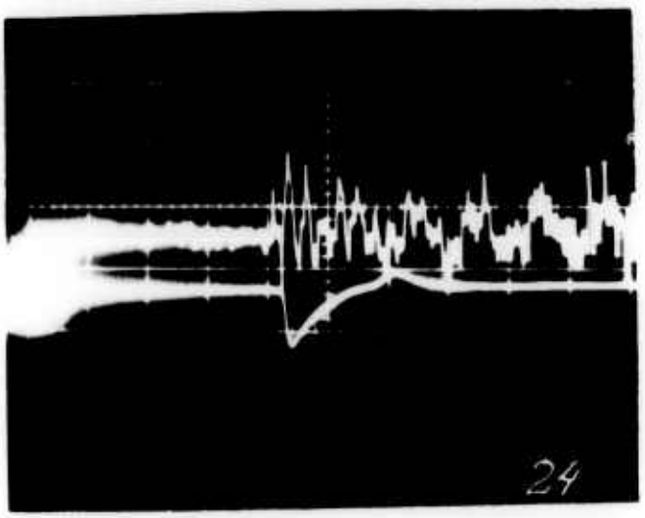

Figure 6.

Shot Number 24
Sweep Speed 50 μsec/cm.
Upper Trace: Pressure Detector
Lower Trace: Interference Signal.

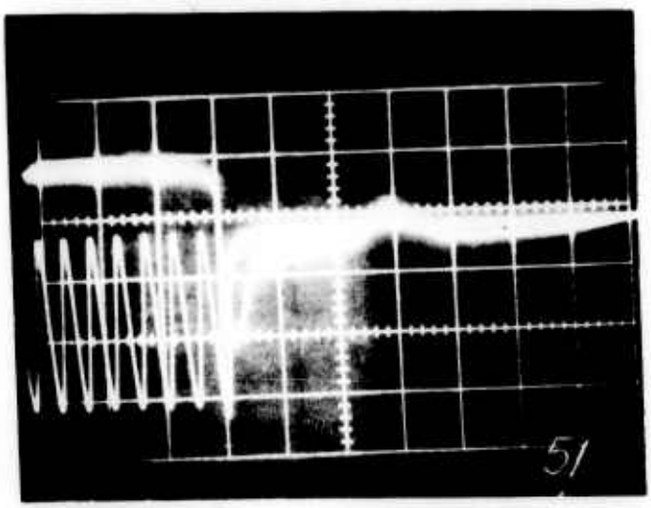

Figure 7.

Shot Number 51
Sweep Speed 100 μsec/cm.
Wavelength 22 cm.
Upper Trace: Signal from electrostatic probe (Amplification 1 V/cm)
Lower Trace: Signal from Microwave detector

A high impedance probe was made and inserted into the shock tube in place of the crystal detector. Following tests with and without microwave signal, typical voltage curves like that in Figure 7 were obtained.

Calculations conducted for a steady state condition of a uniform plasma in contact with a metallic wall indicates that a potential difference ϕ_o given by

$$\frac{e\phi_o}{KT_e} \simeq \frac{1}{2} \ln \frac{M_i}{M_e} \qquad (6)$$

must be established in order to have a zero electron current from the plasma to the wall. With the value of ion-electron mass ratio $\left(\frac{M_i}{M_e}\right)$ for argon, and an electron temperature(T_e) on the order of 10^4 ^oK, equation (6) gives a value of ϕ_o in the range of 3 volts. This value coincides with the measured potential on the electrostatic probe in Figure 7. This interference signal was removed by introducing a small parallel inductance on the RF side of the electric field probe.

The coupling of the microwave generator to the wave guide is an important consideration. The specific coupling condition is that if the wave guide was of infinite length, the reflected power through the antenna would be zero. Stated differently, if a metallic piston is placed in the wave guide, a standing wave pattern would be established such that a linear displacement of the piston would result in a proportional linear shift in a minimum of the standing wave pattern. Or, if an electric field detector is stationary to the wave guide and the piston is linearly displaced, the magnitude of the field will vary sinusoidally with the piston motion.

In the previous section, the character of the plasma generated in the shock tube was described. For the simplest approximation, the generated plasma could be considered as a uniformly ionized slug of gas radially filling the tube and extending about one meter behind the shock front. The electron density of this plasma denoted by n_e could be taken as the thermodynamic equilibrium value. If n_e is so large that the propagation constant k_z in equation (1) becomes an imaginary quantity, the shock front acts like a reflecting piston. The signal from a stationary electric field detector in front of the shock would vary sinusoidally with time as the shock moved towards it.

The time required to complete one sine cycle in the detector signal is related to the shock velocity by

$$\tau = \frac{\lambda_g}{2v}$$

where λ_g is the wave guide wavelength and v is the shock velocity.

Since λ_g and τ can easily be determined to better than 0.1%, the shock velocity can also measure to at least 0.1%.

In Figure 8a, a velocity history can be determined as the shock moves toward the detector at the end of the tube. This history is shown in Figure 8b and is typical of shock tube behavior. In Figure 8a, the increase in amplitude of the detected signal is due to the fact that the microwave signal is attenuated in the wave guide. Hence, the standing wave ratio decreases as the shock interface distance from the detector increases.

As the shock passes the detector, the character of the detected signal changes. To illustrate these changes, the set of graphs in Figure 9 have been prepared. In all cases, the time average of the transverse electric and magnetic field at the wave guide surface are shown. The dotted lines represent field

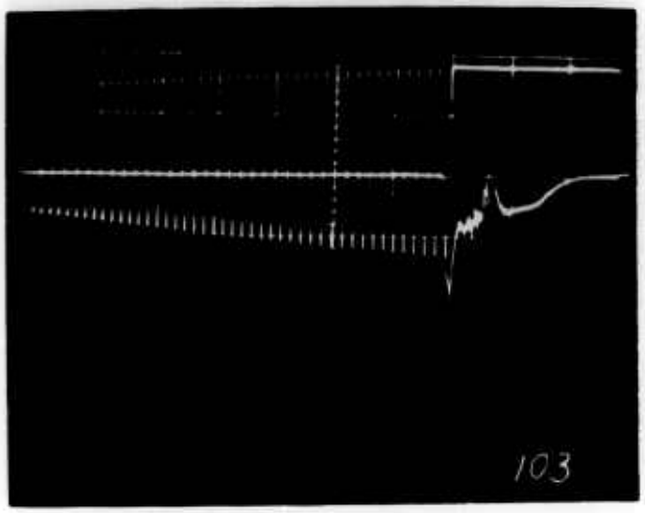

Figure 8a.

Shot Number 103
Sweep Speed .5 msec/cm.
Wavelength 44.4 cm.
Upper Trace: Signal from microwave detector
Lower Trace: Signal from electrostatic probe

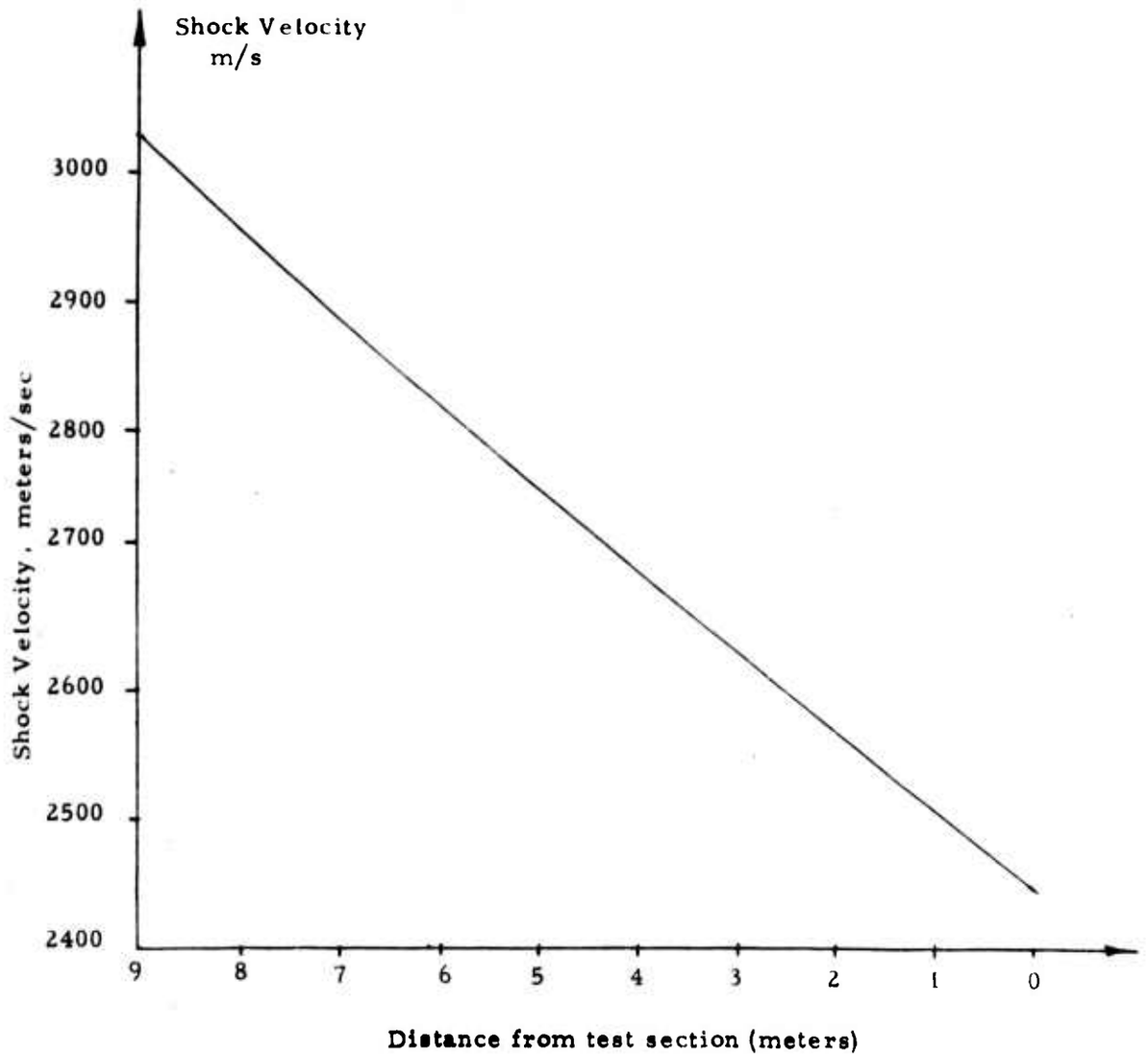

Figure 8b. Shock Velocity Vs Distance from Test Section

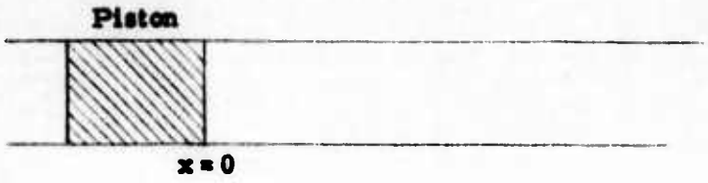

Figure 9a.

Metallic Piston

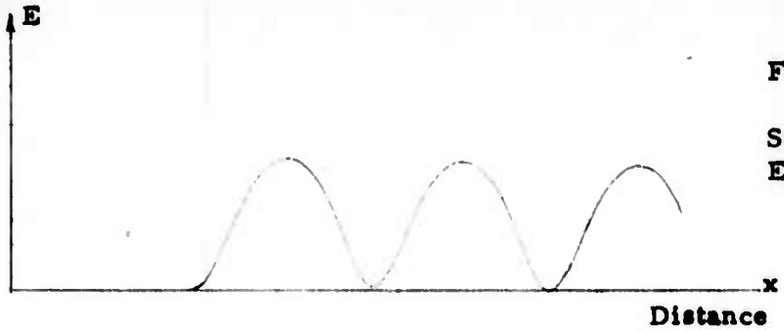

Figure 9b.

Signal from
Electric Field Detector

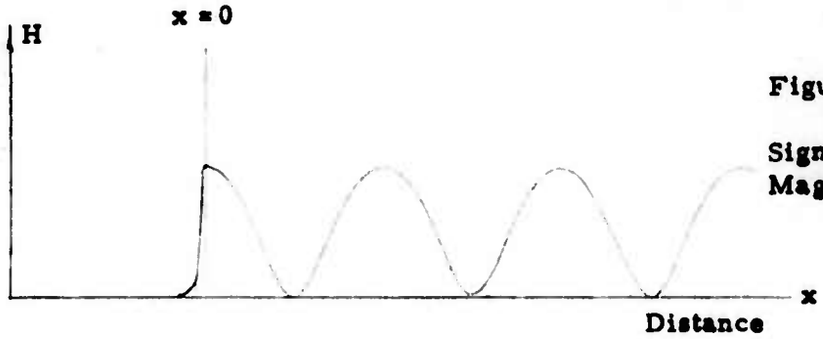

Figure 9c.

Signal from
Magnetic Field Detector

Figure 9d.

Steep Gradient Non-
Uniform Plasma

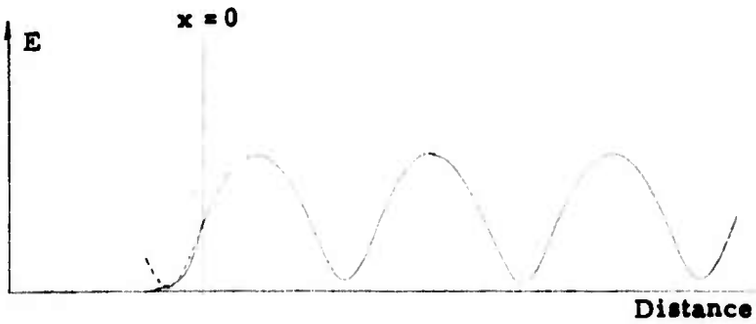

Figure 9e.

Signal from
Electric Field Detector

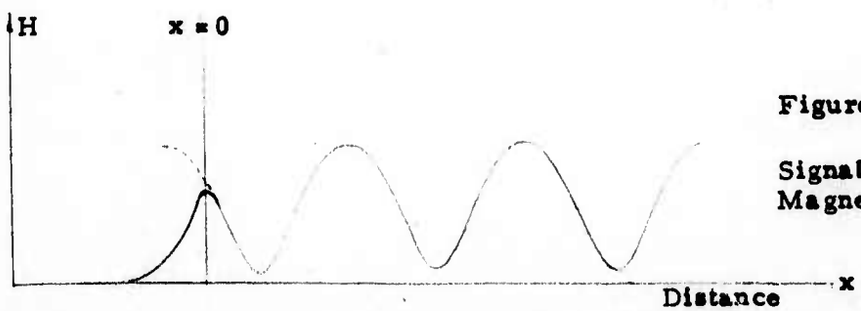

Figure 9f.

Signal from
Magnetic Field Detector

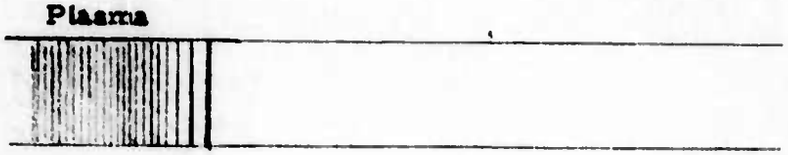

Figure 9g.
Medium Gradient
Non-Uniform Plasma

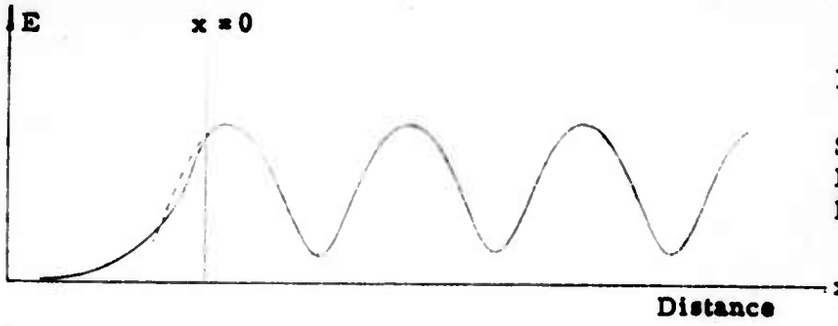

Figure 9h.

Signal from
Electric Field
Detector

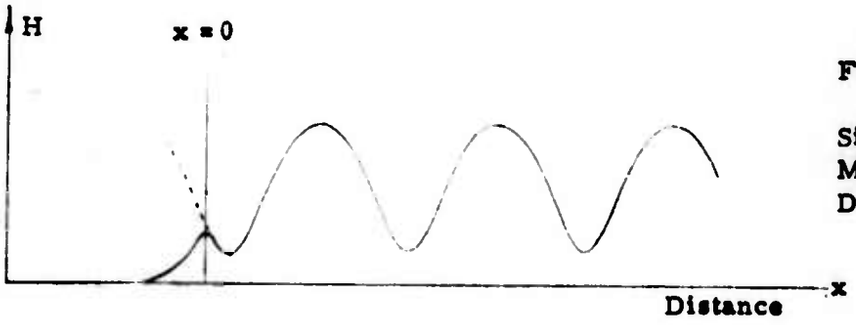

Figure 9i.

Signal from
Magnetic Field
Detector

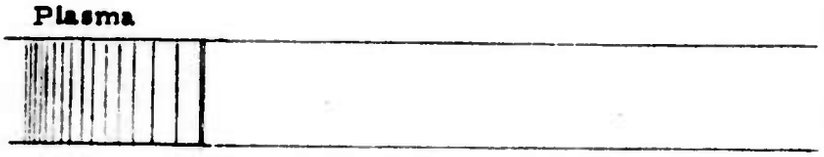

Figure 9j.

Slow Gradient
Non-Uniform Plasma

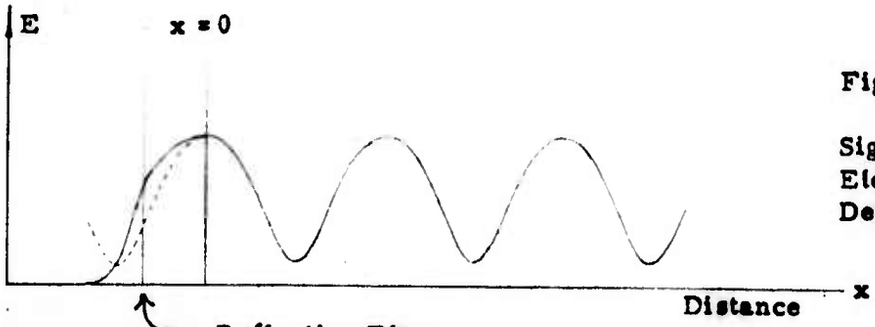

Figure 9k.

Signal from
Electric Field
Detector

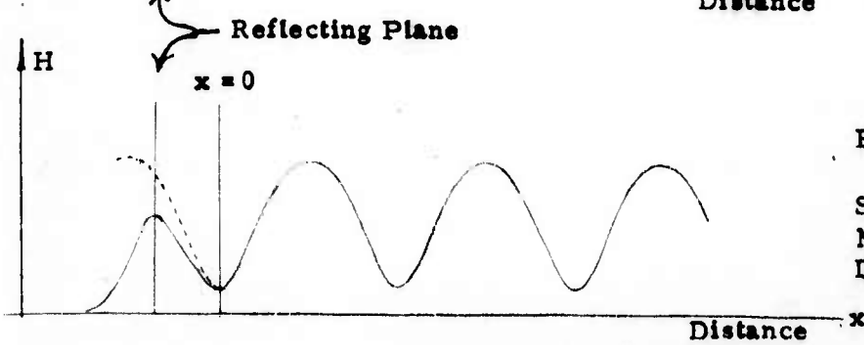

Figure 9ℓ.

Signal from
Magnetic Field
Detector

conditions of the previous cycle so as to contrast the change. If the reflecting surfaces (piston or plasma) are assumed moving, the field conditions are drawn in the frame of reference of the moving system. Hence a stationary detector would measure the field distributions in the reverse order. Since the experimental data have all been obtained using argon shocks, the plasma examples in Figure 9 illustrate field conditions for various axial electron density gradients, assuming some absorption inside the plasma.

In the case (a) of Fig. 9 the penetration inside the metallic piston is very small diminishing to zero as the resistivity approaches zero. Note that the transition in the transverse magnetic field occurs at its maximum and the converse occurs for the electric field. Case (d) for a steep plasma gradient is similar to (a) except that the penetration depth is greater. A typical experimental example of this case is shown in Figure 10. Similarly with case (g), where the plasma gradient is less steep than case (d) the penetration depth has increased and the departure points on the electric and magnetic field increase and decrease respectively. Note that the electric field inside the plasma decreases with a rate changing exponential since the electron density is increasing. Experimental behavior of this type is shown in Figure 11. An enlargement of Figure 11 has been made in Figure 12 where the detected electric field inside the plasma and the electric field of the previous cycle are compared.

Figures 13 and 14 were taken so that it would be possible to discern the departure points. These pictures were made using two electric field detectors. One amplified detector signal was fed to the horizontal deflection plates of a cathode ray tube, the other to the vertical plates. Spacially, these crystals were located several wavelengths apart on the shock tube. The trace becomes unblanked about three cycles before the shock passes the first detector. Hence,

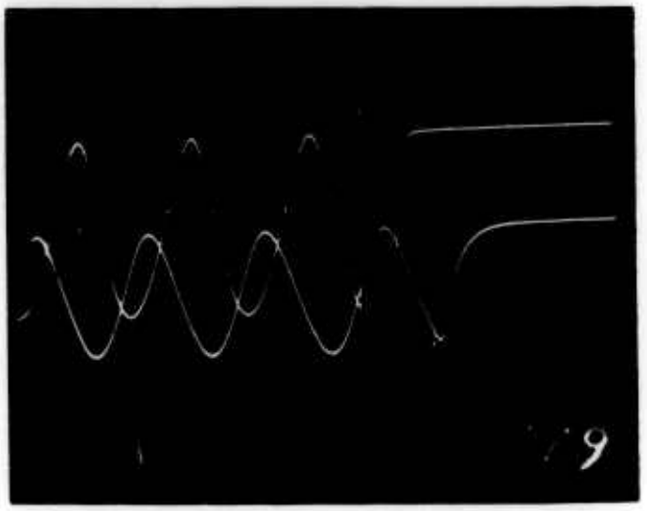

Figure 10.

Shot Number 179
Sweep Speed 20 μsec/cm.
Wavelength 18.9 cm.
Upper Trace: Signal from electric microwave detector
Lower Trace: Signal from magnetic microwave detector

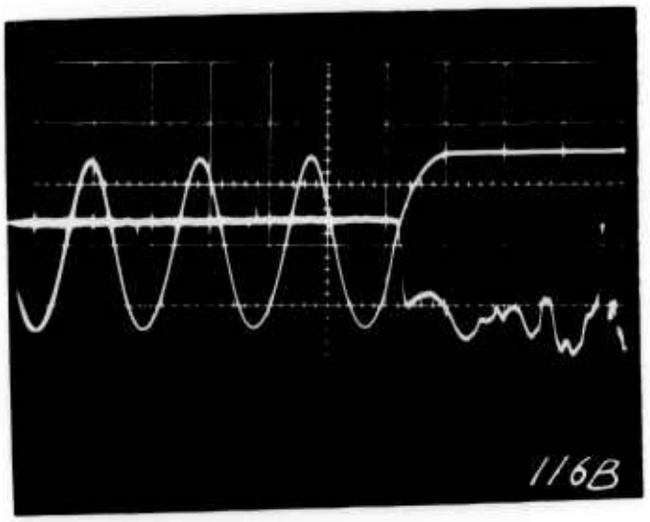

Figure 11.

Shot Number 116B
Sweep Speed 50 μsec/cm.
Wavelength 44.4 cm.
Upper Trace: Signal from electric microwave detector
Lower Trace: Signal from electrostatic probe.

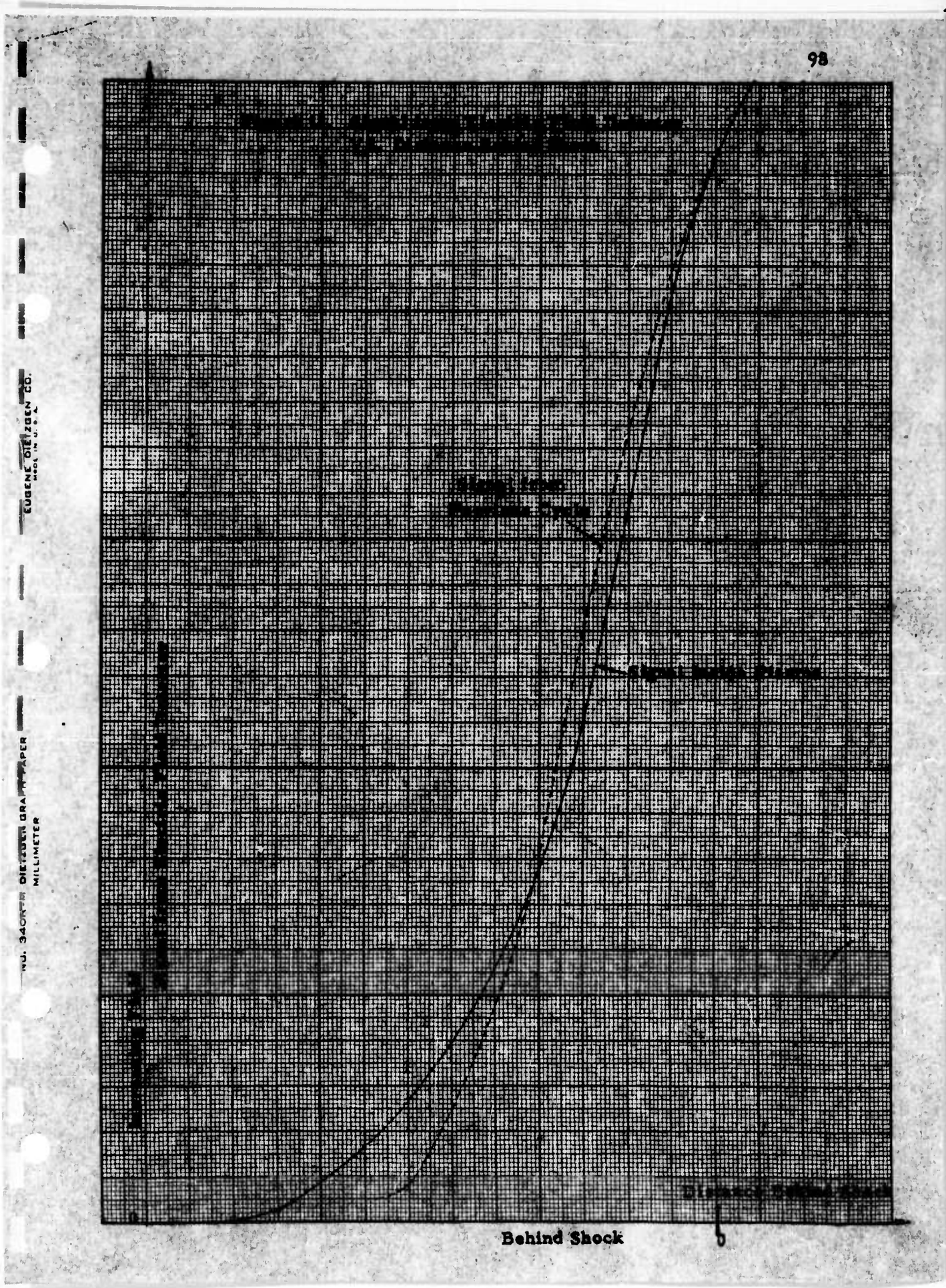
Behind Shock

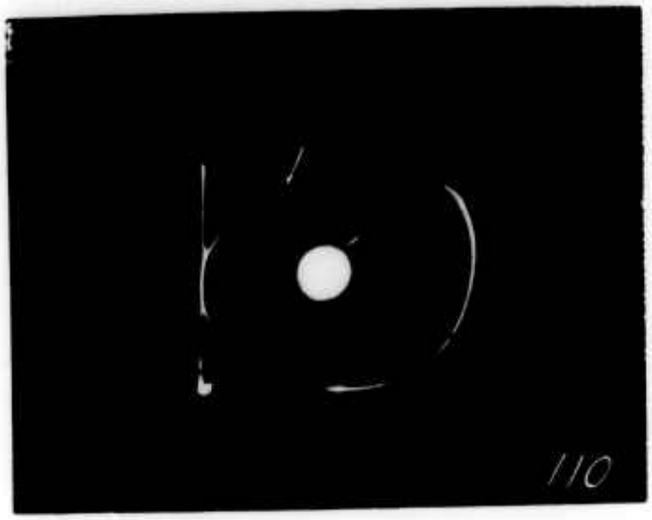

Figure 13.

Shot Number 110
Wavelength 44.4 cm.
Horizontal: Signal from microwave detector
Vertical: Reference signal

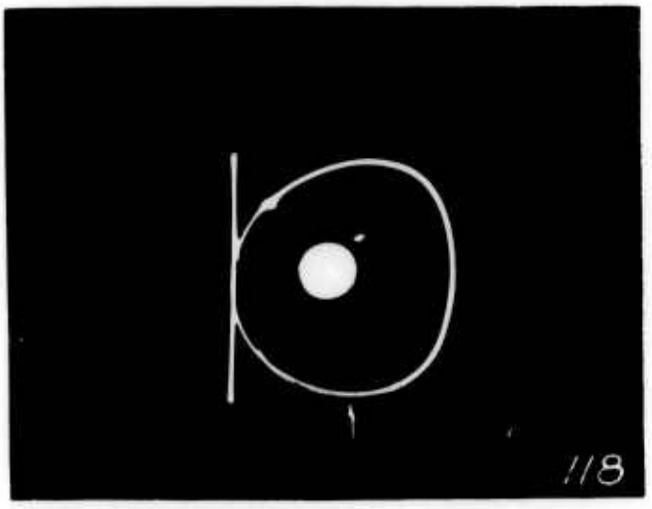

Figure 14.

Shot Number 118
Wavelength 44.4 cm.
Horizontal: Signal from microwave detector
Vertical: Reference signal

the normal standing wave sinusoid is established as an ellipse. (The non-symmetry is due to the nonlinearity of the detectors.) As the shock passes the first detector, the departure is clearly evident. The location of the departure relative to the shock front can be made by using the corresponding linear time scale picture.

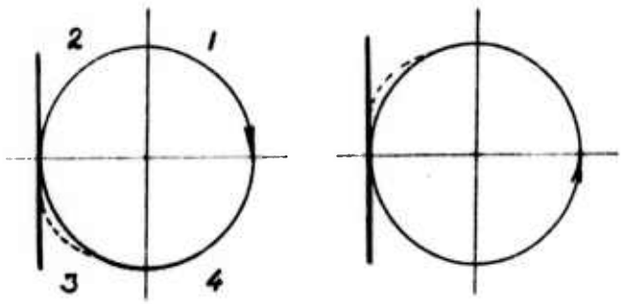

Fig. a.

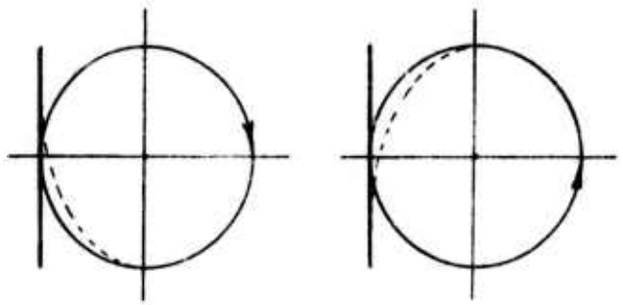

Fig. b.

Vertical - Reference Signal
Horizontal - Detector Signal

Figure 15.

Referring to Figure 15a, note that if the departure occurs on the outside of quadrant 2 or 3, the function is decreasing faster than the sine function and presumably denotes the rate-increasing type of exponential function. However, if the departure is opposite as shown in Figure 15b, the detected signal in the plasma is decreasing slower than the sine function and corresponds to the case described below. The arrows denote the direction of trace.

Case (j) of Figure 9 represents a possible field configuration if a slow axial gradient exists behind the shock. In this case, the critical electron density, where the propagation constant, k_z is zero, is located a long distance behind the physical shock front. Hence there is a region of the plasma behind the shock interface where:

$$\omega_p < \sqrt{\omega^2 - 2.17 \times 10^{20}}$$

In this region, the wave guide wavelength increases as n_e increases. In this case, no well defined point of total reflection occurs, and there is a continuous transition from the propagating wave to a decreasing amplitude of the signal which approaches zero in the region of high electron densities. This phenomena is illustrated in Figures 16 and 17.

It could be noted from Figure 9 that for all cases, the transverse magnetic field plot exhibits an abrupt change in character at the "reflecting point". This is because the magnetic field is always increasing on approach to the transition region. Hence, an abrupt change in slope should occur at the critical region in the case of a sharp transition of the plasma properties. Since the electron density increases as a continuous function, the critical plane of "total reflection" corresponds to a maximum in the magnetic detector signal.

3. INVESTIGATION OF THE PLASMA DENSITY BEHIND AN ARGON SHOCK

In the previous section, the technique for measuring electric and magnetic fields and their relation to the electron density were discussed. In particular, referring to Figure 9 (j and ℓ), the maximum of the magnetic field indicates the "reflecting point". This point is related to the electron density through

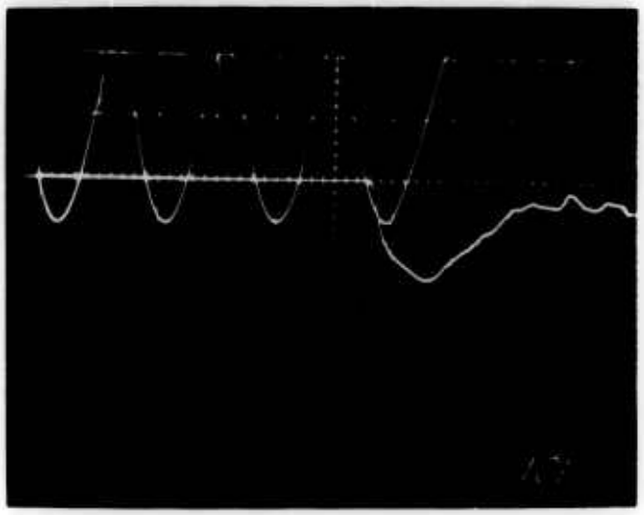

Figure 16.

Shot Number 101
Sweep Speed 50 μsec/cm.
Wavelength 44.4 cm.
Upper Trace: Signal from microwave detector
Lower Trace: Signal from electrostatic probe

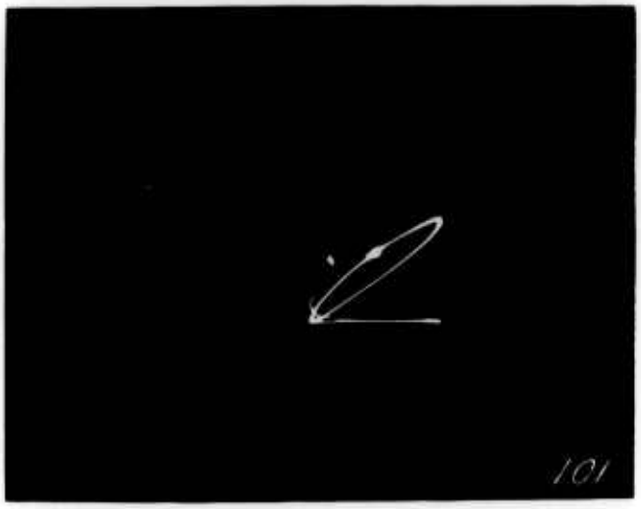

Figure 17.

Shot Number 101
Vertical: Signal from microwave detector
Horizontal: Reference signal

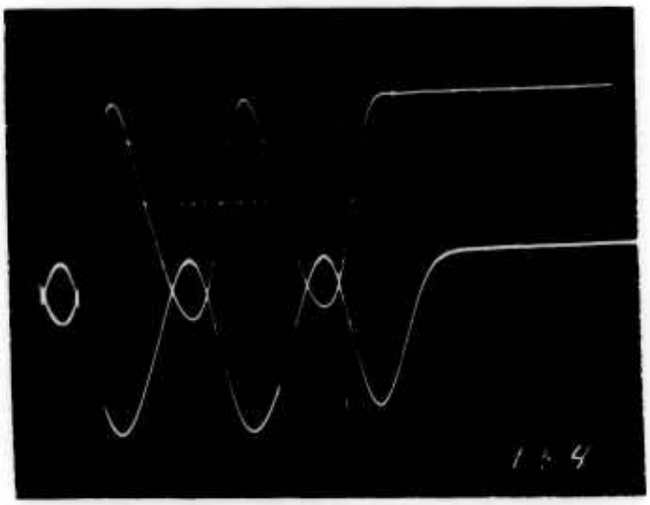

Figure 18.

Shot Number 164
Sweep Speed 20 μsec/cm.
Wavelength 22.49 cm.
Upper Trace: Signal from electric microwave detector
Lower Trace: Signal from magnetic microwave detector
Blanking: Pressure detector

equation (4) assuming the collision frequency zero. Hence, for each microwave frequency used, the electron density at the "reflecting point " is known. Thus, in principle, by repeating the same shock and changing the microwave frequency, a plot of electron density vs distance behind the shock can be made for the range of densities described in Section 2.

This general procedure was used to establish the density profile behind an argon shock for several shock velocities. However, rather than change the frequency between each shot (which is a laborious procedure since the system must be retuned , a series of tests were conducted at each frequency.

To mark the physical arrival of the shock, a crystal pressure probe was mounted flush with the tube's surface. The output from this crystal was fed to a pulse cricuit which in turn cut off the beam intensity of the measuring scope for 5 microseconds. A typical trace of the electric and magnetic probes is shown in Figure 18.

Note that a displacement correction must be made between the signals since the probes are located 3 cm apart along the axis of the tube. This correction is made by first determining the velocity as described in Section 2. Since the distance between probes is known,by using the measured velocity, a time correction of events is made, and the distance between shock arrival and "reflecting point" can be determined.

Using this procedure, Figures 19, 20, and 21 were obtained. From these curves, a composit curve can be drawn showing the electron density as a function of distance behind the shock for various shock velocities (Figure 22). The degree of randomness in the experimental values is due to the uncertainties which

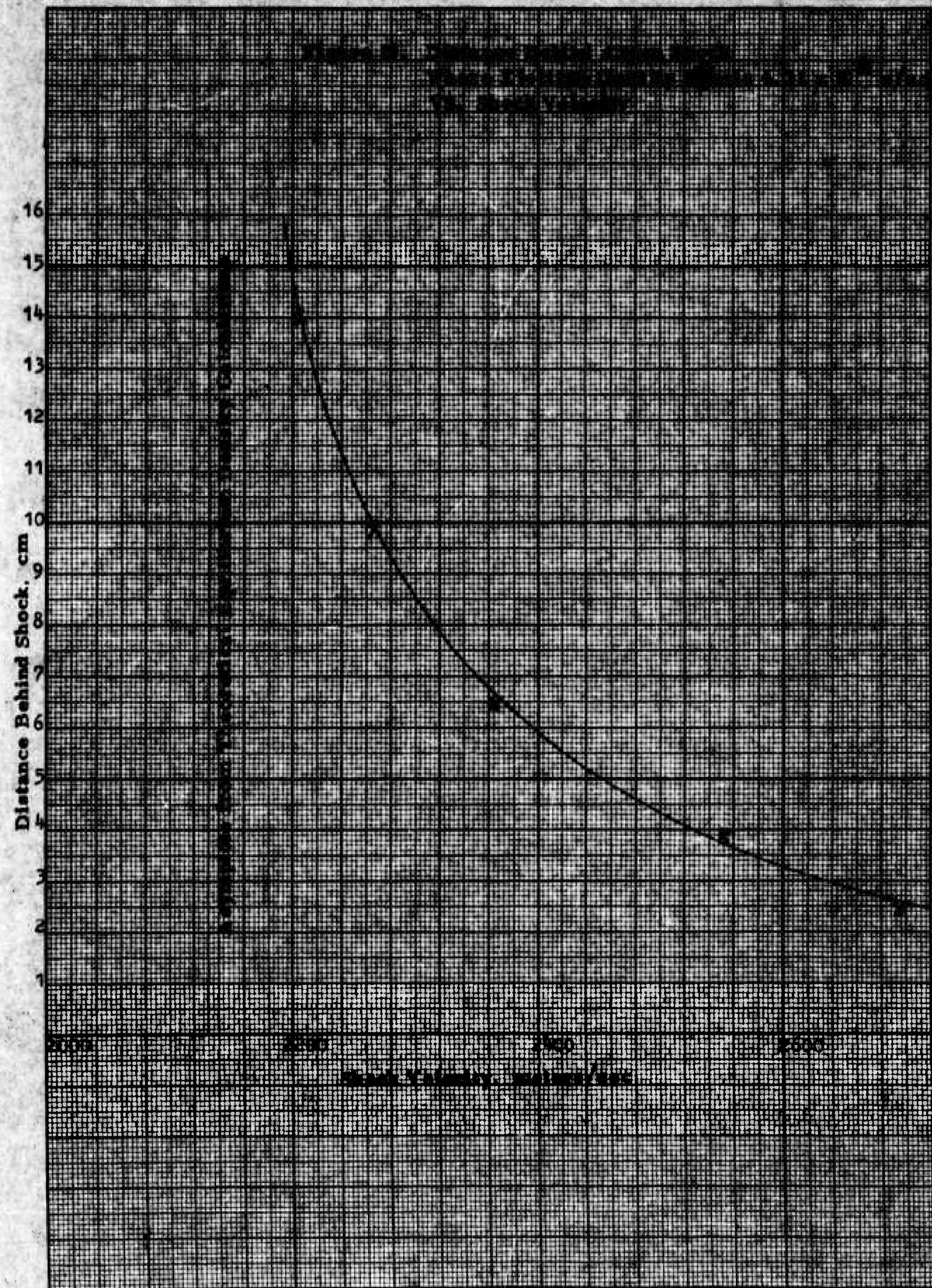

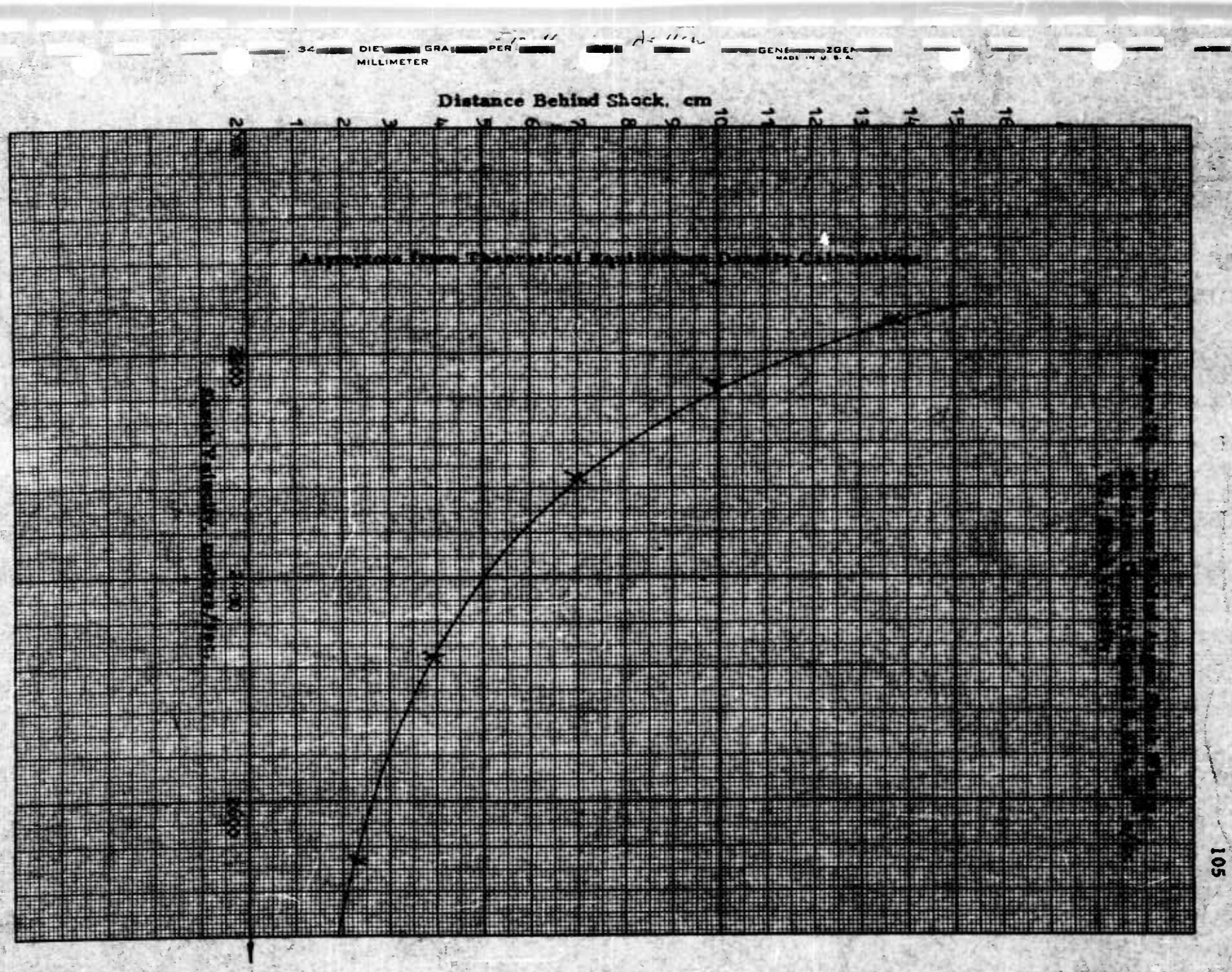
MILLIMETER
MADE IN U.S.A.
Distance Behind Shock, cm
Asymptote from Theoretical Equilibrium Density Calculation

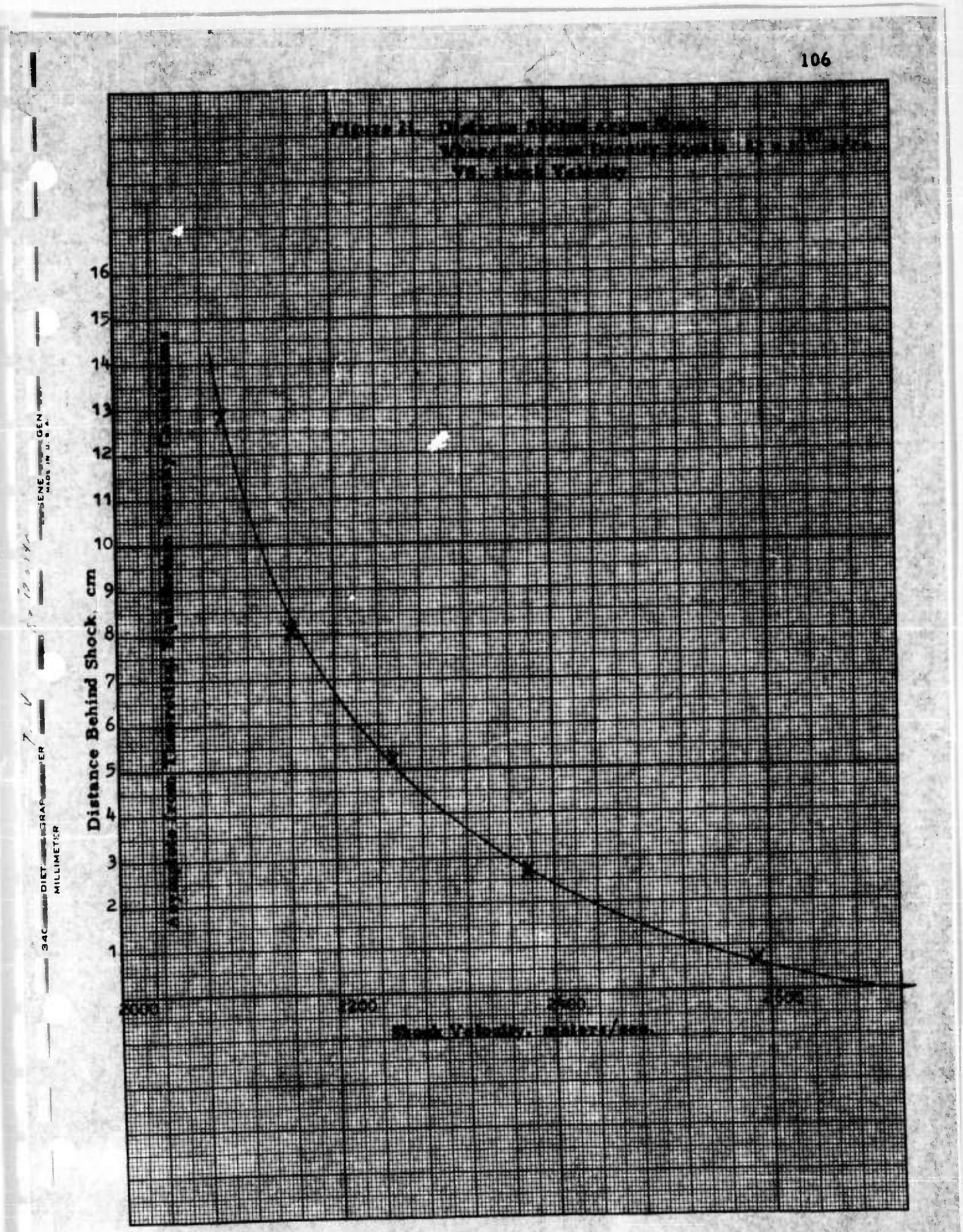
Distance Behind Shock, cm
16
15
14
13
12
11
10
9
8
7
6
5
4
3
2
1
2000
2200
2400
Shock Velocity, meters/sec.

Figure 22. Electron Density VS. Distance Behind Argon Shock

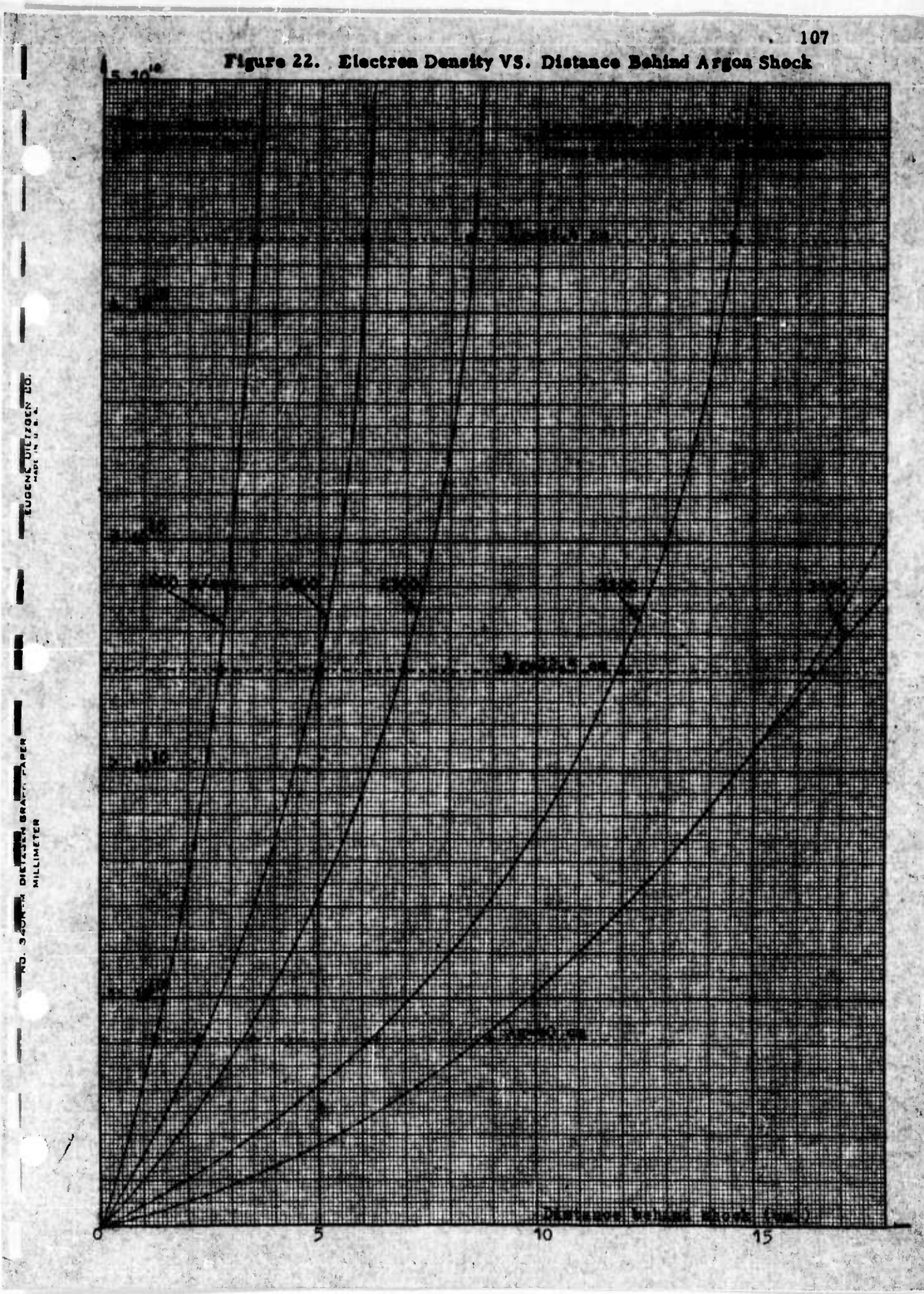

were previously discussed. Actually, the results are surprisingly good taking into account that the ionization rate of argon is a very sensitive function of impurity content.

Since the purpose of this particular investigation was to demonstrate the capability of the measuring technique, no special precautions regarding the impurity of the argon were taken. It might be noted that the data presented was obtained by using argon from the same tank. Upon changing tanks, a completely different set of curves was obtained. The estimated impurity content is between 10^{-3} and 10^{-4} for the data presented.

The theoretical equilibrium electron densities for argon are computed as an appendix to this section. From these results, asymptotes can be located on the curves in Figures 19, 20, 21, and 22. The relation shown between measured and theoretical electron densities indicates the high precision which can be attained with this technique.

An independent correlation of these results is presented in Figure 23. The relaxation time defined by the other investigators refers to the degree of ionization as measured by the luminosity of the plasma. These authors claim a direct relation between the luminosity and the electron density. The point plotted from our data represent a relaxation time defined as the time required for the plasma to attain 60% of its equilibrium value.

Because of the possible ambiguity in the definitions of τ, only an order of magnitude agreement is meaningful. If the results for impurity content in the range of 10^{-3} to 10^{-4} are extrapolated, such an agreement is clearly evident.

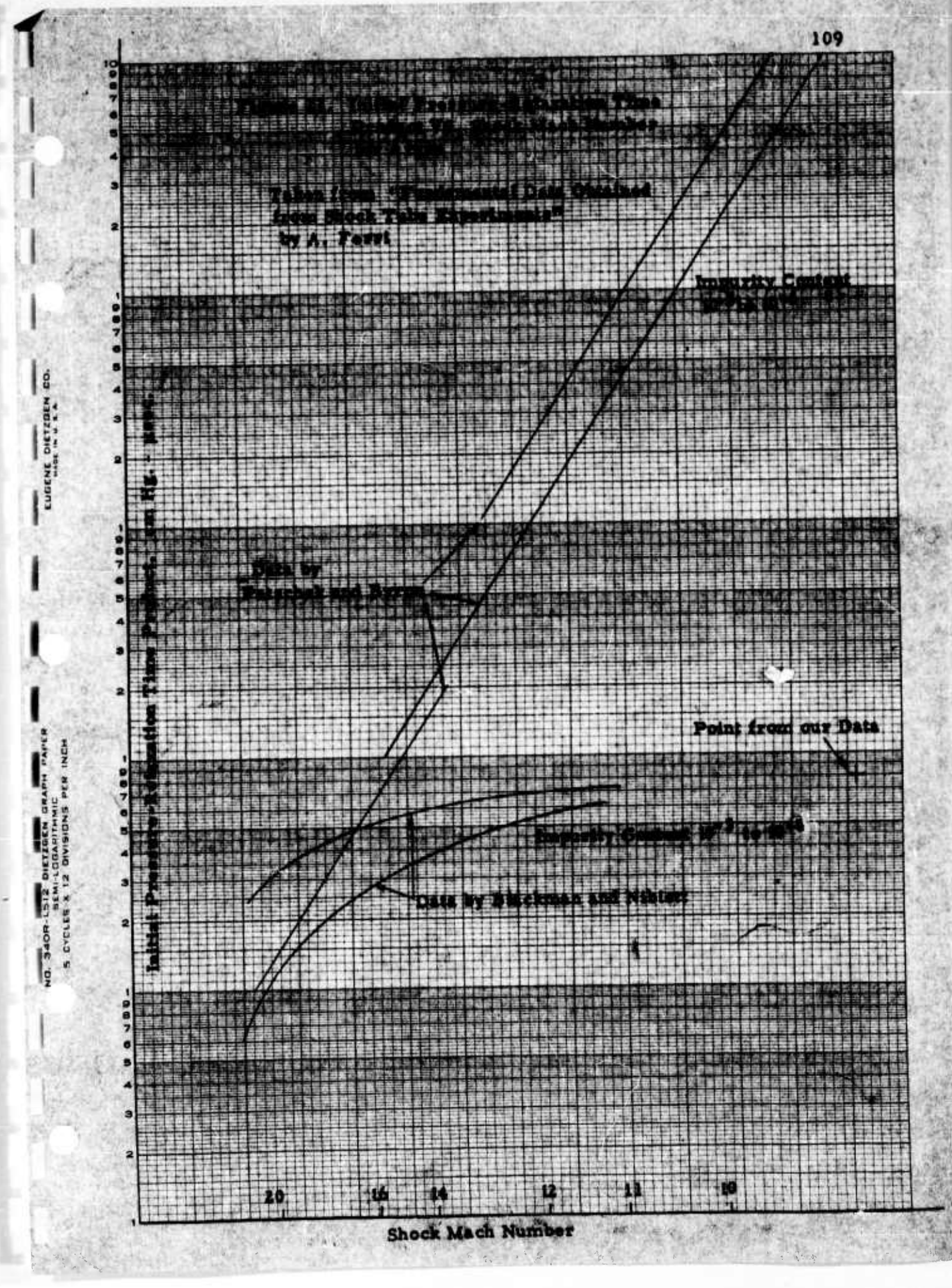
Taken from "Measured Data Obtained from Shock Tube Experiments"
by A. Ferri
Data by
Fairbank and Ferri
Point from our Data
Data by Blackman and Nisbet
Shock Mach Number
Initial Pressure-Ionization Time Product, cm Hg. x μsec.
EUGENE DIETZGEN CO.
NO. 340R-LS12 DIETZGEN GRAPH PAPER
SEMI-LOGARITHMIC
5 CYCLES X 12 DIVISIONS PER INCH

4. FUTURE WORK

Since the argon shock has been demonstrated to be a simple and predictable method of obtaining an axially nonuniform plasma, further experiments will be made using argon to check the analysis of Chapter V. When satisfactory correlation of this analysis has been accomplished, our investigation will be directed toward plasma gradients in air shocks.

APPENDIX A TO CHAPTER IV

EQUILIBRIUM SHOCK CALCULATION FOR PURE ARGON

Equilibrium conditions behind normal shock waves in argon have been computed using a method outlined by E. L. Resler, S. C. Lin, and A. Kantrowitz in The Production of High Temperature Gases in Shock Tubes, Journal of Applied Physics, Vol. 23, No. 12 (December 1952). The calculation considers single ionization of the argon atom, but electronic excitation and multiple ionization are ignored. The assumptions used introduce errors of 1 - 2% at 15,000°K, and are considerably more accurate at lower temperatures.

The conservation equations for mass, momentum, and energy, plus the equation of state and pertinent thermodynamic relationships have been written for argon undergoing the ionization reaction:

$$A \rightleftharpoons A^{+} + e^{-}$$

The subscripts 1 and 2 denote conditions in front of and behind the shock, and the units used are:

density, ρ, slugs/ft^3

pressure, p, atm

velocity, u, a, ft/sec

temperature, T, °K

enthalpy, h, ft^2/sec^2

electron density, n_e, particles/cm^3

and α is the fractional degree of ionization of argon.

$$\rho_1 M_s = \rho_2 \left(M_s - \frac{u_2}{a_1}\right)$$

$$2116.8\, p_1 + \rho_1 a_1^2 M_s^2 = 2116.8\, p_2 + \rho_2 a_1^2 \left(M_s - \frac{u_2}{a_1}\right)^2$$

$$h_1 + \frac{1}{2} a_1^2 M_s^2 = h_2 + \frac{1}{2} a_1^2 \left(M_s - \frac{u_2}{a_1}\right)^2$$

$$h = 5.637 \times 10^3 (1 + a) T + 4.075 \times 10^8 a$$

$$a = \left[2.540 \times 10^5 \frac{p}{T^{5/2}} \exp\left(\frac{1.821 \times 10^5}{T}\right) + 1\right]^{-1/2}$$

$$p = 1.065 (1 + a) \rho T$$

$$a_1 = 61.3\, T_1^{1/2}$$

$$n_e = 7.39 \times 10^{21} \frac{a}{1 + a} \frac{p}{T}$$

An iterative solution scheme was programmed for the Bendix G-15 digital computer using the overrelaxation method. Thus, given input conditions M_s, p_1, and T_1, conditions behind the shock may be obtained.

Figures 24 and 25 present some calculated electron densities as functions of shock velocity and initial pressure. The initial temperature was 300°K, and it was found that the same results are also valid for somewhat lower initial temperatures.

Equilibrium Electron Density (electrons/cc)
Velocity of shock (m/sec.)
1800
2000
2500
3000
EUGENE DIETZGEN CO.
MADE IN U.S.A.
SEMI-LOGARITHMIC
5 CYCLES X 12 DIVISIONS PER INCH

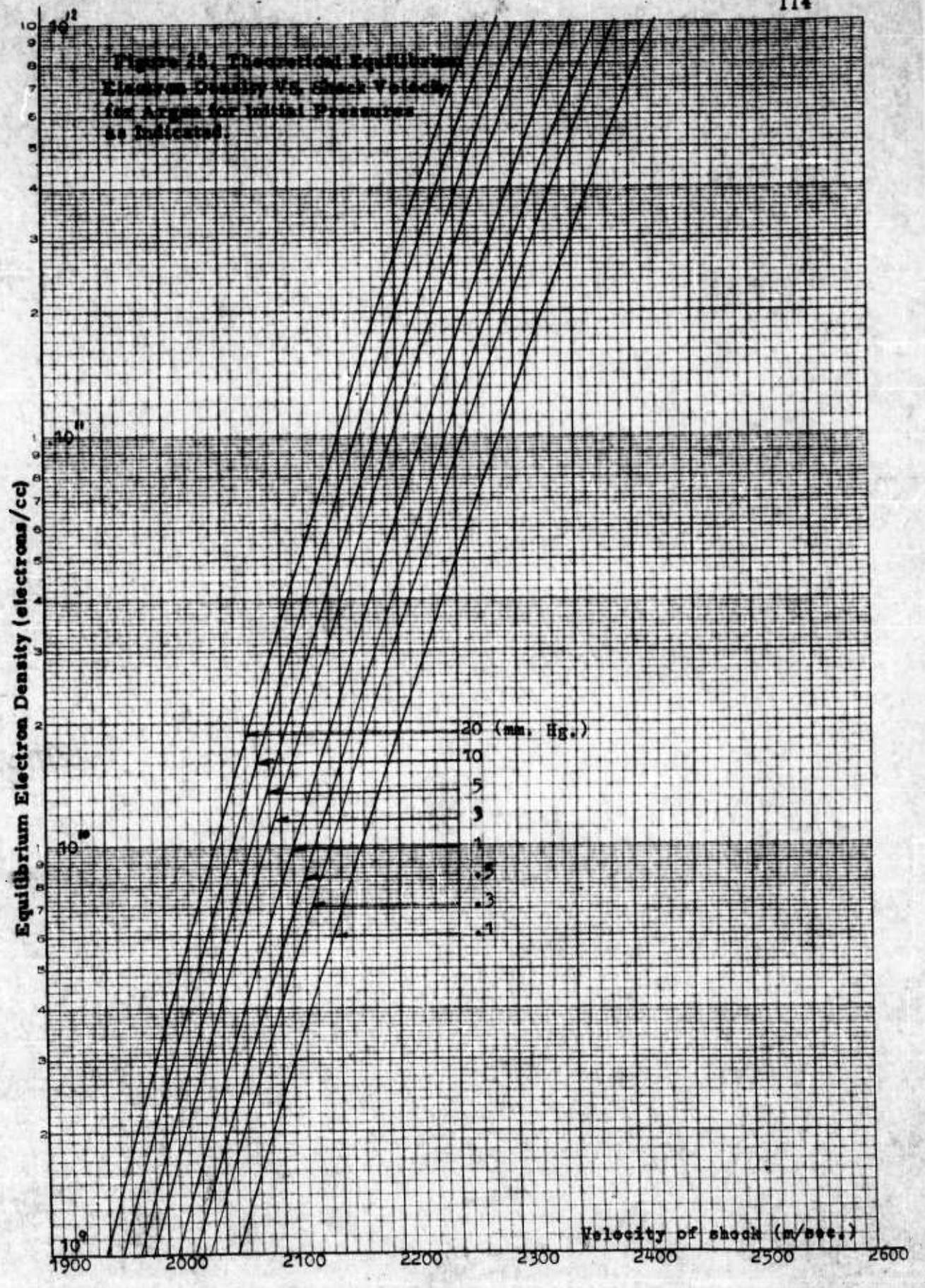

Figure 15. Theoretical Equilibrium Electron Density Vs. Shock Velocity for Argon for Initial Pressures as Indicated.

CHAPTER V

ANALYSIS OF THE ELECTROMAGNETIC FIELD WITHIN A CIRCULAR WAVE GUIDE CONTAINING AN AXIALLY NONUNIFORM PLASMA

INTRODUCTION

The purpose of this chapter is to relate analytically the local electromagnetic properties of the plasma with measurements of certain field parameters at the boundary of the wave guide. In order to fix ideas consider a semi-infinite circular wave guide of radius R whose walls constitute a perfect conductor. Let this guide be filled with a plasma having properties that may vary arbitrarily only in the axial or z-direction. The configuration so described is a simplified representation of the shock tube at any given time during the propagation of the pressure pulse down the tube. Ahead of the disturbance the medium is yet unaffected, and all properties are uniform. As the disturbance is transversed in the z-direction, the pressure and temperature of the medium are drastically altered, as are its properties. Variations of properties and parameters in the radial direction are neglected here, and such effects are discussed elsewhere*.

If electromagnetic radiation is introduced into the end of the tube toward which the pressure pulse is moving, the radiation will progress down the tube through multiple reflections from the perfectly conducting walls of the tube until it encounters the ionized medium at the shock front. At this point reflection and absorption of the radiation will begin to occur and this phenomena will continue as the radiation advances into the plasma until the energy is completely returned or dissipated. The resulting field at any point within the tube is thus

---

* For example, see General Applied Science Laboratories, Inc., Technical Report No. 255.

a composite of the original radiation introduced and that reflected back from that portion of the plasma extending beyond the location in question. Clearly the field pattern will be characteristic of the axial distribution of electromagnetic properties within the tube, for any alteration in this distribution would result in different degrees of absorption and reflection at each point along the tube, and thus the resultant field would be changed.

It will be shown in this chapter that for the simple plasma model studied, namely one described by the two independent properties of collision frequency ν and plasma frequency ω_p, the two characteristic properties may be measured indirectly through measurement of the time-average of the square of the radial component of the electric field and a similar average for the tangential component of the magnetic field and the axial derivatives of these quantities.

In view of the fact that we have assumed that the properties are uniform at any given axial position, such measurements may be carried out at the wall of the tube where $r = R$ rather than by the use of probes immersed in the medium and tending to alter the environment. In order to measure the axial variation, the detector need merely traverse the tube in the axial direction, or, what is equivalent and actually used, a stationary detector measures the desired parameters as the pressure pulse moves down the tube carrying with it the characteristic field distribution.

In the analysis to follow the rationalized mks system of units is used throughout, and the nomenclature is the conventional one and is thus self-explanatory.

I. FIELD EQUATIONS

The electromagnetic field within the wave guide described in the preceding section is determined from the Maxwell equations

$$\nabla \times \bar{E} = -\mu \frac{\partial \bar{H}}{\partial t} \tag{1}$$

$$\nabla \times \bar{H} = \bar{J} + \epsilon \frac{\partial \bar{E}}{\partial t} \tag{2}$$

their associated initial conditions, with the assumption of no net space charge,

$$\nabla \cdot \bar{E} = 0 \tag{3}$$

$$\nabla \cdot \bar{B} = 0 \tag{4}$$

and a momentum equation relating the current density to the electric field:

$$\epsilon \omega_p^2 \bar{E} = \nu \bar{J} + \frac{\partial \bar{J}}{\partial t} \tag{5}$$

The plasma is nonmagnetic and unpolarized so that the permeability μ and permittivity ϵ are the free space values. The plasma frequency ω_p and collision frequency ν are assumed to depend upon the axial coordinate z with the former defined by the relation

$$\omega_p^2 \equiv \frac{ne^2}{m\epsilon} \tag{6}$$

where n is the electron number density, e its charge, and m its mass.

It is of interest to note that for a transverse electric mode ($E_z = 0$) the current given by (5) is also transverse and is thus perpendicular to the gradient of the electron density or plasma frequency. This behavior is consistent with our assumption of a steady distribution of electron density depending upon the axial coordinate alone, and the TE mode will be the only mode considered in this analysis.

The natural system of coordinates for this problem is the circular cylindrical system (r, θ, z) with the positive z-direction being taken as opposite to the direction in which the pressure pulse is moving. The boundary conditions are the conventional ones, namely that the tangential component of the electric field vanish at the surface of the perfect conductor, that the field be finite at the axis of the tube, and that the field vanish infinitely far into the plasma. Expressed mathematically, we have, noting that we have postulated a TE mode for which $E_z = 0$ everywhere,

$$\text{at } r = R: \qquad E_\theta = 0 \tag{7}$$

$$\text{at } r = 0: \qquad \vec{E} \text{ finite} \tag{8}$$

$$\text{as } z \to \infty: \qquad \vec{E} \to 0; \ \vec{H} \to 0 \tag{9}$$

It may be shown that the necessary condition that the normal component of the magnetic field vanish at the wall is automatically satisfied by the above conditions.

Following the usual procedures, the pertinent components of the field satisfying the above relations may be shown to be, apart from a factor $e^{i\omega t}$,

$$E_r = \frac{1}{r} J_n(\gamma_k r)\, e^{in\theta} w(z) \qquad (n \geq 1) \tag{10}$$

$$H_\theta = \frac{i}{\mu\omega} \frac{w'}{w} E_r \qquad \left(w' \equiv \frac{dw}{dz}\right) \tag{11}$$

where J_n is the Bessel function of the first kind of order n and the constant γ_k may have any of the discrete values given by the roots of

$$J_n'(\gamma_k R) = 0 \tag{12}$$

The function $w(z)$ is the solution of

$$w'' + \left(\frac{\omega^2}{c^2} \kappa^2 - \gamma_k^2\right) w = 0 \tag{13}$$

$$w = w' \to 0 \quad \text{as} \quad z \to \infty \tag{13a}$$

where ω is the circular frequency of the introduced radiation and c the free space velocity of light,

$$c^2 = \frac{1}{\mu \epsilon} \tag{14}$$

The parameter κ is the so-called complex refractive index of the medium and is defined by the expression

$$\kappa^2 \equiv 1 - \frac{\phi^2}{1 - i\psi} \tag{15}$$

with $$\phi \equiv \frac{\omega_p}{\omega} \tag{16}$$

$$\psi \equiv \frac{\nu}{\omega} \tag{16a}$$

It should be noted that κ is a function of z so that the solution of equation (13) must in general be determined numerically.

Finally, we define for convenience the quantity

$$A_{nk}(\theta) \equiv i \frac{J_n(\gamma_k R)}{\mu \omega R} e^{in\theta} \tag{17}$$

so that at the surface of the wave guide we may express the two field components of interest in the form

$$E_r = - i\omega\mu A_{nk} w(z) \tag{18}$$

$$H_\theta = A_{nk} w'(z) \qquad \underline{r = R} \tag{19}$$

In all that precedes it is of course understood that the actual field is given by the real parts of the complex expressions which appear above after first multiplying by the factor $e^{i\omega t}$.

2. EXPRESSIONS RELATING AXIAL VARIATION OF FIELD TO $(E_r^2)_{AV}$ AND $(H_\theta^2)_{AV}$

It may be shown that the value of $(E_r^2)_{AV}$, which denotes the time-average of the square of the radial component of the electric field is given exactly by the relation

$$(E_r^2)_{AV} = \frac{1}{2} E_r E_r^* \tag{20}$$

where E_r on the right side of the equation is the complex expression given by equation (10) or (18) and E_r^* denotes its complex conjugate obtained by replacing i with -i in the original expression. Similarly,

$$(H_\theta^2)_{AV} = \frac{1}{2} H_\theta H_\theta^* \tag{21}$$

where H_θ on the right side of the equation is the complex representation of the field given by equation (11) or (19). In each case the factor $e^{i\omega t}$ disappears and further, because of the manner in which the θ-dependence enters, namely in the form $e^{in\theta}$, this factor also disappears when multiplied by its conjugate. Thus, the quantities $E_r E_r^*$ and $H_\theta H_\theta^*$ depend upon only the radial and axial coordinates. In particular, at r = R, we have using equations (18) and (19),

$$2(E_r^2)_{AV} = E_r E_r^* = \omega^2 \mu^2 A_{nk} A_{nk}^* w w^* \tag{22}$$

$$2(H_\theta^2)_{AV} = H_\theta H_\theta^* = A_{nk} A_{nk}^* w' w'^* \qquad \underline{r = R} \tag{23}$$

The importance of these relations lies in the fact that the axial distribution of the quantities ww^* and $w'w'^*$ may thus be determined at the surface of the wave guide for any mode through measurement of the two quantities $(E_r^2)_{AV}$ and $(H_\theta^2)_{AV}$. We may now use these measurements to determine κ.

3. DETERMINATION OF THE SQUARE OF THE LOCAL COMPLEX REFRACTIVE INDEX, κ^2

The complex retractive index κ is related to the function w(z) through the differential equation (13), or equivalently

$$\frac{\omega^2}{c^2}\,\kappa^2 - \gamma_k^2 = -\frac{w''}{w} \tag{24}$$

For convenience, we now define the complex function F(z) by the left side of (24), namely

$$F(z) \equiv \frac{\omega^2}{c^2}\,\kappa^2 - \gamma_k^2 \tag{25}$$

We desire the real and imaginary parts of F(z), and thus through (25), determine κ.

The real part of F(z), using (24) and (25) is evidently given by

$$2\,\mathrm{Re}\,F \equiv 2F_r = -\frac{w''}{w} - \frac{w''^*}{w^*} = -\frac{w''w^* + w''^* w}{ww^*} \tag{26}$$

Noting that the derivative of the conjugate is equivalent to the conjugate of the derivative, i.e.,

$$w'^* \equiv w^{*\prime} \tag{27}$$

and using the identities

$$(w'w^*)' \equiv w''w^* + w'w^{*\prime} \tag{28a}$$

$$(w^{*\prime}w)' \equiv w^{*\prime\prime}w + w^{*\prime}w' \tag{28b}$$

Equation (26) may be written

$$2F_r = -\frac{(ww^*)'' - 2w'w^{*\prime}}{ww^*}$$

and

$$F_r = \frac{w'w^{*'}}{ww^*} - \frac{1}{2}\frac{(ww^*)''}{ww^*} \tag{29}$$

Referring now to equations (22) and (23), we have

$$F_r = \omega^2\mu^2\,\frac{H_\theta H_\theta^*}{E_r E_r^*} - \frac{1}{2}\frac{(E_r E_r^*)''}{E_r E_r^*} = \omega^2\mu^2\,\frac{(H_\theta^2)_{AV}}{(E_r^2)_{AV}} - \frac{1}{2}\frac{(E_r^2)''_{AV}}{(E_r^2)_{AV}} \tag{30}$$

and thus F_r is determined in terms of measured quantities.

The procedure for determining the imaginary part of F is similar, but not as straightforward. Analogous to equation (26), we have

$$2i\,F_i = -\frac{w''}{w} + \frac{w''^*}{w^*} = \frac{\left[ww^*\left(\frac{w'^*}{w^*} - \frac{w'}{w}\right)\right]'}{ww^*} \tag{31}$$

and by an obvious transformation

$$F_i = -\frac{\left[ww^*\,\mathrm{Im}\,\frac{w'}{w}\right]'}{ww^*} \tag{32}$$

The function w'/w may be determined in the following way. First we note that

$$\frac{w'}{w} + \frac{w'^*}{w^*} = \frac{(ww^*)'}{ww^*} \equiv a \tag{33}$$

where a is a measurable function. Also, another measurable function is

$$\frac{w'w^{*'}}{ww^*} \equiv b \tag{34}$$

Solving (33) and (34) simultaneously for w'/w, we have

$$\frac{w'}{w} = \frac{a}{2}\left[1 \pm \sqrt{1 - 4\,\frac{b}{a^2}}\right] = \frac{1}{2}\,\frac{(ww^*)'}{(ww^*)}\left[1 \pm \sqrt{1 - 4\,\frac{(w'w^{*'})(ww^*)}{[(ww^*)']^2}}\right] \tag{35}$$

Returning to equation (32) we now have, substituting from equation (35),

$$\text{Im}\ \frac{w'}{w} = \pm\ \frac{1}{2}\ \frac{(ww^*)'}{(ww^*)}\ \sqrt{4\ \frac{(w'w^{*\prime})\ (ww^*)}{[(ww^*)']^2} - 1} \tag{36}$$

$$F_i = \pm\ \frac{\left[(ww^*)'\ \sqrt{4\ \frac{(w'w^{*\prime})\ (ww^*)}{[(ww^*)']^2} - 1}\right]'}{2\ ww^*} \tag{37}$$

Using again equations (22) and (23), we have finally

$$F_i = \pm\ \frac{\left[\sqrt{4\omega^2\mu^2\ (H_\theta^2)_{AV}\ (E_r^2)_{AV} - \left[(E_r^2)'_{AV}\right]^2}\right]'}{2\ (E_r^2)_{AV}} \tag{38}$$

The choice of sign in equation (38), as will be seen in the next section, is made to yield a positive collision frequency.

The real and imaginary parts of κ or κ^2 may now be determined directly from equation (25),

$$\kappa^2 = \frac{c^2}{\omega^2}\ F + \frac{c^2}{\omega^2}\ \gamma_k^2 \equiv R + iI \tag{39}$$

Thus,

$$\text{Re}\ \kappa^2 \equiv R = \frac{c^2}{\omega^2}\ \left[F_r + \gamma_k^2\right] \tag{40}$$

$$\text{Im}\ \kappa^2 \equiv I = \frac{c^2}{\omega^2}\ F_i \tag{41}$$

4. PLASMA FREQUENCY AND COLLISION FREQUENCY

The desired quantities ω_p and ν, or what is equivalent, ϕ and ψ are now readily found. From the definition of κ^2, equation (15), we have

$$\kappa^2 = \left(1 - \frac{\phi^2}{1+\psi^2}\right) - i \frac{\psi\phi^2}{1+\psi^2} \equiv R + i I \tag{42}$$

Solving for ψ and ϕ^2, we have

$$\psi = \frac{I}{R-1} \tag{43}$$

$$\phi^2 = (1 - R) + \frac{I^2}{(1-R)} = (1 - R)(1 + \psi^2) \tag{44}$$

Using equations (40) and (41), we have

$$\psi = \frac{F_i}{F_r + \gamma_k^2 - \frac{\omega^2}{c^2}} > 0 \tag{45}$$

and

$$\phi^2 = \left[1 - \frac{c^2}{\omega^2}(F_r + \gamma_k^2)\right](1 + \psi^2) \tag{46}$$

The plasma properties are thus determined by the measured quantities through the use of equations (30) and (38) for F_r and F_i.

UNCLASSIFIED